AD-A080 960 ELECTROCHEMICAL TECHNOLOGY CORP SEATTLE WASH F/G 11/3
DETERMINATION OF THE EFFECT OF COMPOSITION, STRUCTURE AND ELECT--ETC(U)
DEC 79 T R BECK N00014-79-C-0021
UNCLASSIFIED NL

1 OF 2
AD-
A080960


1.0
1.1
1.25
1.4
1.6
1.8
2.0
2.2
2.5
2.8
3.2
3.6
4.0
4.5
5.0
5.6
MICROCOPY RESOLUTION TEST CHART
NATIONAL BUREAU OF STANDARDS-1963-A

Contract No. N00014-79-C-0021

LEVEL II

12

DETERMINATION OF THE EFFECT OF COMPOSITION, STRUCTURE AND ELECTROCHEMICAL MASS TRANSPORT PROPERTIES ON ADHESION AND CORROSION INHIBITION OF PAINT FILMS

Annual Progress Report No. 1
For the Period: October 1978 through October 1979

Prepared for
UNITED STATES NAVY
Naval Ocean Research and Development Activity
Bay St. Louis, Missouri 39520

By:
ELECTROCHEMICAL TECHNOLOGY CORP.
3935 Leary Way N.W.
Seattle, WA 98107

Principal Investigator

THEODORE R. BECK

TABLE OF CONTENTS

UNCLASSIFIED

SECURITY CLASSIFICATION OF THIS PAGE (When Data Entered)

REPORT DOCUMENTATION PAGE	READ INSTRUCTIONS BEFORE COMPLETING FORM
1. REPORT NUMBER	2. GOVT ACCESSION NO. 3. RECIPIENT'S CATALOG NUMBER
4. TITLE (and Subtitle) Determination of the Effect of Composition, Structure and Electrochemical Mass Transport Properties on Adhesion and Corrosion Inhibition of Paint Films	5. TYPE OF REPORT & PERIOD COVERED Annual progress rept. no. 2 Oct 78-Oct 79, 6. PERFORMING ORG. REPORT NUMBER
7. AUTHOR(s) T. R. Beck Theodore	8. CONTRACT OR GRANT NUMBER(s) N00014-79-C-0021
9. PERFORMING ORGANIZATION NAME AND ADDRESS Electrochemical Technology Corp. 3935 Leary Way N.W. Seattle, WA 98107 392 075	10. PROGRAM ELEMENT, PROJECT, TASK AREA & WORK UNIT NUMBERS
11. CONTROLLING OFFICE NAME AND ADDRESS United States Navy Naval Ocean Research and Development Activity Bay St. Louis, Missouri 39520	12. REPORT DATE Dec [redacted] 79 13. NUMBER OF PAGES 168
14. MONITORING AGENCY NAME & ADDRESS (if different from Controlling Office) 12 175	15. SECURITY CLASS. (of this report) Unclassified 15a. DECLASSIFICATION/DOWNGRADING SCHEDULE

16. DISTRIBUTION STATEMENT (of this Report)

Reproduction in whole or in part is permitted for any purpose of the United States Government

17. DISTRIBUTION STATEMENT (of the abstract entered in Block 20, if different from Report)

18. SUPPLEMENTARY NOTES

None

19. KEY WORDS (Continue on reverse side if necessary and identify by block number)

Paint, epoxy, polyurethane, vinyl, paint formulations, infrared, ultraviolet, mechanical properties, x-ray, pores, diffusion, adhesion, corrosion

20. ABSTRACT (Continue on reverse side if necessary and identify by block number)

Seven different paint systems were formulated to meet military specifications of paints used by the Navy. These included three vinyl resins, two polyurethanes, and two epoxy resin systems. Unpigmented free films of all of these systems were prepared for various physical and chemical measurements. Chemical formulas, molecular weights, and structures of these resins are known. Three characterization tests were used, infrared and ultraviolet spectroscopy and dynamic mechanical properties measured on a Rheovibron instrument. The loss

DD FORM 1 JAN 73 1473 EDITION OF 1 NOV 65 IS OBSOLETE

Unclassified

SECURITY CLASSIFICATION OF THIS PAGE (When Data Entered)

392 075

20.

tangent for all of the systems rapidly increased around or slightly above room temperature. The nonlinear changes in mechanical properties around and above room temperature are indicative of structural changes that would certainly influence mass transport properties of the films.

Transport properties are required for the mathematical model that has been formulated for transport of ionic species and water through paint films under concentration and potential gradients and measurements were started. The transport parameters will be related to chemical and structural properties of the polymer systems to obtain a more fundamental understanding of the effect of paint properties on the mechanism of corrosion protection. Small angle x-ray scattering measurements were made on five of the polymer systems at Oak Ridge National Laboratory to determine the size of voids or pores in the polymers in order to correlate transport properties. Only preliminary results are in, but the data indicate that the voids are smaller than 15 to 30 Å.

Preliminary adhesion measurements were made for seven paints on steel substrates. Measurements of cutting force on steel knives with appropriate cutting angles were converted to surface energy of adhesion by means of fracture-mechanics type equations. In all cases, wetting with water decreases adhesion to a very low level in a matter of tens of minutes. For times of wetting on the order of an hour, the adhesive strength increases to its original value upon drying of the film. Times for loss and regain of adhesion are the same order of magnitude as for water transport measurements on free films.

ACKNOWLEDGMENT

Many people contributed to this program and are acknowledged here in the order of their contributions in the results and discussion section. Dr. H. A. Newey and Mr. C. J. Busso, consultants in resin and polymer technology, Lafayette, California, provided sources of materials and formulations for paints meeting appropriate military specifications and information on composition and structure. Professor J. C. Seferis, Department of Chemical Engineering, University of Washington, Seattle, provided guidance on measurements of physical and mechanical properties. Mr. A. R. Wedgewood, a student of Prof. Seferis and a part-time employee of Electrochemical Technology Corp. (ETC), measured IR and UV spectra and dynamic mechanical properties of the paint films. Dr. R. T. Ruggeri, research chemical engineer at ETC, was responsible for measurements of transport properties of paint films and the adhesion measurements. He participated in the overall planning of the program and in interpretation of results. Mrs. S. G. Chan, chemist at ETC, measured ionic capacities of paint films. Mr. Michael LaScala, chemical technician at ETC, made measurements of diffusion coefficients, water absorption, and other properties related to mass transport. Mr. Farrel W. Lytle made the small angle x-ray scattering measurements on the paint films to determine pore size at Oak Ridge National Laboratory. He was assisted by Dr. R. W. Hendricks and Dr. J. S. Lin who operate the facility under a National Science Foundation grant. Mr. W. C. Chan, chemical engineering graduate student, University of Washington, worked at ETC in the summer of 1979 on adhesion measurements. Finally, acknowledgment is given to Mr. P. Olson, Experimental Research Equipment Co., whose creative abilities and mechanical skill have made possible the special machines and equipment for measurement of adhesion and other physical properties.

1.0 INTRODUCTION

Natural organic coating materials have been used since antiquity for decoration and for protection of structures (1). The Egyptians learned to use natural pigments in binders of gum arabic, egg, and beeswax. Bitumen has been used at least since Biblical times to conserve the wooden hulls of ships. During the Middle Ages linseed oil was introduced as a binder by artists and then by craftsmen. Shellac made its appearance in Europe from the Far East during the seventeenth century. These were essentially the only coatings used up to the present century.

Synthetic resins introduced in the period of 1920 to 1950 now dominate the coatings field (1). These include in chronological sequence, phenolics, alkyds, chlorinated rubber, vinyls, urea resins, melamine resins, polyurethane, silicone resins, and epoxide resins. The vinyl, polyurethane and epoxide resin systems are now extensively used for military aircraft and ships. Appropriate corrosion-inhibiting and coloring pigments are added to suit the purpose.

Protection against corrosion of structural metals is one of the primary objectives of coatings for military systems. Corrosion protection is in part achieved by the polymer film properties and in part by incorporation of corrosion inhibitors. In spite of the long-time usage of coatings for corrosion protection, the mechanism of protection is still incompletely understood. The research described in this report is based on the premise that further improvements in coating life and protective ability could be made if there were a better, more-quantitative, understanding of the mechanism of corrosion inhibition by paints.

It has long been known that paint films are readily permeable to water and oxygen. These species can diffuse through paint films orders of magnitude faster than is required by observed corrosion rates under films (2). In 1948, Bacon, Smith, and Rugg (3) showed by means of extensive tests with painted rods that corrosion resistance is directly related to surface resistance of the films. Films with resistance greater than 10^8 ohm cm^2 gave good long-term protection, but films with

resistance less than 10^6 ohm cm^2 permitted corrosion within days or weeks.

Research on the protective properties of paints during the past three decades has shown that film resistance tends to decrease with time. This phenomenon has been attributed to development of pores in the film normal to the surface. Brasher and Nurse (4) suggested the following sequence: random water absorption, reorientation of the film and linking of the water clusters to form pores, establishment of equilibrium between pores and solution, and finally, onset of corrosion. Cherry and Mayne (5) observed a sharp drop in film resistance after a given exposure time and a change from "activated" to pore diffusion. For the initial, activated diffusion, the film resistance increased with concentration of NaCl in the immersion solution. They termed this "I" or inverse relation to solution resistance. Kittelberger and Elm (6) had already shown that water absorption by films decreases with sodium chloride concentration in the solution due to osmotic pressure. For the pore-type diffusion, observed by Cherry and Mayne, the film resistance was directly related to solution resistance and this was termed "D" type. Kendig and Leidheiser (7) recently measured changes in electrical permittivity of films versus frequency as a function of exposure time and interpreted their results in terms of development of pores.

Although indirect evidence indicates development of pores in paint films, no direct measurements of their size, shape, and distribution have been reported in the literature. On the other hand, in the field of ion-exchange membranes, such measurements have recently been described (8). Small angle x-ray scans and transmission electron microscopy have been used to characterize the pore structure in the du Pont Nafion membranes. These techniques were believed to be applicable in studies of paint films.

Electrochemical Technology Corp. (ETC) began studies of transport properties of paint films and initiation of corrosion through work done on an Air Force Office of Scientific Research contract (AFOSR) in 1976 (9). This work was proposed in response to a need for a better under-

standing of how paint films protect expressed by Air Force personnel at the AFOSR/AFML Corrosion Workshop (10) held in Dayton, Ohio on 17-18 September 1975. Review of the paint literature showed that, relative to the immense practical importance of the field, the number of quantitative papers was very sparse and the data were quite fragmentary. A comprehensive one-dimensional mathematical model for transport processes in paints was therefore formulated, including all mobile species, ionic, solute, and solvent. All required parameters, diffusion coefficients, transference numbers, water absorption coefficients, etc., were measured on a military-specification polyurethane paint and used in the model. Computer implemented calculations have shown the relative importance of the fifteen input parameters and have demonstrated the internal consistency of the data.

During this prior work, a need became evident to relate transport properties of paint films to their chemical and physical structure. Also a wide variety of paint systems used in practice needed to be studied. Due to the proprietary, competitive nature of the paint industry it was not possible to obtain known chemical compositions and structures for military-specification paints. Therefore consultants were hired to provide information for formulation of appropriate paint systems.

Contacts with Navy personnel (11, 12) indicated several problems concerning paint that are important to the Navy:

- It is desired to increase paint life from a current three years up to ten years.
- More quantitative prediction and measurement of performance and condition of paint films is needed.
- Improvements in paint adhesion, in particular, resistance to cavitation forces, is needed.
- It is desired to resolve the effect of cathodic protection on adhesion of paints, particularly for vinyl coatings.

The practical importance of adhesion dictated that studies of adhesion should be initiated at ETC and related to the work on transport

properties of paint films.

Reporting of the work accomplished during the first year on this contract is divided into five main areas: 1. composition of paints, 2. characterization by IR and UV spectroscopy and by dynamical mechanical methods, 3. measurement of properties important to mass transport through paint films, 4. small angle x-ray scattering measurements, and 5. adhesion measurements. Each of these areas is described in a separate section of this report and has its own set of references. In addition, Appendices A to D contain detailed data and derivations pertaining to characterization of the polymers.

REFERENCES (Section 1.0)

1. P. Nylen and E. Sunderland, Modern Surface Coatings, Interscience, New York, 1965.

2. J. F. O. Mayne, Chemistry and Industry, p 518, March 20, 1965.

3. R. C. Bacon, J. J. Smith, and F. M. Rugg, Ind. Eng. Chem., 40, 161 (1948).

4. D. M. Brasher and T. S. Nurse, J. Appl. Chem., 9, 96 (1959).

5. B. W. Cherry and J. E. O. Mayne, 1st International Congress on Metallic Corrosion, London, 1962.

6. W. W. Kittelberger and A. C. Elm, Ind. Eng. Chem., 39, 876 (1976).

7. M. W. Kendig and H. Leidheiser, J. Electrochem. Soc., 123, 982 (1976).

8. T. D. Gierke, "Ionic Clustering in Nafion Perfluorosulfonic Acid Membranes...," presented at The Electrochemical Society, October 1977, Atlanta.

9. AFOSR Contract, F49620-76-C-0029, A Study of Transport Properties and Initiation of Corrosion Under Paint Films, Final Report, December, 1979.

10. Proceedings of AFOSR/AFML Corrosion Workshop, Dayton, Ohio, 17-18 September 1975.

11. Telephone call to Ed Morganstern, Naval Ship Engineering Center, Crystal City, Va., October 5, 1977.

12. Telephone call to Herman Preiser, Naval Ship R&D Center, Annapolis, Md., October 28, 1977.

2.0 SUMMARY AND CONCLUSIONS

Seven different paint systems were formulated to meet military specifications of paints used by the Navy. These included three vinyl resins, two polyurethanes, and two epoxy resin systems. Unpigmented free films of all of these systems were prepared for various physical and chemical measurements. Chemical formulas, molecular weights, and structures of these resins were provided by paint chemist consultants. In addition, characterization tests were carried out on commercial-airplane polyurethane and epoxy resin systems which were under study on another contract.

Three characterization tests were used, infrared and ultraviolet spectroscopy and dynamic mechanical properties measured on a Rheovibron instrument. The purpose of obtaining the IR and UV spectra was to establish baseline data for comparing chemical and structural changes in the films as a function of time and exposure to various environments. The IR spectra obtained agreed with published spectra which were available for some of the resin systems.

Loss tangent and elastic modulus were measured with the Rheovibron for each polymer system in a temperature range from -160°C to +140°C. A striking observation was that the loss tangent for all of the systems rapidly increased around or slightly above room temperature. The glass transition temperatures, defined by the maximum in the loss tangent, varied from >40°C to 98°C for the various films. The nonlinear changes in mechanical properties around and above room temperature are indicative of structural changes that would certainly influence mass transport properties of the films. Changes in humidity from zero to 100 percent produced changes in loss tangent for all of the films at room temperature. The real part of the modulus decreased for all films with increasing humidity; this was attributed to the plasticizing effect of water.

Measurements of transport properties of the seven films of known composition were begun. These properties are required for the mathematical model that has been formulated on another contract for transport of ionic

species and water through paint films under concentration and potential gradients. Diffusion coefficients, solubilities, ionic capacity, etc., are required as input data. A nearly-complete set of data was previously obtained for the commercial airplane polyurethane, and model calculations have been performed giving consistent calculational results. An objective of the present work is to relate the transport parameters to chemical and structural properties of the polymer systems and thus obtain a more fundamental understanding of the effect of paint properties on the mechanism of corrosion protection.

Small angle x-ray scattering measurements were made on five of the polymer systems at Oak Ridge National Laboratory. The purpose was to determine the size of voids or pores in the polymers in order to correlate transport properties. There is much speculation in the paint literature concerning pore size. Only preliminary results are in from the Oak Ridge measurements, but the data indicate that the voids are smaller than 15 to 30 Å. Furthermore, the measured voids are smaller in the vinyl systems, in agreement with lower measured ionic conductivities. It is planned to refine the calculations using a program at Oak Ridge to obtain void size distributions for each polymer.

Preliminary adhesion measurements were made for seven paints on steel substrates. Measurements of cutting force on steel knives with appropriate cutting angles were converted to surface energy of adhesion by means of fracture-mechanics type equations. In all cases, wetting with water decreases adhesion to a very low level in a matter of tens of minutes. For times of wetting on the order of an hour, the adhesive strength increases to its original value upon drying of the film. Times for loss and regain of adhesion are consistent with water transport measurements on free films. Similar results were obtained with sodium chloride solutions except that adhesion recovery was spotty indicating weak spots in the films.

In this first year of work, much effort went into obtaining and characterizing the polymer films and developing techniques. In the second year, it is planned to emphasize the transport measurements and

model calculations and measurements of adhesion. The objective will be to pull all of the parts together into a coherent picture relating transport behavior of the films to their chemical composition and structure. It is hoped that adhesion measurements will give a sensitive measure of incipient corrosion which can be correlated with the mass transport model. Obtaining exact paint formulations has paved the way to a vast literature on polymers, much more sophisticated than the paint literature, and has accelerated our progress in understanding the behavior of paints.

3.0 RESULTS AND DISCUSSION

3.1 Formulation of Known-Composition Paints

Two consultants with long-time experience in polymers and paints, Dr. H. A. Newey and Mr. C. J. Busso, provided formulations of known compositions of vinyl, epoxy, and polyurethane paint systems meeting appropriate military specifications. During preparation of the initial proposal (1), it was determined by contacts with paint formulators and raw materials suppliers that the paint industry is extremely competitive and that the only way to obtain known-composition paints was through consultants. Appropriate Military Specification numbers for paints used by the Navy were obtained from NSRDC at Annapolis (2).

The paint systems procured (3, 4) are given in the following subsections. The code name given each paint for internal use at ETC is given in parentheses by each paint.

3.1.1 System I, Epoxy Resin Coating that Meets MIL-P-24441 (E Epoxy)

This coating consists of an epoxy resin, Shell EPON 815, and a polyamide curing agent. The epoxy resin is a mixture of the diglycidyl ether of bisphenyl A (90% by weight) and butyl glycidyl ether (10% by weight). The curing agent is a more-complex amine mixture, mainly Versamid 280B75 plus Genamid 2000 and MEK solvent (formulas given). In curing the amine, hydrogens add to the epoxide groups in the epoxy resin by the reaction:

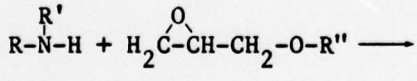

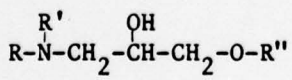

The epoxy group reacts with both amine hydrogen on the terminal primary amine groups. The polyfunctional amines, Versamid 280 and Genamid 2000, react by this simple addition reaction with EPON 815 to give a cross-linked thermoset film.

3.1.2 System II, MIL-P-15328D, Formula 117 (VR2)

The structure of Bakelite Vinyl Butyral Resin XYGL can be best described by telling how it is made. Vinyl acetate is polymerized to a linear polymer and then saponified to remove most of the acetate groups leaving hydroxyl groups. Part of these hydroxyl groups is reacted with butyraldehyde, which forms an acetal with adjacent hydroxyl groups. The final product may be represented by the following structure:

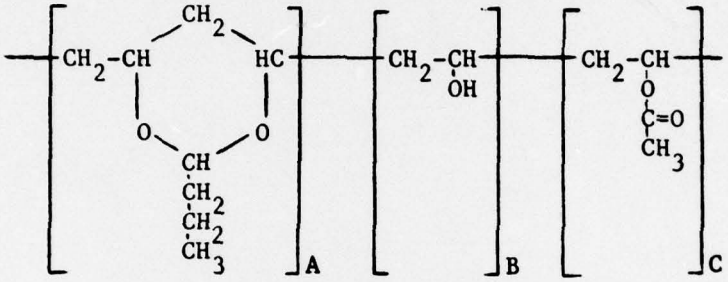

Units of A, B, and C are randomly distributed along the molecular chain. In Bakeline XYHL there is approximately 80% by weight A, 19.5% by weight B, and 0.5% by weight C. The molecular weight is about 30,000.

3.1.3 System III, MIL-P-15929C, Formula 119 (VR3)

Bakelite vinyl resin VAGH is a copolymer of vinyl chloride and vinyl acetate where a fraction of the acetate groups have been saponified to hydroxyl groups. It can thus be described as a copolymer of vinyl chloride, vinyl acetate, and vinyl alcohol, and can be represented by the formula:

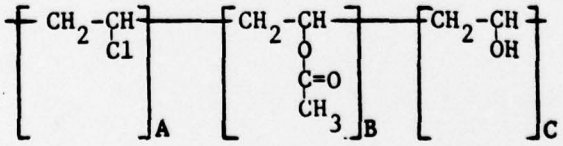

These units are randomly distributed along the molecular chain. Bakelite VAGH is 91% by weight A, 3% by weight B, and 6% by weight C. The average molecular weight is 23,100 and it has a glass transition temperature of 79°C.

Tricresyl phosphate is a plasticizer for the resin. It has the structure:

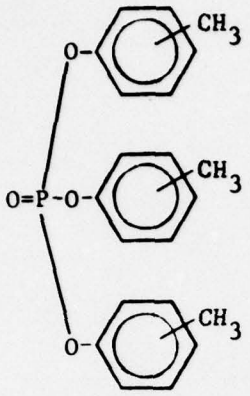

It does not react chemically but only dissolves in the vinyl resin.

3.1.4 System IV, MIL-P-15931, Formula 121 (VR4)

Bakelite Vinyl Resin VYHH is a random linear copolymer of vinyl chloride (86% by weight) and vinyl acetate (14% by weight). Again, tricresyl phosphate is the plasticizer. The rosin in the formula is largely abietic acid with other related compounds. Abietic acid has the following structure:

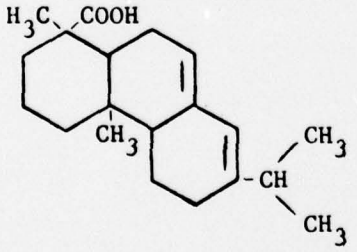

The rosin contributes to the hardness of the coating and helps adhesion. The coating dries by the evaporation of the solvent and no chemical reaction takes place between the components.

3.1.5 System V, EPONOL Resin Coating (A Epoxy)

EPONOL 55 is a thermoplastic resin related to epoxy resin. The structure of the repeating unit is generally represented by the formula:

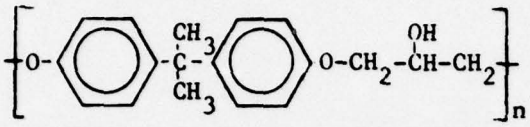

where n is about 25. There is some branching of the chain and the end groups are probably phenol or alcohol groups. While the chemical structure is similar to the epoxy resins, the molecular weight is high enough that good films are formed merely by evaporation of the solvent without the need of a curing agent.

3.1.6 System VI, Ketimine-Epoxy Coating (K Epoxy)

To explain the chemical composition of this coating we must first explain what a ketimine curing agent is, and how it works. The ketimine H-2 is formed from ethylenediamine and methyl isobutyl ketone by the splitting out of water as follows:

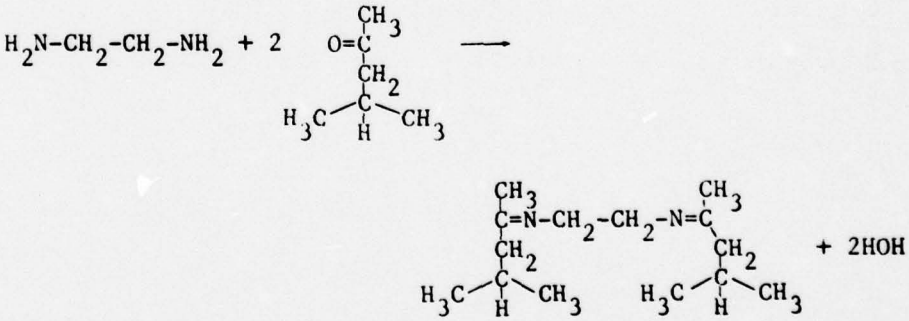

Ketimine H-2

When applied in a coating, this ketimine readily reacts with the moisture of the air which breaks it back to ethylenediamine and methyl isobutyl ketone. (The reverse of the above equation.) The methyl isobutyl ketone evaporates from the coating and the ethylenediamine is the real curing agent. Ethylenediamine cures epoxy resins by a simple, clean-cut addition

of the amine hydrogen to the epoxide groups. This reaction is shown in the following equation using a monoepoxide for illustrative purposes:

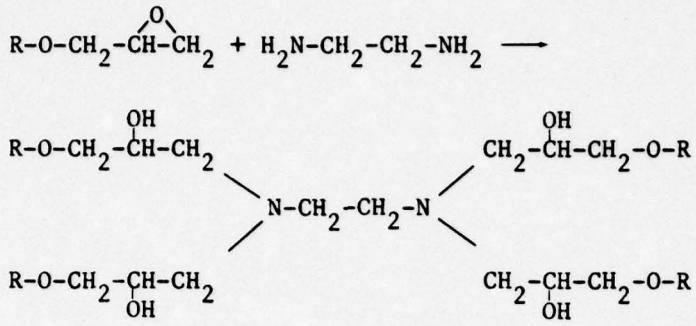

Since in the actual coating the epoxy resin is close to difunctional and the ethylenediamine is tetrafunctional, the addition reaction gives a cross-linked system with well-defined structure.

The epoxy resin in this coating consists of two parts. It is mainly the diglycidyl ether of bisphenol A.

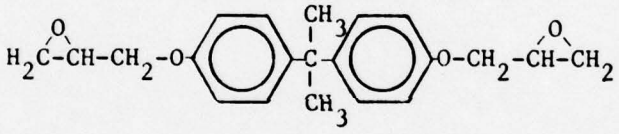

To lower the viscosity and cut down the cross-link density, this diglycidyl ether of bisphenol A is diluted with a minor amount (about 10%) of a monofunctional epoxy compound, butyl glycidyl ether.

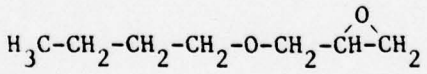

The phenol in the formula is merely present as a catalyst to speed up the reaction between amine hydrogens and epoxy groups.

3.1.7 System VII, MIL-C-81773B A/S (N PUR)

This is a two part coating. Part I is a solution of polyester resin having free hydroxyl groups. A typical product of this type would be

prepared by reacting a glycol, phthalic anhydride and a triol to yield the following resin structure:

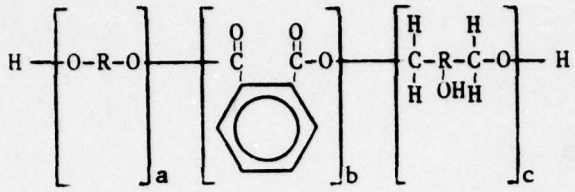

Component II is a solution of Desmodur N. This is a biuret derived from hexamethylene diisocyanate:

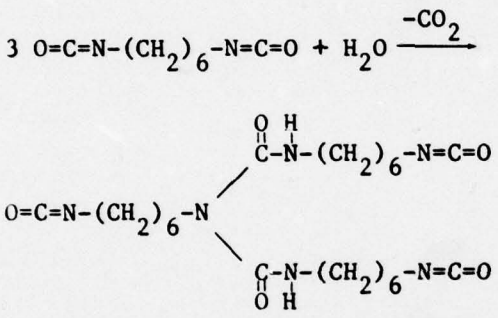

Desmodur N is sold by Mobay Chemical as a 75% solids solution in 1/1 by volume ethylglycol acetate/xylene solvent; designation of the solution is Desmodur N-75.

Cross-linking these systems results from the isocyanate-hydroxyl reaction to produce a urethane linkage:

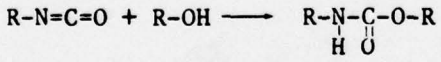

Stoichiometry for this system is 1:1, Component I:Component II, by volume. Films of these coatings should be fully cured after eight hours at 77° F.

All of the components for the seven paints were procured and free films of all were made by spraying on decal paper and stripping in water. To date only unpigmented films have been made.

In addition to these systems, some testing was done on two airplane paint systems studied on another contract. These were both commercially

important, modern, two-part polymer systems, without pigments, obtained from the Boeing Commercial Airplane Company, Kent, Washington. One was a polyurethane, Desoto, Inc., Chemical Coatings Div., Berkeley, California, meeting Boeing material specification BMS-10-60D-TYII and Mil C-83286. The code name given to this system was System VIII or O PUR. The other paint was an epoxy, Koppers Co., Andrew Brown Div., Kent, Washington and was given the code name System IX or O epoxy. No information was obtainable on the exact formulations of these systems.

A clear methacrylate paint in a spray can was used in some of the adhesion tests described in Section 3.5 to check with literature data obtained with the hesiometer on methacrylate systems.

REFERENCES (Section 3.1)

1. Electrochemical Technology Corp., proposal 7803, "Determination of the Effect of Composition, Structure, and Electrochemical Mass Transport Properties on Adhesion and Corrosion Inhibition of Paint Films," April 1978.

2. T. R. Beck, Telephone call to H. Preiser, NASRD, Annapolis, MD, February 23, 1978.

3. Letter, Newey & Busso Associates, to Electrochemical Technology Corp., December 11, 1978.

4. Ibid, January 29, 1979.

3.2 Characterization by IR and UV Spectra and Dynamic Mechanical Properties

Introduction

Initial characterization of the nine unpigmented paint systems being used in the transport, corrosion, and adhesion studies has been completed. The paint systems investigated include three vinyl resins, two polyurethanes, and four epoxy systems. The compositions for seven of these systems were provided by Newey and Busso (1, 2), and are designated as Systems I-VII as given in Section 3.1. The remaining two systems were the polyurethane, System VIII, and the epoxy, System IX.

The determination of the structure-property relations for each paint system is essential for understanding their observed behavior and for developing methods by which their performance can be improved. Numbers of techniques are available, including infrared, ultra-violet, NMR, x-ray diffraction, rheooptical, and dynamic mechanical, by which the polymeric structure can be characterized. In this study, infrared, ultraviolet, and dynamic mechanical techniques were used.

A polymer is a large molecule built up by the repetition of one or more different kinds of small chemical units, linked together by strong covalent bonds. The repetition of these chemical units in some cases, results in the formation of linear or branched chains. In other cases, these chains may be interconnected forming a three-dimensional network. Whether the polymer forms a linear, branched, or network structure is determined by the properties of the chemical unit (functionality) and the reaction conditions. The resulting structure greatly influences the polymer's properties; for example, most linear polymers can be made to soften and then be molded by the application of heat and pressure, while cross-linked or network structures are in general stable to heat and cannot be made to flow. The three vinyl resin systems (Systems II, III, and IV) are linear chain molecules, one epoxy system (System V) is moderately branched, while the remaining five systems form network structures.

In addition to providing sites for cross-linking, the chemical structure of the repeating units determines the nature of the chain end groups,

the main chain structure of the polymer, and the type of chain substituents (OH, Cl, COOH, etc.).

Although the influence of the end groups on physical properties is usually small, due to the high degree of polymerization, the effect of these end groups on chemical properties cannot be neglected. In the case of the amine cured epoxy systems (System I, VI, IX), the unreacted epoxide groups, which remain after undergoing the normal cure process, are potential sites for further reaction.

The geometrical arrangement and chemical structure of the main chain greatly influences the polymer morphology and the mobility of the polymer chains. Arrangements fixed by chemical bonding in the molecule, such as cis and trans isomers are described as configurations. The configuration of a polymer chain cannot be altered unless chemical bonds are broken and reformed. Arrangements which arise from the rotation about single bonds such as the plannar zig-zag and helical forms are described as conformations.

In the case of two of the vinyl resins (Systems III and IV), the main chain consists of only carbon atoms, and may be arranged in a syndiotactic isotactic or atactic configuration (?). (In the syndiotactic arrangement, all side groups to chain face "up" or "down"' in isotactic, the groups alternate; in atactic, the groups are random.) To illustrate the importance of chain configuration on the polymer's properties, consideration to the polyvinyl chloride polymer (PVC) will be given. Since vinyl resin Systems III and IV are 91% and 86% vinyl chloride by weight (1), similar effects might be expected in these systems. X-ray, infrared, and high resolution NMR studies on PVC prepared by free radical polymerization above room temperature suggest an approximately 65% syndiotactic configuration (4). Under these conditions, the polymer is somewhat branched and only slightly crystalline. As the temperature of free radical polymerization is lowered, the degree of syndiotacity increases. This results in a decrease in the extent of branching and an increase in crystallinity. These morphological changes are attributed to the increased chain ordering, and result in increased melting point and glass transition temperatures (4). Other polymer properties are also expected to change as a result of these

morphological changes.

In the case of the epoxy systems, the chain backbone consists of bulky ring structures in addition to C, O, and in all but System V, N atoms. These ring structures decrease the number of conformations available to the polymer, due to increased steric hinderance, and result in increased chain rigidity.

The type of substituents on the polymer chain determines the kinds of secondary forces acting between the molecules, the molecular packing, and extent of steric hinderance. The high molecular weight of polymers enhances the normally weak secondary forces of attractions between molecules, resulting in many of the excellent properties of polymers. Some of the more important kinds of secondary forces in polymers, are Van der Waals, dipole interaction, and dispersion forces. Polyvinyl chloride is a strongly polar polymer, and many of its properties are attributed to the strong dipole intermolecular attraction forces which result.

In addition to these kinds of interaction forces, the hydrogen bond is particularly important in many polymeric systems. Hydrogen bonding usually occurs between a hydrogen attached to an acidic group, such as a hydroxyl, carboxyl, amine or amide group, and a basic group. The basic group is usually an oxygen as in a carbonyl, ether, or hydroxyl group; a nitrogen as in amines or amides; and occassionally a halogen group. Hydrogen bonds formed between the carbonyl and amine groups in the polyurethane systems (Systems VII and VIII) are extremely important to the properties of these polymers.

The size of the chain substituents determines how close the molecular chains can pack and their mobility. In the vinyl butyral resin (System II), the size of the acetal side group prevents the polymer chains from packing close together. The result is that the secondary forces between the chains are decreased, so that the polymer is self-plasticized. Also, the repeat units in the vinyl butyral polymer contain dipolar side groups which are bridged across alternate chain carbon atoms. These dipoles therefore are unable to rearrange independent of the main chain. Since the magnitude of the interaction forces between dipoles depends on their alignment, this condition is expected also to lower the interaction forces.

In conclusion, measurement of appropriate physical and chemical properties allow the determination of the polymer's structure. From this information, the cause and effect of structural changes can be determined.

3.2.1 Experimental Methods

Dynamic Mechanical Properties

Dynamic mechanical property measurements on the films as a function of temperature give information on phase transformations. These measurements were made in the laboratory of Prof. J. C. Seferis, ETC consultant, at the University of Washington, Department of Chemical Engineering.

Dynamic mechanical data were obtained using the Rheovibron DDV-11B, manufactured by Toyo Measuring Instrument Co. Ltd., Tokyo, Japan. The operating principle of the Rheovibron consists of applying a sinusoidal displacement to one end of the sample and monitoring the stress response at the other end. For a viscoelastic material, the stress response will lead the strain input by phase lag angle δ. For a perfectly-elastic solid, $\delta = 0°$, while for a viscous liquid, $\delta = 90°$. The Rheovibron measures directly the tangent of the phase lag angle δ and the magnitude of the complex modulus $|E^*|$ and/or compliance $|S^*|$ which are defined as:

$$(E^*) = \frac{\sigma_o}{\varepsilon_o}, \quad |S^*| = \frac{1}{|E^*|} = \frac{\varepsilon_o}{\sigma_o} \tag{1}$$

where ε_o and σ_o are the amplitude of the strain input and stress response ouput respectively. From this information, the real (elastic component) and imaginary (viscous component) of the complex modulus and/or compliance can be calculated as follows:

$$\begin{aligned} E^* &= E' + E'' & S^* &= S' - S'' \\ E' &= E^* \cos\delta & S' &= S^* \cos\delta \\ E'' &= E^* \sin\delta & S'' &= S^* \sin\delta \end{aligned} \tag{2}$$

$$\tan\delta = \frac{E''}{E'} = \frac{S''}{S'}$$

These properties were measured as a function of temperature at a frequency of 11 Hz. The sample chamber was purged with dry N_2 gas to obtain 0% humidity conditions.

Measuring the temperature dependence of these material descriptors (E', E", S', S") provides the mechanical spectrum from which structural and compositional effects on the mechanical properties can be determined.

Using a plexiglas humidity chamber, dynamic mechanical properties were measured at room temperature as a function of percent relative humidity. Zero percent humidity was obtained by using a layer of desiccant on the bottom of the chamber. The desiccant was replaced by saturated salt solutions which produce known relative humidity conditions (5), and water which gives 100% relative humidity conditions. The salts used in this study and the resulting humidities at 25°C are, $MgCl_2 \cdot 6\ H_2O$ (33.2%), $Na_2Cr_2O_7 \cdot 2\ H_2O$ (53.8%), NaCl (75.8%), and KNO_3 (92.0%). Data were also taken at room conditions, and a sling psychrometer was used to determine the relative humidity.

Equilibrium was assumed to be reached after one hour of exposure for the vinyl resin and polyurethane systems. This time was based on the results obtained in absorption studies (see Section 3.3) and was confirmed by taking data after 1 and 10 hours of exposure for each paint system at one or more humidity conditions. For the epoxy system studied, it was assumed that 8 hours would be sufficient for equilibrium to be reached. This time was verified by taking data at 8 and 16 hours of exposure at 100% relative humidity.

Infrared Spectroscopy

Although the infrared spectrum (0.8 - 50. μm) is characteristic of the whole molecule, certain groups of atoms give absorption bands at or near the same frequency regardless of the rest of the structure. The energy absorbed by these molecular groups is converted to stretching and bending vibrations in the molecule. Since all polymers possess specific absorption bands in the infrared part of the spectrum, infrared spectroscopy is one of the most useful tools for the analysis of polymeric

structure. Some applications of the infrared spectrum for the analysis of polymeric structure include: 1. the identification of unknown samples by comparison to reference compounds, 2. compositional determinations in polymers and copolymers, 3. the measurement of structural factors such as branching, cross-linking, and crystallinity, 4. studies of the steric and conformational order of the polymer chains, 5. determination of the nature and amounts of plasticizers, additives, and impurities, and 6. studies on the extent of hydrogen bonding in the polymer system. Furthermore, a number of reviews (6, 7, 8, 9) have discussed other applications of infrared spectroscopy to the study of polymeric materials.

Quantitative analysis of infrared spectra generally involves either the application of the Beer-Lambert law (7) or the determination of the intensity ratios of different absorption peaks (9). The Beer-Lambert law relates the absorption, A, to the samples thickness, b (cm), and the concentration of the absorbing species, c (gmole/liter), by the molar extinction coefficient, ε, as follows

$$A = \varepsilon bc \tag{3}$$

The absorbance A is given in terms of the incident intensity, I_o, and the transmitted intensity, I, by

$$A = \log_{10} \frac{I_o}{I} \tag{4}$$

The Beer-Lambert law is not always obeyed because the molar extinction coefficient is greatly affected by environmental changes. Consequently, plots of band absorbance ratios vs compositions have found extensive application in correlating absorbance intensity to composition.

Hydrogen bonding alters the absorption frequencies of both the proton donor and acceptor, (e.g., NH and C=O respectively) for both the stretching and bending bands. In general the stretching band of the proton donor is moved to lower frequencies, while the stretching frequency of the acceptor group is also shifted but to a lesser degree. The bending vibration of the donor group is usually shifted to higher frequency, but to a lesser extent than that of the stretching mode (9). In addition, both intermolecular and intramolecular bonding can occur, each of which alter

the spectrum.

Observations of shifts and intensity changes of the spectrum peaks allows for qualitative and quantitative analysis of the polymer's structure. In this work, infrared absorbance spectra were measured at the University of Washington Department of Chemistry using three different Perkin-Elmer spectrophotometers. The instruments used were the 727-B, 283, and 257 models. Samples were prepared as free films, liquids and as KBr discs (9). The initial results and conclusions derived from these spectra are presented along with the discussion of each paint system.

Ultraviolet Spectroscopy

The absorption of radiation energy by chemical compounds in the ultraviolet region of the spectrum is dependent on the electronic structure of the molecule. The absorption energy is quantized and results in the excitation of a single electron from a ground state orbital (π, σ, or n) to an excited or antibonding orbital (π^* or σ^*). The relative ease with which the various transitions occur is summarized in Fig. 3.2.1. Although the energy scale in this Fig. is relative, it can be readily seen than a $n \rightarrow \pi^*$ transition requires less energy than a $\pi \rightarrow \pi^*$ transition, and that both of these transitions require less energy than a $\sigma \rightarrow \sigma^*$ transition.

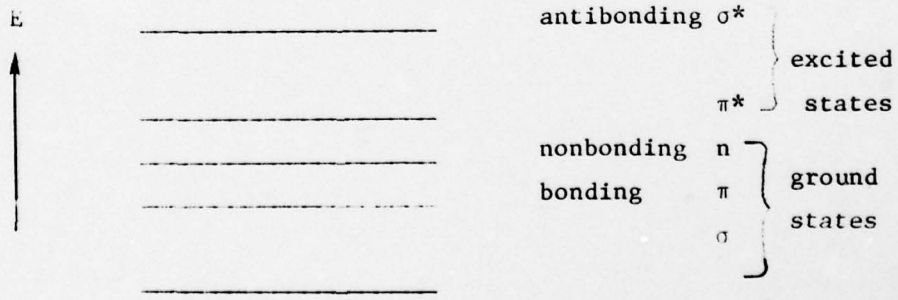

Fig. 3.2.1. The electronic energy levels of various bond orbitals on a relative energy scale.

The energy absorbed in an electronic transition, ΔE, is given by the following relationship (10):

$$\Delta E = h\nu = \frac{hc}{\lambda} \tag{5}$$

where h = Plank's constant

c = velocity of light

ν = frequency

λ = wavelength

The energy absorbed, ΔE, is equal to the difference between the ground and excited state. In addition it can be seen from Eq. 5 that the smaller the energy difference, the longer the wavelength of absorption.

Since the energy absorbed by a particular electronic transition is quantized, a discrete absorption line for each transition is expected. These discrete lines are observed for simple molecules in the gaseous state. However, in the case of a complex molecule, such as a polymer, the multiplicity of the vibrational sublevels and the closeness of their spacing cause these discrete lines to overlap. This results in the observation of broad absorption bands.

Saturated compounds which contain σ-electrons exclusively, can undergo only $\sigma \rightarrow \sigma^*$ transitions. Since ΔE for such a transition is relatively large, these compounds absorb at short wavelengths on the order of 200 nm or less. Since atmospheric absorption starts near wavelengths of 200 nm and extends into the shorter wavelength region, these absorptions can be only examined through vacuum ultraviolet spectroscopy.

As a result of the atmospheric absorption and the nonavailability of a vacuum UV spectrophotometer, only the 200-380 nm region of the UV was investigated. There are numbers of compounds which contain covalently bonded unsaturated molecular groups which absorb in this region. These groups are called chromophores and contain both π and n electrons. These electrons can undergo three transitions. These are the $n \rightarrow \sigma^*$, $\pi \rightarrow \pi^*$, and $n \rightarrow \pi^*$ transitions. Many of the absorptions observed in the long wavelength region of the UV (200-380 nm), result from the low energy $n \rightarrow \pi^*$ transition.

Two types of chromophores found in the different paint systems being investigated are the carbonyl and benzene ring. The carbonyl group contains σ, π, and n electron pairs. Saturated ketones and aldehydes display three transitions. The $\pi \rightarrow \pi^*$ and $n \rightarrow \sigma^*$ transitions are observed at 150 and 190 nm respectively, while the $n \rightarrow \pi^*$ transition occurs in the 270-300 nm range. Benezene absorbs at 184, 204, and 256 nm, with the 204 and 256 nm bands resulting from $n \rightarrow \pi^*$ transitions. More information on these and other chromophores is given by Silverstein et al., (10).

The monitoring of wavelength shifts and changes in the intensity of the spectrum peaks gives information on the effects of solvents and substitutions of different groups. For example, hydrogen bonding to the carbonyl group in a saturated ketone lowers the energy level of the n orbitals. This results in a shift of the absorption peak to lower wavelengths. The substitution of OH and Cl groups to a chromophore such as a benzene ring, alters both the wavelength and intensity of the absorption.

In addition to the detection of structural differences as those described above, quantitative analysis of the UV absorbance can be done using the Beer-Lambert law given as Eq. 4. This relation is generally used to correlate the absorption and the concentration of the absorbing species.

The ultraviolet absorbance spectra given in this work, were measured at the University of Washington Department of Chemistry using the Varian Super Scan 3 UV - visible spectrophotometer. Samples were prepared as free films, which were placed directly in the UV beam path, and as dilute solutions made using solvents which are transparent in the UV. Specific results for the polymer systems investigated are given in the sections which follow.

3.2.2 Vinyl Resin Systems

System II (VR2)

This resin is a vinyl butyral, which is essentially a random linear copolymer consisting of approximately 80% n-butyl acetal, 19.5% vinyl

alcohol and 0.5% vinyl acetate by weight (1). This composition can be verified by chemical analysis of the hydroxyl, acetate, and combined butyraldehyde content (11). X-ray data indicate that a vinyl butyral polymer with approximately this composition is substantially amorphous (12). Other properties such as specific gravity, refractive index, moisture permeability, and the linear expansion coefficient are given in Roff and Scott (12).

The character of the acetal and hydroxyl side groups results in the considerable polarity and high degree of hydrogen bonding observed in this polymer. These factors result in the polymer's solubility in polar solvents and good adhesion properties to a variety of surfaces. Also, the acetal and hydroxyl side groups provide potential reactive sites for post cure (13). Although the acetal rings restrict rotation due to steric hinderance, the long n-alkyl side chain tends to cause the main chains of the polymer to be apart. This creates a large free volume and decreases the polar interactive forces between the chains. The net effect is that the polymer is self-plasticized and therefore has a lower modulus, higher flexibility, and a lower glass transition than would be observed if the n-alkyl side chain was replaced by a hydrogen (e.g., polyvinyl formal).

Dynamic Mechanical

The dynamic mechanical properties measured at a frequency of 11 Hz are given in Fig. 3.2.2. A large relaxation peak denoted by α was observed at 72°C in the plot of tan δ vs temperature. A broad secondary relaxation denoted by β was observed to occur over the -80° to -50°C temperature range.

The α relaxation has been attributed to the material's glass transition, Tg, by comparisons to the results of other investigators (14, 15, 16, 17). The glass transition temperature identifies the phase change from a glassy thermoplastic to a rubber-like material (18, 19). This transition is associated with abrupt changes observed in a number of the polymer's properties; for example, the volume, refractive index, modulus, and the loss tangent.

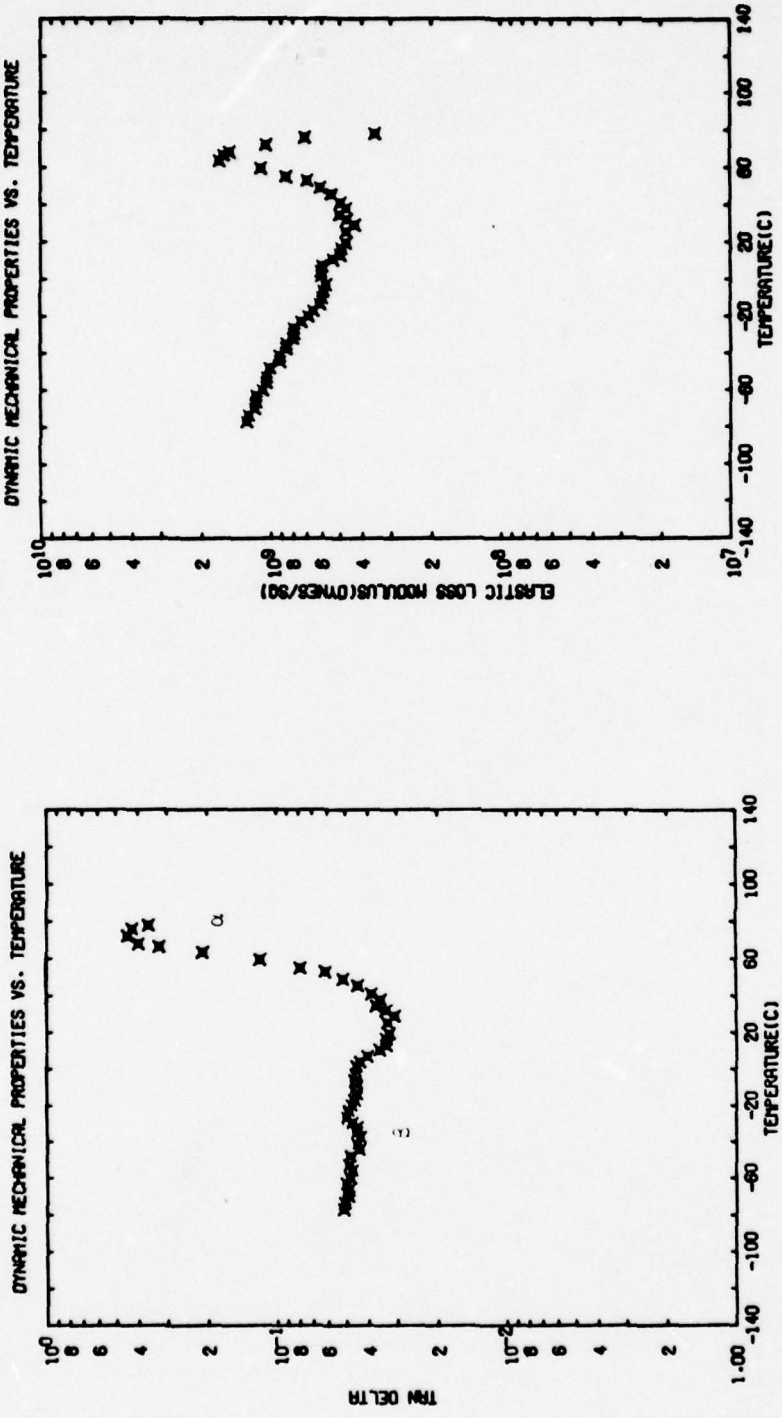

Fig. 3.2.2. Dynamic mechanical properties of paint System II (VR2) as a function of temperature at 11 Hz.

The glass transition temperature measured is a function of composition, frequency or rate of experimentation, and the method of determination. Most random copolymers exhibit their Tg, between the Tg's of the homopolymers from which they are comprised. The Tg for polyvinyl alcohol (PVOH) and polyvinyl butyral (12% polyvinyl-alcohol content) are given by Nielsen (20) as 85°C and 49°C respectively. The Tg for polyvinylbutyral is given for a 12% PVOH content, since the procedure for producing a polyvinyl acetal, as described by Newey and Busso (1) results in a random copolymer containing polyvinyl alcohol because 100% acetalisation cannot be attained. Fitzhugh and Crozier (14) measured the torsion modulus for a polyvinyl butyral-polyvinyl alcohol copolymer system as a function of temperature and percent PVOH content. From these data they evaluated the inflection temperature, T_i, and the softening temperature, T_s, which may be considered as estimates of the Tg at low frequencies. Their results showed that the Tg increased with PVOH content and are summarized in Table 3.2.1. A number of relationships between the Tg and composition of a random copolymer have been developed and are discussed in detail in Appendix A. The increase in Tg with PVOH content observed (see Table 3.2.1) is consistent with these relationships.

The glass transition is a rate-dependent phenomenon; for example, a faster heating rate leads to a higher Tg being measured. Equivalently, higher frequencies of experimentation result in a higher Tg being measured. In Fig. 3.2.3 the Tg determined by previous investigators (21, 22, 23) from the maximum observed in either the dielectric loss tangent ($\tan \delta_\varepsilon$), the mechanical loss tangent ($\tan \delta_\varepsilon$), the dielectric loss, ε'', or the loss modulus E" are plotted as log frequency versus 1/Tg.

The Tg determined from the dynamic mechanical data presented in this work are given in Table 3.2.2. These values are plotted in Fig. 3.2.3; along with the results of other investigators (21, 22, 23) for comparison. Reasonable agreement between the present work and their work was found.

Varieties of other experimental methods have been used to determine the Tg of a polymer. Some of these methods include dilatometry (16), refractive index (24), and specific volume measurements. Since each experiment measures a different polymer property, variations are often

Table 3.2.1

Tg of Polyvinyl Butyral vs PVOH Content

% PVOH	T_i	T_s
25.6		64
18.0	61	62
16.0		61
12.1	48	49

Table 3.2.2

Method	Tg
Loss Tan δ	72
Loss Modulus	63.5

Table 3.2.3

Maximum tan δ Peak Temperature (°C)

Relaxation	System VIII	System VII
α	61	70
β'	-8	-10
β	-60	-70
γ	<-140	<-140

Peak	Symbol	% PVOH	Experiment	Ref.
Tan δ_ε	▲	12-13	Dielectric	23
Tan δ_ε	■	36.6	Dielectric	21
ε''	●	12-13	Dielectric	22
Tan δ_E	▼	36.6	Mechanical	21
Tan δ_E	□	20	Mechanical	This work
E''	○	20	Mechanical	This work

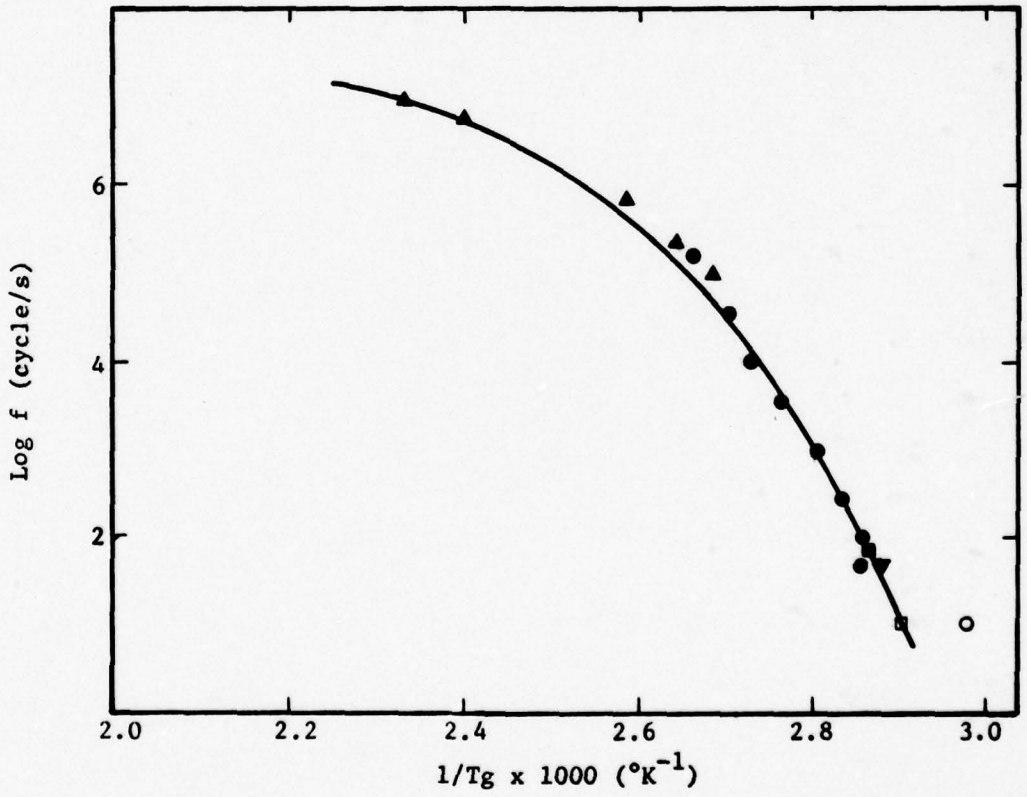

Fig. 3.2.3. Frequency dependence of Tg for paint System II (VR2) from dielectric and mechanical experiments.

observed in the Tg determined by each method.

For comparison, the results of Takahashi (16) obtained at 50 Hz are given in Fig. 3.2.4. The α transition is at about 75°C for the sample cured at 170°C for 30 min and 95°C for the sample cured at 200°C for 30 min. The β transition, although observed, is not fully resolved in these data. The cause of the β transition has not yet been identified, and further literature review on this subject is required. The dielectric loss at 60 Hz is also given, with a maximum at 75°C also being displayed. The general trends observed in Takahashi results (see Fig. 3.2.4) are in agreement with those found in this work (see Fig. 3.2.2).

It can be seen from Fig. 3.2.3 and Fig. 3.2.4 that dielectric results correlate reasonably well with mechanical results for this polymer. A possible explanation of this observation is that the permanent dipoles in this molecule, as a result of the bridge attachment of the acetal groups across adjacent carbons, are unable to reorient independent of the main chain. Therefore the dielectric relaxation observed in this polymer involve simultaneous main chain and side chain motions. Since these are the same motions involved in the mechanical relaxations, the correlation between dynamic mechanical and dielectric properties is understandable (25).

The effect of moisture on the dynamic mechanical properties of VR2 was investigated at 22°C. The results are summarized in Fig. 3.2.5, where the loss tangent (tan δ) and storage modulus (E') are plotted against percent relative humidity. Since the water content in the polymer at equilibrium increases with percent relative humidity, the increase in tan δ and decrease in modulus observed, were attributed to a plasticizing effect of water. Takayanagi (26) in studying the effect of moisture on polyvinyl alcohol concluded that the plasticization effect of water results from the breakage of intermolecular hydrogen bonds by the absorbed water molecules. The lessening of these intermolecular interactions results in increased chain mobility as detected by the increase in tan δ, and a decrease in the modulus. The importance of moisture effects on the polymer properties is clear from the magnitude of the changes observed in the dynamic mechanical properties. Specifically the measured storage modulus

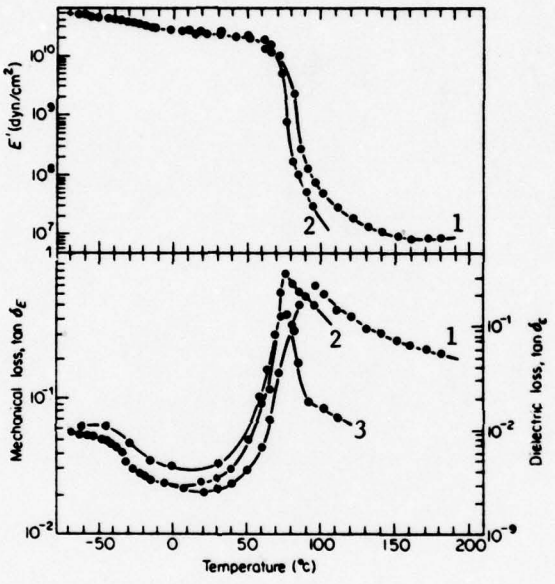

Fig. 3.2.4. Temperature dependence of E' and the mechanical and dielectric tangents for polyvinyl butyral. 1: mechanical at 50 c/s, sample cured at 200°C for 30 min; 2: mechanical at 50 c/s, sample cured at 170°C for 30 min; 3: dielectric at 60 c/s, sample cured at 200°C for 30 min (4).

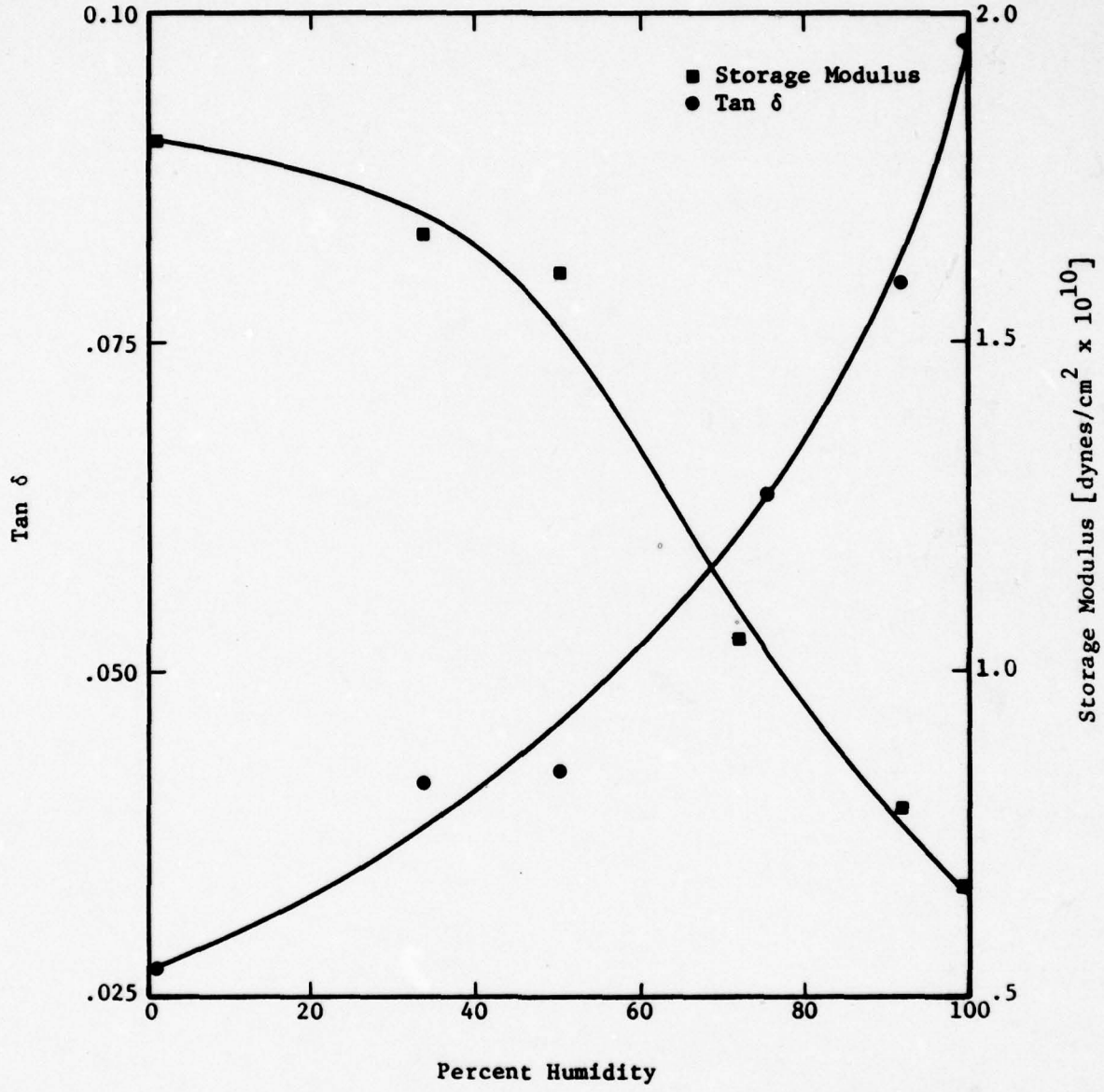

Fig. 3.2.5. Dynamic mechanical properties of paint System II (VR2) as a function of relative humidity at 22°C and 11 Hz.

at 100% relative humidity conditions was found to be less than one-half that of the dry sample.

Infrared Spectroscopy

The two infrared spectra obtained for VR2 are given as Fig. B-1 and Fig. B-2 in Appendix B. The spectrum given in Fig. B-1 was obtained from a sample prepared as a solvent-cast free film, while the spectrum in Fig. B-2 was obtained from a disc prepared by dispersing the polymer powder as supplied by Union Carbide Corporation in a KBr powder. The one-to-one peak correspondence between these two spectra indicates that little or no residual solvent remains in the free film after drying.

These spectra were found to be in excellent agreement with spectra published by Haslam et al., (6) and Hummel (8) for polyvinyl butyral. All of these spectra are characterized by two rather broad bands of high inensity at 1000 and 1140 cm^{-1}. These absorptions are characteristic of the ether structure (C-O-C) in this polymer. The presence of residual polyvinyl acetate groups is usually indicated by a weak carbonyl absorption together with a 1243 cm^{-1} absorption band (6). The lack of the carbonyl absorption is indicative of the low polyvinyl acetate content suggested by Newey and Busso (1). The approximately 20% polyvinyl alcohol content in this polymer is characterized by the broad OH stretching peak observed at 3440 cm^{-1} in these spectra. Elliot (27) and Hennicker (9) have discussed the effect of hydrogen bonding on the OH stretching, as to shift its absorption frequency from the 3550-3650 range to the 3350-3450 range. The exact location of this peak depends, in addition to the extent of hydrogen bonding, on the properties of the solvent, which in this case is the polymer. It is concluded that the OH groups in this polymer are almost completely involved in hydrogen bonding.

Another characteristic of the polyvinyl butyral spectrum is a very broad and intense absorption band which covers the 350-700 cm^{-1} range (see Fig. B-1). This band has been attributed to the overlap of a sequence of strong absorption bands due to the in-plane and out-of-plane C-O-C bending vibrations (8).

The infrared spectrum has been used by other investigators to monitor the degradation of polyvinyl butyral due to the action of gamma radiation in the presence of oxygen by observing the formation of carbonyl groups (9).

Ultraviolet Spectroscopy

The ultraviolet spectrum obtained for Paint System II (VR2) is given as Fig. C-1 in Appendix C. Further analysis of this spectrum is still required.

System III (VR3)

Vinyl resin VR3 is a random copolymer, consisting of 91% vinyl chloride, 3% vinyl acetate and 6% vinyl alcohol by weight, which has been plasticized with 9.5% by weight tricreysl phosphate (TCP) (1). Even though approximately 9 out of every 10 repeat units in the copolymer is a vinyl chloride, the copolymerization with vinyl acetate and vinyl alcohol alters the polymer properties from those expected for 100% PVC in a number of significant ways. Two such effects are that the increased irregularity in the chain decreases the crystallinity, and the acetate side groups result in the polymer being somewhat less polar (13).

The effect of the copolymer composition on the Tg in this resin is less clear than in the case of VR2. The Tg's of the corresponding homopolymers which make up the VR3 copolymer are 32°C for polyvinyl acetate (PVAc) (19, 29), 80°C for polyvinyl chloride and 85°C for polyvinyl alcohol (PVOH) (19). According to the rules for the effect of composition on the Tg of a random copolymer, given in Appendix A, the resulting Tg should be increased due to the PVOH content and decreased due to the PVAc content from the 100% PVC value. Extension of equation A2 in Appendix A to three components predicts the resulting Tg to be 78.6°C.

The plasticizer, tricreysl phosphate (TCP), is a liquid added to the polymer to improve its flow properties and decrease the brittleness. The use of plasticizers with polyvinyl chloride type polymers, which are generally hard, brittle, glass-like solids, to obtain a polymer with the properties of a soft, flexible and tough material is a common commercial

practice (28). The plasticizer brings about these property changes by dissolving in the polymer and lowering its glass transition temperature. For practical reasons, the plasticizer must be compatible with the polymer and relatively nonvolatile. For these reasons, they are usually liquids with molecular weights in the hundreds. TCP, whose formula is $(CH_3C_6H_4O)_3PO$, has a molecular weight of 368. The depression of the Tg by the addition of a diluent such as TCP, can be approximated by the following linear function for low TCP concentrations (19):

$$Tg = Tg' - KW_1 \tag{6}$$

where W_1 is the weight fraction diluent, Tg' is the glass transition of the nonplasticized polymer, and K is a coefficient which is dependent on both the polymer and diluent (19). Similar linear relations as a function of volume fraction plasticizer have also been proposed (20). The effect of plasticizer on dynamic mechanical data results in lowering the temperature of maximum damping (tan δ) and broadening the transition region.

Dynamic Mechanical

The dynamic mechanical data for VR3 was obtained at 11 Hz and is given in Fig. 3.2.6. A large relaxation denoted by α was observed in the tan δ vs temperature curve. The α relaxation was assigned as the material's glass transition by comparison to the results of other investigators (15, 19, 30).

To determine the properties of the copolymer resin and the compositional effects of the TCP plasticizer, two special composition samples having 0% and 17.2% TCP by weight were made. The dynamic mechanical properties of these samples were obtained at 11 Hz and are plotted in Fig. 3.2.7 including the results given in Fig. 3.2.6 for comparison. For all three compositions the large relaxation observed corresponds to the material's glass transition. The effect of increased TCP content was observed to broaden and shift this relaxation (the glass transition) to lower temperatures. This shift of the material's glass transition was monitored by the temperature of the maximum in the loss modulus, E", versus temperature curve, since the experimental limits of the Rheovibron prevented determination of

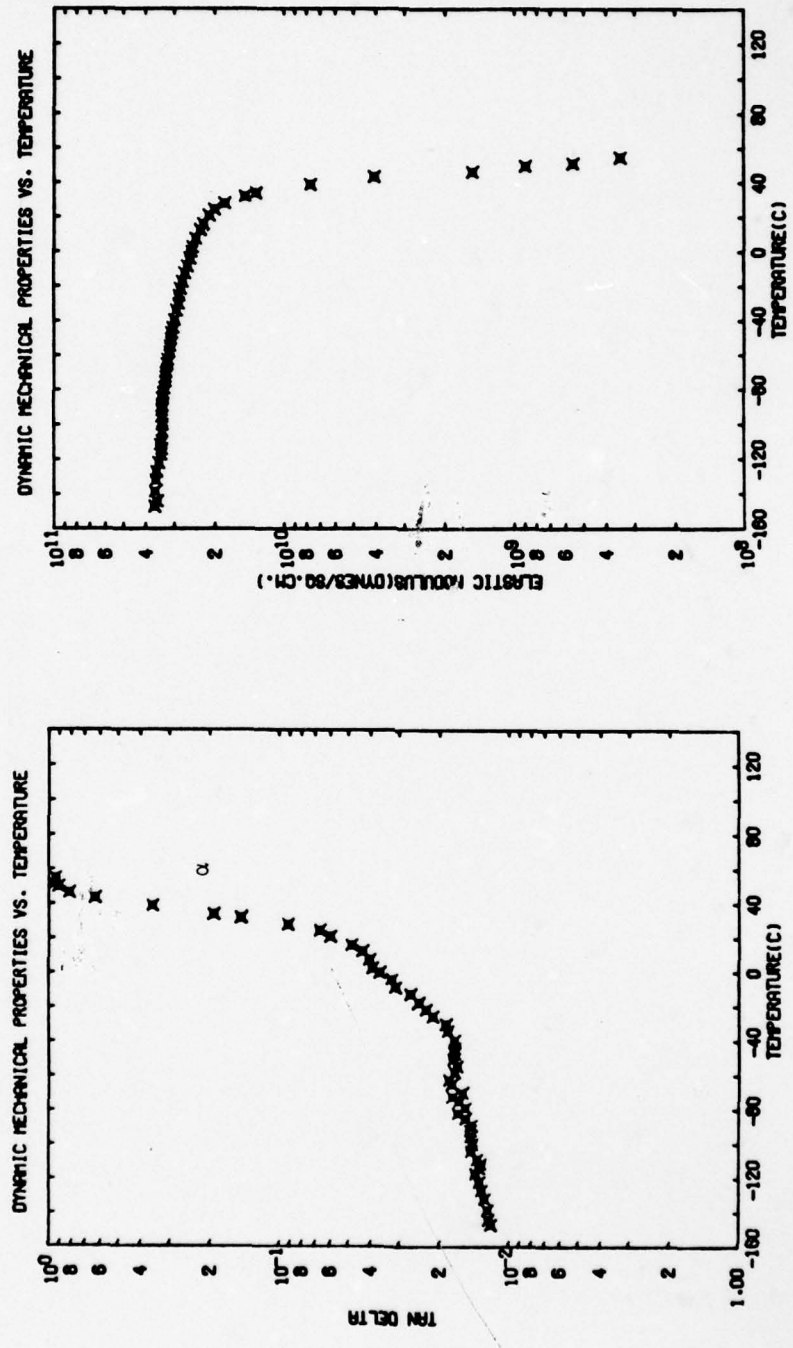

Fig. 3.2.6. Dynamic mechanical properties of paint System III (VR3) as a function of temperature at 11 Hz.

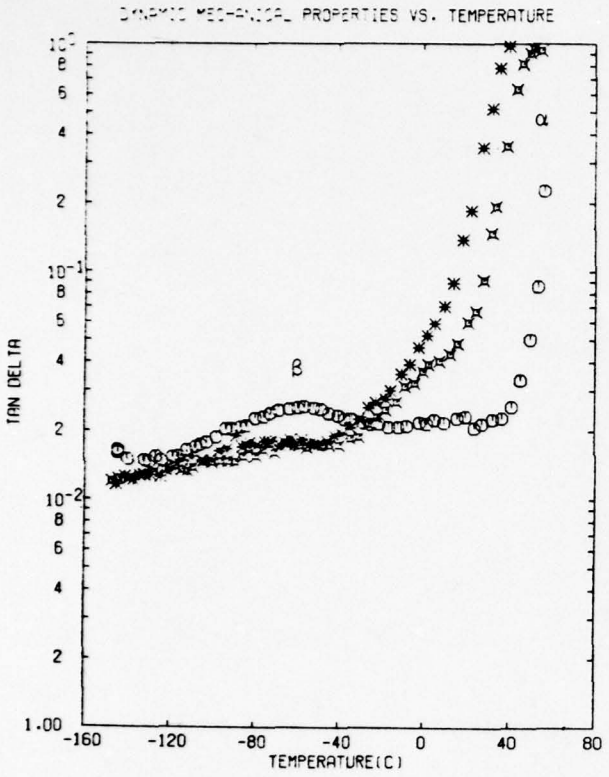

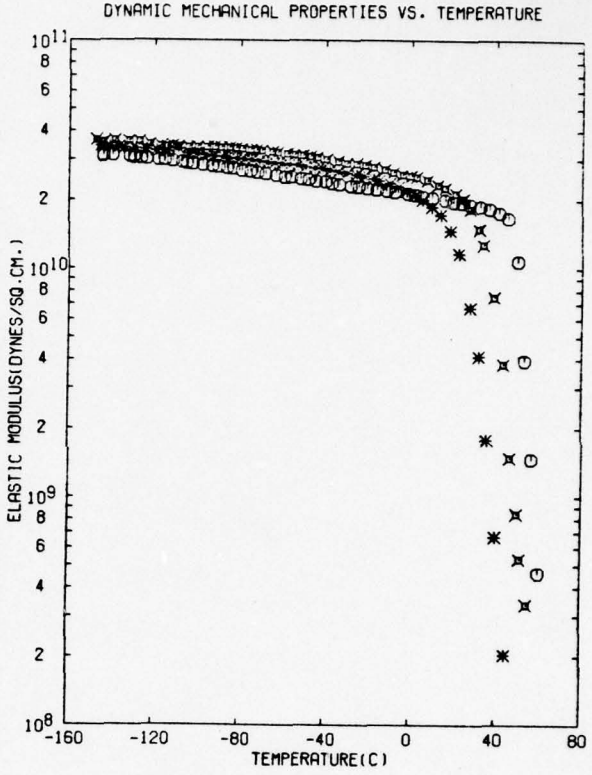

Fig. 3.2.7. Dynamic mechanical properties of paint System III (VR3) and two special paints as a function of temperature at 11 Hz. The weight percent TCP of these paints are as follows; ⓞ 0%, ⋈ 9.5%, and ✱ 17.2%.

the maximum in the tan δ versus temperature curve. In Fig. 3.2.8 the temperature of the maximum in the loss modulus is plotted against the weight fraction TCP. The linear dependence of Tg with weight fraction TCP suggested by Eq. 6 is seen to correlate over the concentration range investigated.

A second relaxation denoted by β was observed at -56°C in the tan δ versus temperature curve, obtained for the unplasticized resin. A similar relaxation has been observed at -50°C at 1 Hz for the polyvinyl chloride homopolymer (31). A number of mechanisms have been proposed for the β relaxation (32), including a crank shaft motion of the main chain. As can be seen in Fig. 3.2.7, the addition of TCP plasticizer resulted in the β relaxation being completely damped out. This is consistent with the observations of Pezzin (31), who reported complete elimination of the β relaxation peak with the addition of 12 parts diethylhexyl phthalate plasticizer per hundred parts polyvinyl chloride.

The effects of moisture on the dynamic mechanical properties of VR3 were measured at 25°C, and the results are presented in Fig. 3.2.9. Only slight plasticization of this resin with increased relative humidity was observed. This plasticization resulted in a small increase in tan δ, and the modulus measured at 100% humidity was 87% of the 0% humidity value.

Infrared Spectroscopy

To analyze the structure of the copolymer resin used in VR3, two spectra of the unplasticized composition were run. These spectra are given as Figs. B-3 and B-4 in Appendix B. The spectrum given as Fig. B-3 was obtained from the special sample containing 0% TCP by weight prepared as a solvent-cast free film. The spectrum given in Fig. B-4 was obtained using a sample made by mixing the polymer powder as supplied by Aldrich Chemical Co., Inc., with KBr powder and pressing into a disc.

Close comparison of these two spectra shows a number of differences. Firstly, even though the hydroxyl group absorption was split into two peaks, one at 3560 and the second at 3440 cm^{-1} in both spectra the relative intensities were not the same. In the case of the KBr disc the

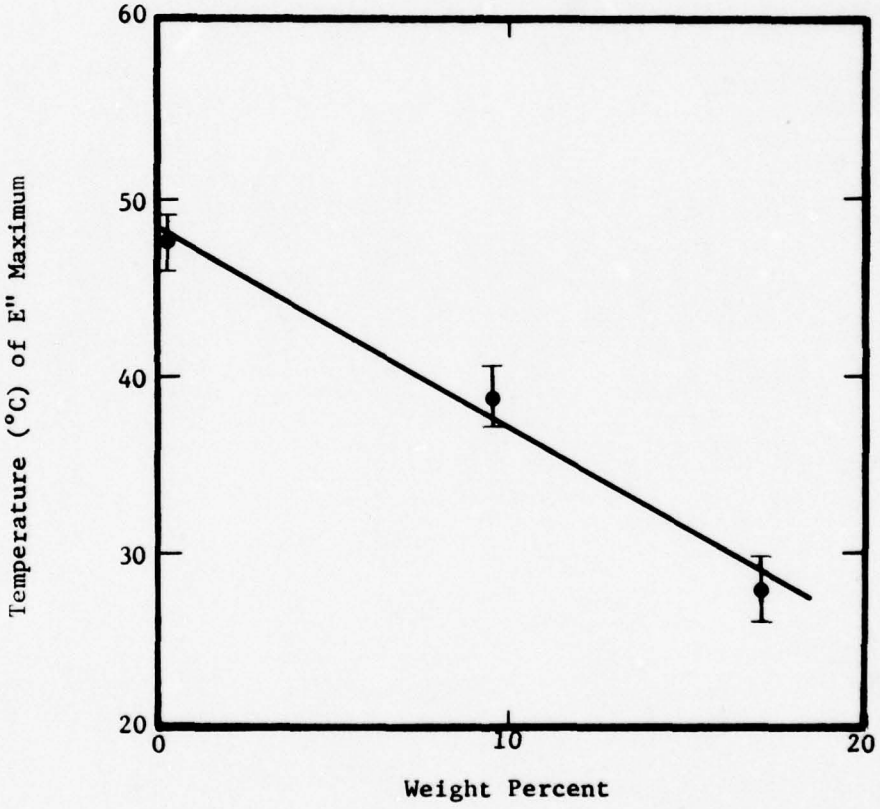

Fig. 3.2.8. The temperature of the maximum in the loss modulus vs temperature curve obtained at 11 Hz are given as a function of weight percent TCP plasticizer.

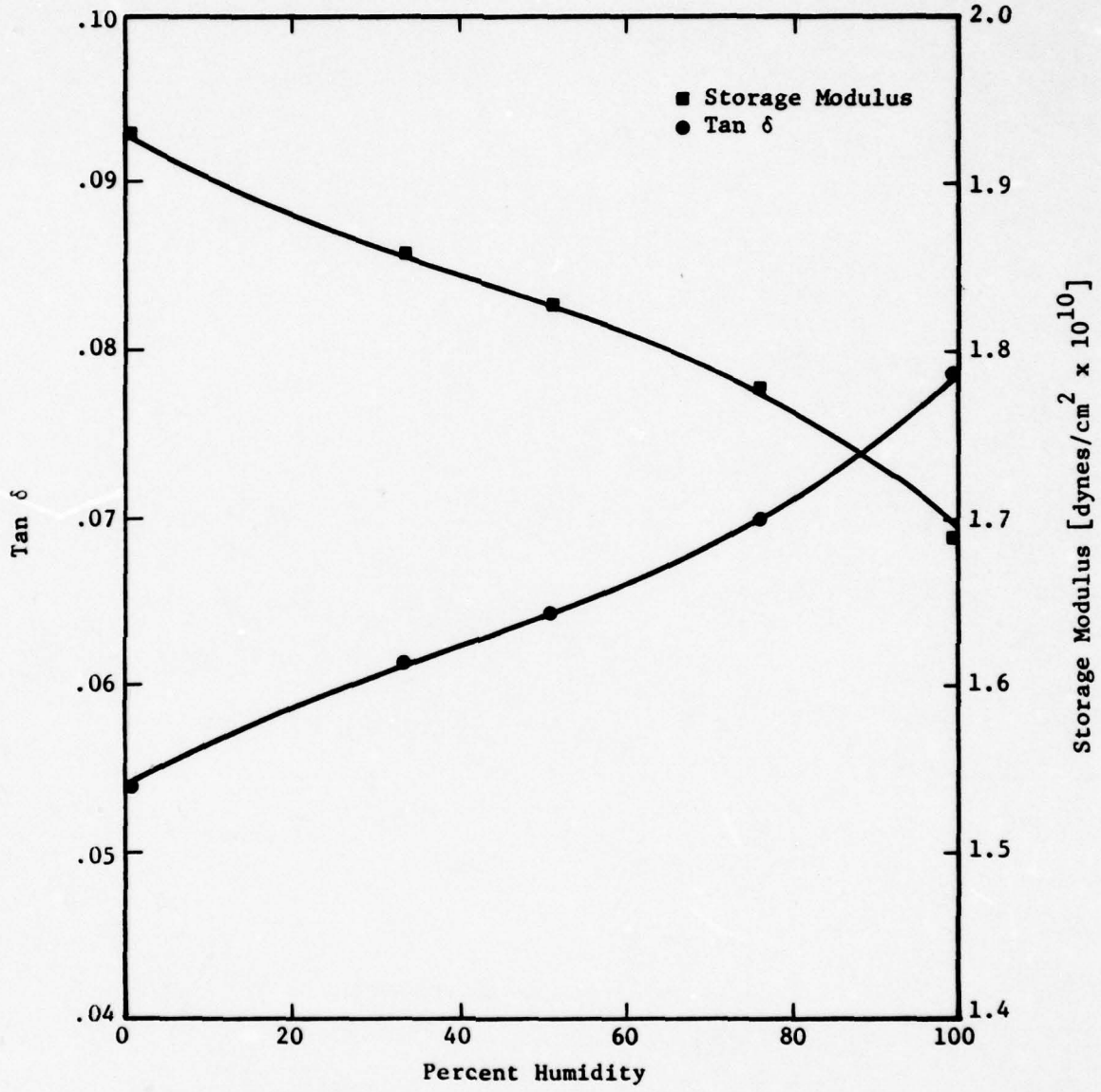

Fig. 3.2.9. Dynamic mechanical properties of paint System III (VR3) as a function of percent relative humidity at 25°C and 11 Hz.

3560 cm^{-1} absorption was greater than the 3440 cm^{-1} absorption, while for the solvent-cast sample the opposite was observed (see Figs. B-3 and B-4). Specifically, the ratio of the absorption at 3440 cm^{-1} (A_{3440}) and that at 3560 cm^{-1} (A_{3560}) were .87 for the KBr disc sample and 1.20 for the solvent-cast free film. From the discussion given in the infrared section for VR2, the absorption at 3560 cm^{-1} was attributed to the stretching of nonhydrogen bonded OH groups, while the 3440 cm^{-1} absorption was attributed to the stretching of hydrogen bonded OH groups. This result indicates increased hydrogen bonding of the OH groups in the solvent-cast film.

A second difference was observed in the 1700-1740 cm^{-1} carbonyl absorption band region. In the solvent-cast film spectrum, this absorption band was split into two peaks, one at 1731 cm^{-1} and a second at 1701 cm^{-1}, while in the KBr disc sample only a single peak at 1735 cm^{-1} was observed. The discussion by Hennicker (9) suggests that an absorption at 1742 cm^{-1} is due to the stretching mode of a nonhydrogen bonded carbonyl group, while an absorption at 1700 cm^{-1} is due to the stretching mode of a hydrogen bonded carbonyl group. West and Cooper (33) observed this peak splitting in a polyurethane system, with the hydrogen bonded and nonhydrogen bonded peaks being resolved at 1703 cm^{-1} and 1733 cm^{-1} respectively.

The result of this analysis indicates increased hydrogen bonding in the solvent-cast free film, of both the hydroxyl and carbonyl groups compared to that observed in the KBr disc sample. This observation may be in part due to differences in the solvent interaction properties. In the case of the KBr discs the solvent is KBr, while in the solvent-cast films the solvent is the polymer itself. The spectrum observed for the solvent-cast film is therefore more indicative of the polymer's structure.

A comparison to a vinyl chloride-vinyl acetate copolymer spectrum published by Haslam (6) shows that the presence of the hydroxyl group is indicated by the 3560 and 3440 bands already discussed and an increase in the 1100 cm^{-1} absorbance due to the presence of the C-O band of the secondary alcohol group. Also these spectra are to be compared to the spectrum of a vinyl chloride-vinyl acetate-vinyl alcohol system which has been published (34).

To investigate the effect of the TCP plasticizer on the polymer structure, infrared spectra of the 9.5% and 17.2% by weight composition films were taken, and the results are given as Figs. B-5 and B-6 respectively. A spectrum on the TCP plasticizer is given as Fig. B-7 to help with the identification of changes in these spectra due to the plasticizer. This spectrum compares well with the results of Hummel (8).

Direct comparison of the infrared spectrum with and without plasticizer allowed the identification of six distinct peaks due to the plasticizer in the polymer resin. These peaks may be used to monitor changes in the plasticizer composition among other things. The frequencies of these absorption peaks are approximately 778, 1140, 1481, 1498, 1580, and 1603 cm^{-1}.

In Fig. 3.2.10 the ratio of the absorbance to the sample thickness is plotted against the TCP concentration (units of g/liter), for the 1580 and 1603 cm^{-1} bands. The TCP concentration was obtained using a density of 1.4 g/cm^3 (12) for the copolymer and 1.17 g/cm^3 for the TCP plasticizer, and assuming that the volumes are additive. From the slopes of the lines given in Fig. 3.2.10, the molar extinction coefficient $\varepsilon(cm^2/g \times 10^5)$ was determined using Eq. 3 to be 2.87 ± .25 for the 1580 cm^{-1} band and 2.37 ± .08 for the 1603 cm^{-1} band.

The effect of the TCP plasticizer on the hydrogen bonding in this polymer is given in Fig. 3.2.11, where the ratio of the 3440 and 3560 cm^{-1} absorbances (A_{3440}/A_{3560}) and the ratio of the 1703 and 1733 cm^{-1} absorbances (A_{1703}/A_{1733}) for the solvent cast films is plotted against weight percent TCP. Recalling the cause of each absorbance, it is readily seen that the increase in the A_{3440}/A_{3560} ratio indicates an increase in the relative hydrogen bonding of the hydroxyl groups. The decrease in the A_{1703}/A_{1733} ratio indicates a decrease in the hydrogen bonding of the carbonyl groups. From this result it was hypothesized that the TCP plasticizer perferentially hydrogen bonds to the hydroxyl groups and as a result breaks bonds between the hydroxyl and carbonyl groups. Further studies of this phenomena are required. In conclusion, information on the composition and structure of the VR3 can be obtained from infrared spectroscopy.

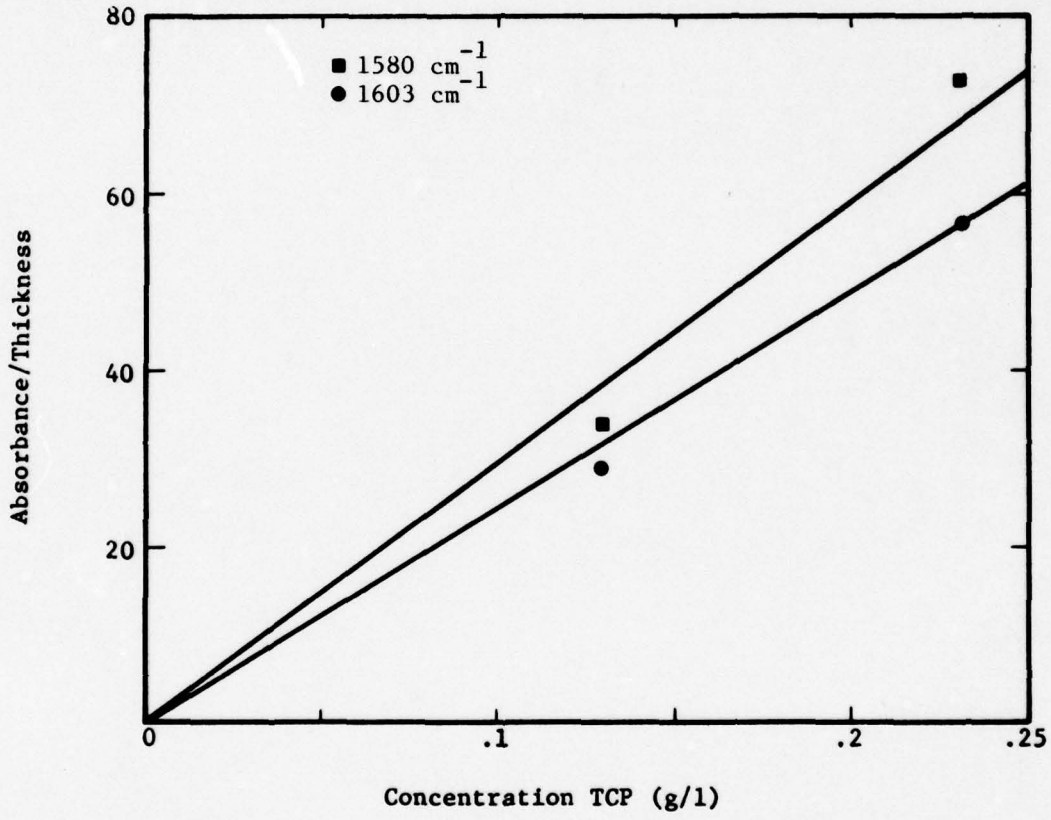

Fig. 3.2.10. The ratio of absorbance to sample thickness versus the concentration of TCP in the copolymer used in paint System III (VR3).

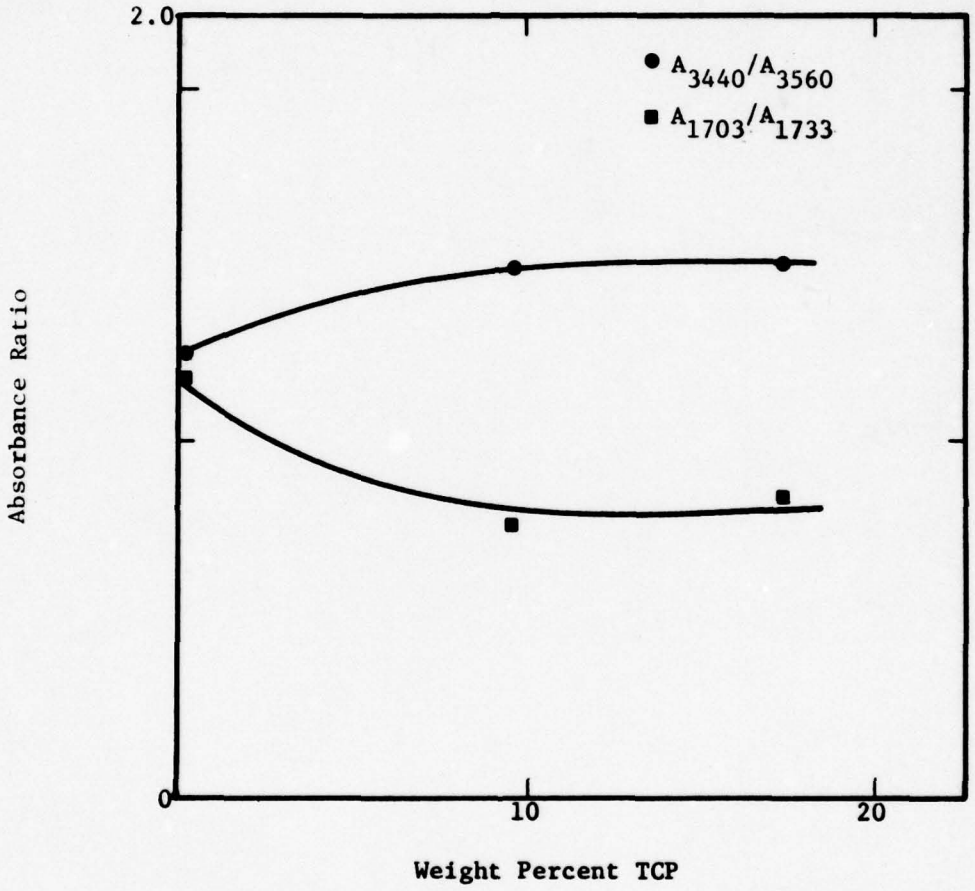

Fig. 3.2.11. The effect of TCP content on hydrogen bonding for paint System III (VR3) monitored by plotting the following absorbance ratios; ● A_{3440}/A_{3560} and ■ A_{1703}/A_{1733}.

Ultraviolet Spectroscopy

The ultraviolet absorbance spectra of the three film compositions are given in Fig. C-2 in Appendix C. The absorbances plotted are on a relative scale and are not absolute. The addition of the TCP plasticizer to the copolymer, results in an absorbance in the 234-285 nm range. Two peaks in this absorbance spectrum are observed at 265 and 272 nm, along with a slight shoulder at 257 nm. This absorbance has been attributed to the benzene ring structure and the phosphate oxygen double bond in the TCP molecule. The benzene ring normally absorbs at a wavelength of 256 nm. This absorbance appears to have been shifted to higher wavelengths by, among other things, the substitution of a methyl group on the benzene ring (10). For comparison, an absorbance spectrum for TCP dissolved in ethanol, which is a window solvent from 205 nm and up, is given as Fig. C-3. The wavelengths of the absorbance peaks were found to be the same as those found for TCP dissolved in the polymer (see Fig. C-3). Additional work is required to obtain a better understanding of the ultra-violet spectrum, which will hopefully lead to an improved understanding of the polymer structure.

System IV (VR4)

This resin system consists of an 86% vinyl chloride and 14% vinyl acetate by weight random copolymer which has been mixed with tricreysl phosphate (TCP) plasticizer and a gum rosin hardener. The final resin composition contains 42% copolymer, 16% TCP plasticizer, and 42% rosin hardener by weight (1).

Copolymerization of PVC with PVAc results in improved flow properties by reducing the regularity of the polymer structure, thus lowering the interaction forces between the chains. As reported by Wyman (35) the copolymerization of vinyl chloride with vinyl acetate also results in a decrease of the glass transition temperature with increasing vinyl acetate content. Recalling that the Tg of these homopolymers are 32°C for polyvinyl acetate and 80°C for polyvinyl chloride, this trend is consistent with the behavior predicted by the relations given in Appendix A. Furthermore, the

copolymerization with polyvinyl acetate results in a polymer with good adhesion properties (11) and an increased solubility in the usual solvents used for lacquers (8).

The dependence of the Tg for a polyvinyl chloride-polyvinyl acetate copolymer on weight percent TCP was studied by Clash and Rynkiewicz (15). They reported that the glass transition temperature decreased linearly with increasing TCP content over the 0-30 weight percent range studied.

Dynamic Mechanical

In Fig. 3.2.12 the dynamic mechanical properties obtained at 11 Hz for VR4 are given. Two relaxation in the tan δ vs temperature curve were observed, and are designated by α and β. The β peak displayed its maximum at -8°C while the maximum of the α peak was not identified as a result of the instrument's limitations. The α peak was attributed to the material's glass transition, by comparison to the result of the other investigators (15, 19, 30). To identify the cause of the β relaxation, the properties of the copolymer resin, and the effects of the rosin hardener and the TCP plasticizer, three special composition paints were made. The compositions of these special paints are as follows: 100% copolymer, the copolymer plasticized with 27.6% by weight TCP, and the copolymer with 50% by weight rosin. In Fig. 3.2.13 the dynamic mechanical spectrum obtained for the copolymer only and the copolymer plasticized with 27.6% by weight TCP are given. In both of these spectra, a single relaxation, attributed to the glass transition, was observed. As was found for VR3 the effect of the plasticizer was to shift the glass transition to a lower temperature. In Fig. 3.2.14 the dynamic mechanical data of the copolymer only and copolymer with 50% rosin by weight are given. The large relaxation denoted by α observed for both polymers is again attributed to the material's glass transition. In the case of the paint system containing 50% by weight rosin, a secondary relaxation denoted by β was observed at 12°C. From these results it was concluded that the β relaxation observed for the VR4 system (see Fig. 3.2.12) was due to an activity in the rosin component of the paint. Further comparison of these spectra shows that the effect of the TCP plasticizer is to shift both the α and β relaxation to lower

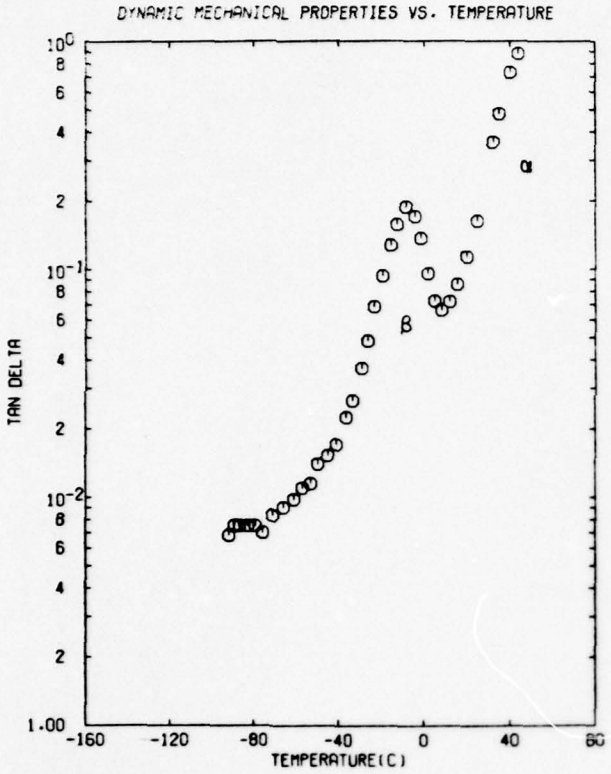

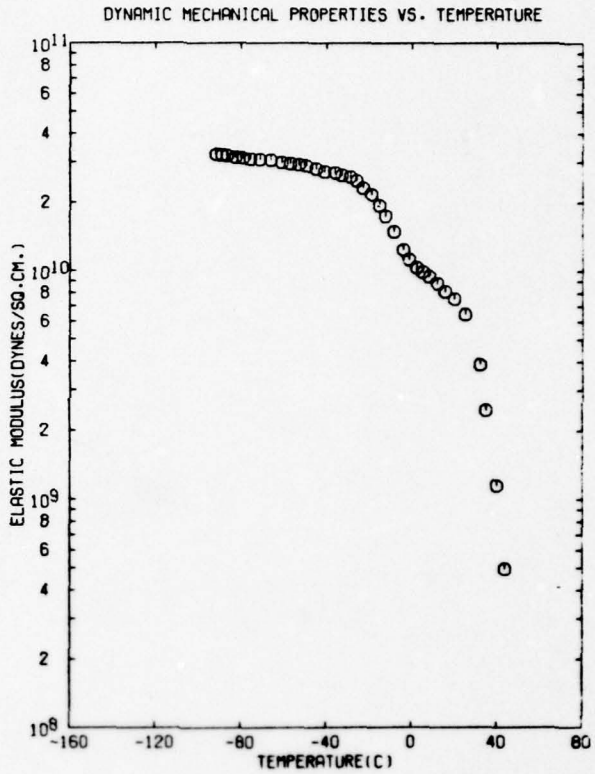

Fig. 3.2.12. Dynamic mechanical properties of paint System IV as a function of temperature at 11 Hz.

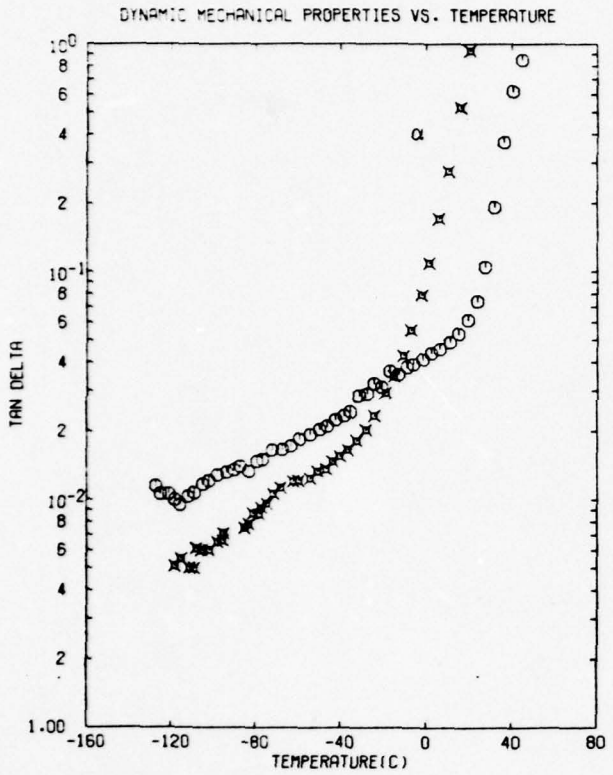

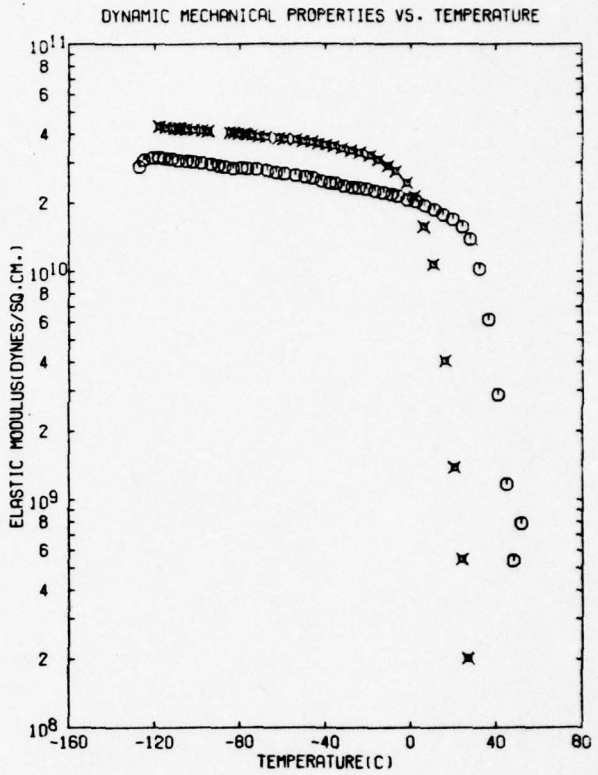

Fig. 3.2.13. Dynamic mechanical properties for two of the special paints made for the study of paint System IV, as a function of temperature at 11 Hz. These systems are; ⊙ the copolymer only, and ✱ the copolymer and 27.6% by weight TCP.

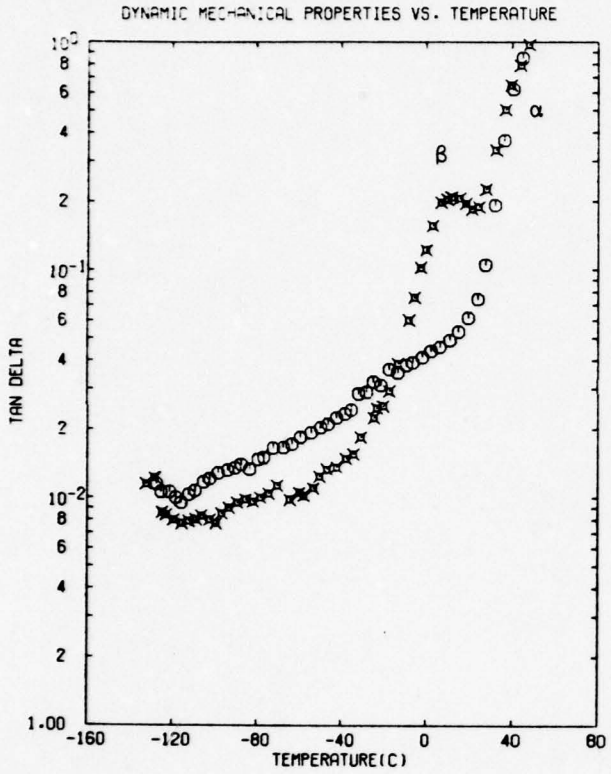

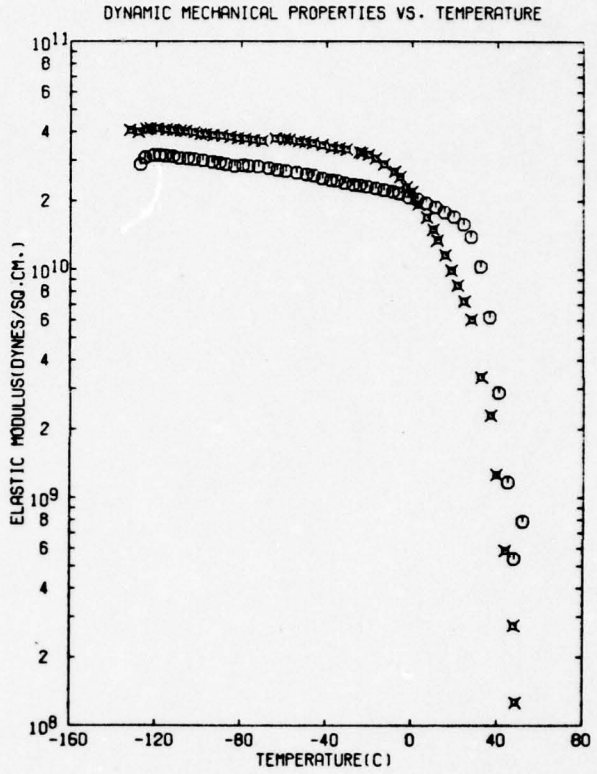

Fig. 3.2.14. Dynamic mechanical properties for two of the special paints made for the study of paint System IV as a function of temperature at 11 Hz. These systems are; ⏲ the copolymer only, and ⌘ the copolymer with 50% by weight rosin.

temperatures. In Fig. 3.2.15 the VR4 paint and the special paint system containing copolymer mixed with 50% rosin are plotted together for comparison. The α relaxation was shifted by $\sim 5^{\circ}C$ by the addition of 16% TCP by weight, while the β peak was shifted by $20^{\circ}C$. This result indicates that the interactions of the TCP plasticizer with the copolymer component are different from those with the rosin component; additional study is required to resolve these differences.

The effect of humidity on the dynamic mechanical properties of both VR4 and the special paint system containing the copolymer with 50% by weight rosin were measured at $22^{\circ}C$. These results are presented as Figs. 3.2.16 and 3.2.17 respectively. The effect of increased humidity on VR4 resulted in decreasing both the modulus and the loss tangent. At first the decrease in the loss tangent with increased humidity seems inconsistent with the effects usually associated with plasticization such as increased chain mobility resulting in an increase in the loss tangent. Upon closer analysis the decrease in the loss tangent was attributed to the shift of the β relaxation to lower temperatures with increased plasticizer content. As shown in Fig. 3.2.15, as the β peak is shifted to lower temperatures, a valley forms between the α and β relaxation. In the temperature range where the valley occurs, a decrease in the loss tangent with increased plasticizer content would be observed. Assuming water plasticizes the material in a similar manner as the TCP plasticizer, the observed decrease in tan δ with increasing humidity can be associated with the plasticizing effect of water. The decrease of the modulus observed was moderate with the 100% relative humidity value being 80% of the 0% humidity value. This behavior is also associated with the plasticizing effect of water in the polymer.

For the copolymer containing 50% rosin by weight (see Fig. 3.2.17) the loss tangent was observed to pass through a maximum with increasing relative humidity while the modulus measured at 100% humidity was 50% of the value obtained at 0% humidity conditions. The decrease in loss tangent with increasing humidity at high relative humidities can be explained in the same way the results for VR4 (see Fig. 3.2.16) were explained. The increase of the loss tangent with increasing humidities at low humidity conditions is not fully understood.

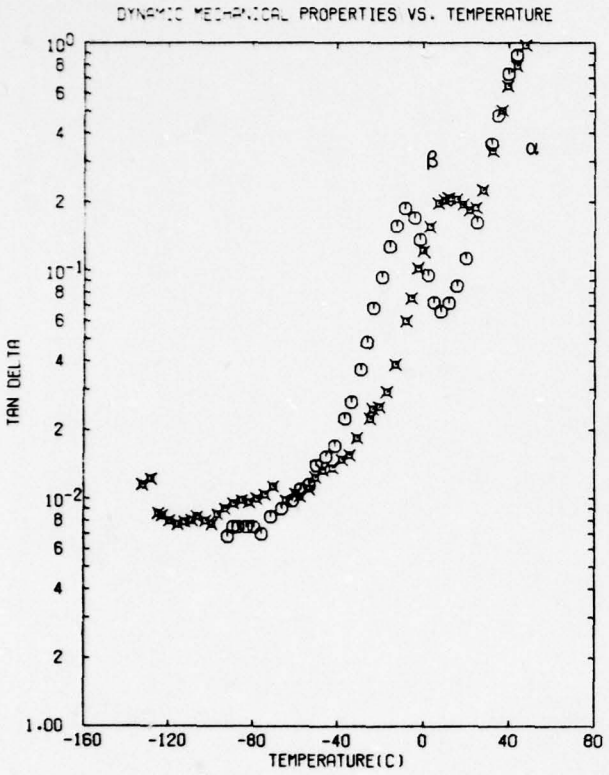

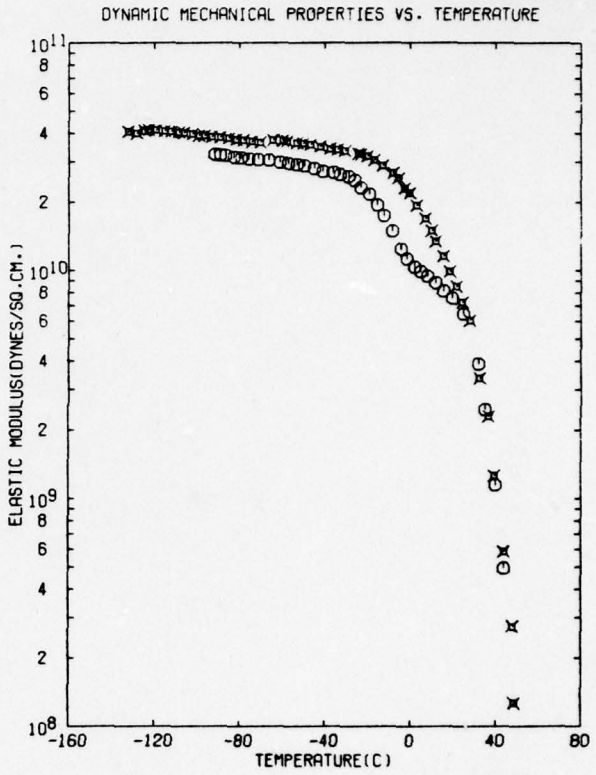

Fig. 3.2.15. Dynamic mechanical properties for paint System IV Φ and the special paint containing copolymer and ⋈ 50% by weight rosin as a function of temperature at 11 Hz.

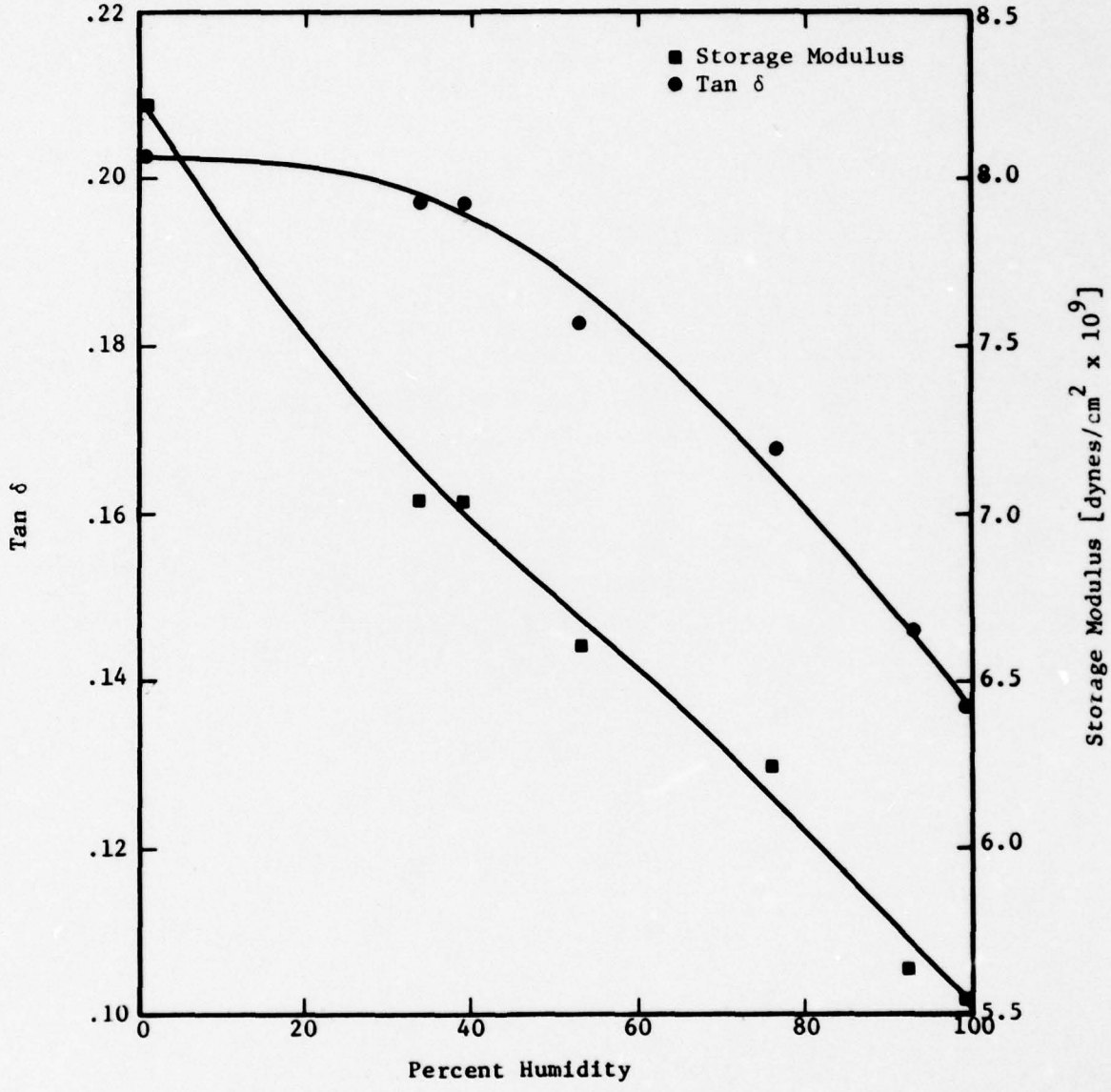

Fig. 3.2.16. Dynamic mechanical properties of paint System IV as a function of relative humidity at 22°C and 11 Hz.

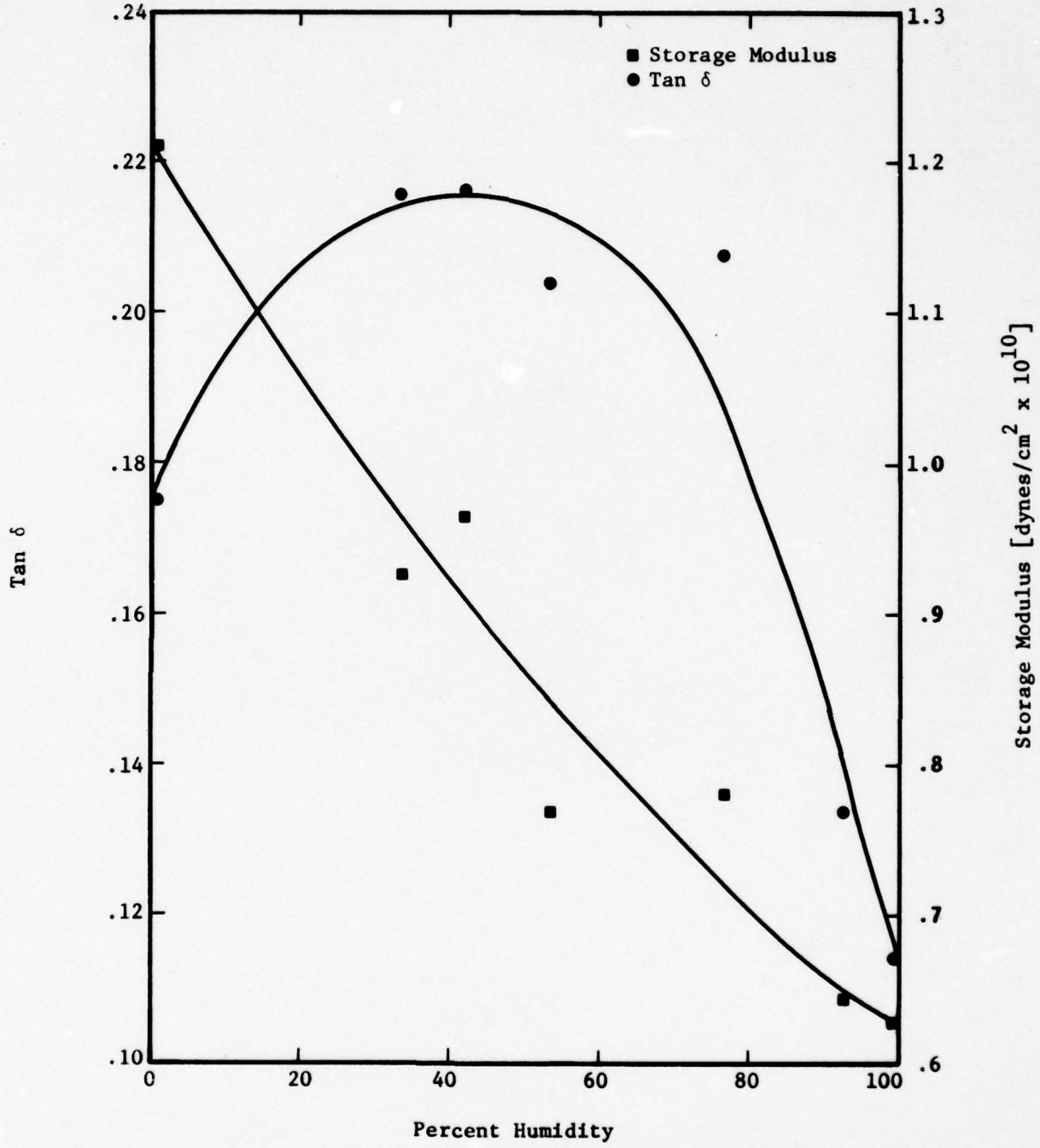

Fig. 3.2.17. Dynamic mechanical properties of the special paint containing copolymer and 50% rosin by weight is given as a function of percent relative humidity at 11 Hz and 22°C.

It is proposed that the rosin be treated as a filler in future work. A discussion on modeling fillers is given in Appendix D.

Infrared Spectroscopy

Two spectra of the copolymer in this resin were obtained and are given as Figs. B-8 and B-9 in Appendix B. The spectrum given in Fig. B-8 was taken on a solvent-cast film sample, while the spectrum given as Fig. B-9 was obtained from a KBr sample made from the resin powder supplied by Union Carbide Corporation. Comparison of these spectra to each other showed no marked differences.

The spectrum of the vinyl acetate-vinyl chloride copolymer is straight-forward, because the major bands of both the polyvinyl chloride and vinyl acetate are evident in the copolymer spectrum. This copolymer system is usually identified by the strong vinyl acetate bands occuring at approximately 1026, 1212, 1379, and 1739 cm^{-1} and a strong vinyl chloride absorption at 615 cm^{-1}. Visual comparison of these spectra to a series of spectra presented by Haslam (6) for different vinyl acetate vinyl chloride content was made. The spectra obtained in this work compared well to the spectrum he presented for 16% vinyl acetate content.

The composition of a vinyl acetate-vinyl chloride copolymer can be accurately determined by infrared spectroscopy by a number of quantitative methods. The methods frequently used involve measurement of the 1730-1740 cm^{-1} absorbance. Also according to Haslam measurement of the 4651 cm^{-1} absorbance gives an accurate determination of the acetate content. Haslam also states that measurement of the 6135 cm^{-1} absorbance can be used to determine the free acetate monomer content present in the polymer. At this time the infrared spectrometers available to us do not measure in this frequency range of the spectrum. Hennicker (9) presented a calibration curve for the ratio of the 1730 and 1435 cm^{-1} absorbance against percent vinyl acetate content. This calibration curve is presented as Fig. 3.2.18 along with the result obtained from the spectra of the solvent-cast film presented in Fig. B-8. An absorbance ratio of 2.74 was obtained which corresponds to 15% vinyl acetate content. The 15% and 16% vinyl acetate

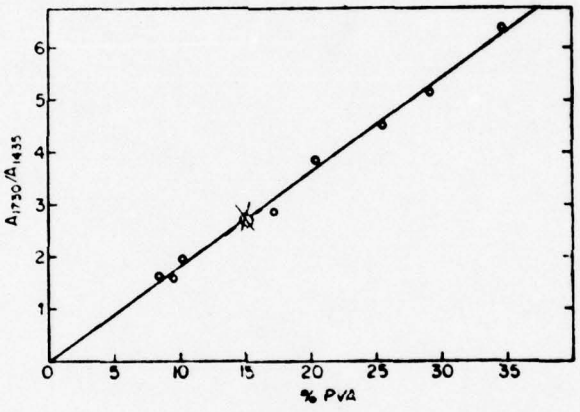

Fig. 3.2.18. Calibration curve for the determination of polyvinyl acetate in p.v.c.-p.v.a. copolymers. The absorbance ratio of C=O to CH_2 is plotted against concentration of p.v.a. (9). ⊠ The results from this work are plotted for comparison.

contents determined using these two methods discussed are in close agreement with the 14% vinyl acetate content suggested by Newey and Busso (1).

In Fig. B-10 the infrared spectrum obtained for the rosin hardener prepared as a KBr disc sample is presented. Hummel (8) has given an infrared absorption spectrum obtained for the same type of rosin along with a discussion of some of the characteristic absorption peaks. The spectrum obtained in this work compared well with the spectrum he presented. The hydroxyl stretching was observed at 3420 cm^{-1} and the carbonyl absorption was obtained at 1690 cm^{-1}. Absorption at these frequencies suggest that these groups are hydrogen bonded.

In Fig. B-11 the infrared spectrum of the copolymer plasticized with 27.6% by weight TCP is given. A thinner sample having the same composition is required to obtain better resolution of the 900-1400 cm^{-1} range of the spectrum. Three absorption peaks were observed in this spectrum which identifies the presence of the TCP plasticizer in the paint. The absorbance peaks occur at 1610, 1588, and 778 cm^{-1}. As was the case for VR3, these peaks can be used to monitor the plasticizer content in the paint film. The carbonyl absorption was observed at 1740 cm^{-1} indicating that little or no hydrogen bonding occurs as a result of the addition of the TCP plasticizer to the copolymer resin.

In Fig. B-12 a spectrum obtained on the copolymer mixed with 20% by weight rosin hardener is given. The split in the carbonyl absorption into peaks at 1703 and at 1745 cm^{-1} was attributed to the presence of hydrogen bonded and unbonded carbonyl groups.

In Fig. B-13 the spectrum for the copolymer containing 50% rosin by weight is given, while in Fig. B-14 the spectrum for the normal VR4 composition is given. The resolution of these spectra is poor due to the strong absorbance of the rosin peaks. To improve the resolution, thinner films of both samples need to be run.

Ultraviolet Spectroscopy

In Fig. C-4, given in Appendix C, the spectra for the copolymer only,

the copolymer with 27.6% by weight TCP plasticizer and the normal VR4 composition are given. The spectrum of the copolymer only, has a slight absorption in the 260-280 nm wavelength range. This absorption is characterized by three peaks occurring at 268, 272, and 275 nm and has been associated with the carbonyl groups in the polyvinyl acetate unit since carbonyl is known to absorb in the 270-300 nm range (10). The addition of TCP plasticizer resulted in an absorbance in the 230-290 nm range. The three peaks observed for the TCP plasticizer in ethanol (see Fig. C-3) have become one broad absorption due to the additional absorption of the carbonyl groups in the copolymer. The normal VR4 spectrum resulted in one broad absorption from which no information on the rosin hardener component or the TCP plasticizer could be obtained.

In Fig. C-5 in Appendix C, the spectra of the rosin hardener in ethanol and the copolymer containing 20% rosin by weight are given. The rosin hardener is characterized by three absorption peaks, occurring at the 235, 243, and 252 nm and a shoulder observed over the 260-300 nm wavelength range. The absorption peaks correspond to the unsaturated ring structure in the rosin (10). The shoulder was associated with the carbonyl in the carboxylic acid group in the rosin. The absorbance spectrum obtained for the copolymer film containing 20% by weight rosin displays the same three peaks at approximately the same wavelength as were observed for the rosin in the ethanol solvent. Further analysis of these spectra is still required.

3.2.3 Polyurethane Systems VII and VIII

Two polyurethanes were studied in this work. The first was a commercial paint manufactured by Desoto Inc., and has been designated as System VIII, or O PUR. The composition of this paint is not known. The second paint, designated as System VII, or N PUR, was made in-house and its composition was given by Newey and Busso (1). The major components of this paint are a linear polyester prepolymer which is coupled through urethane linkages with an isocyanate buiret to form a cross-linked block copolymer. The mechanical properties of a polyurethane are the result of the degree of cross-linking, segmental flexibility, chain entaglements,

segmental campatibility, Van der Waals forces, and hydrogen bonding (36). The incompatibility of the segments in the polyurethane structure have been observed in many cases to result in the formation of domain structures (37, 38). Many of the mechanical properties observed in polyurethanes have been associated with this phase separation. Hydrogen bonding and other secondary attractive forces contribute largely to the mechanical properties of polyurethanes. For this reason the mechanical properties are very dependent on temperature. Specifically, increased temperature results in the rapid deterioration of mechanical properties, due to the breakage of hydrogen bonds and other secondary bonds (39). In general, coatings based on polyurethane have very good resistance to abrasion and solvent attack, along with good flexibility and impact resistance (3, 40). Additional information on polyurethane systems can be obtained elsewhere (12, 41).

Dynamic Mechanical

The 11 Hz dynamic mechanical properties for systems VIII and VII are given in Figs. 3.2.19 and 3.2.20, respectively. Four relaxations labeled α, β', β, and γ were observed in the loss tangent versus temperature curve for both of these paints. The temperature location of the maximum of these peaks is given in Table 3.2.3. By comparison to the work of Jacobs and Jenckel (42, 43) given in Fig. 3.2.21a, the α, β, and δ relaxations were identified as follows: the α relaxation is the glass transition, the γ relaxation has been associated with motions of the CH_2 sequences in isocyanate segment, and the β relaxation is associated with the effects of absorbed water in the films. The effect of moisture on the dynamic mechanical spectrum was investigated in detail by Jacobs and Jenckel (43) and their results are summarized in Fig. 3.2.21b. As shown, the effect of increased water content is to increase the β transition while shifting its maximum to lower temperature. The γ transition is decreased in magnitude and shifted to lower temperature with increased moisture content. Correlations have been obtained between these kinds of shifts and moisture content for other materials (44), thus making dynamic mechanical measurements a useful means for determining the effect of moisture.

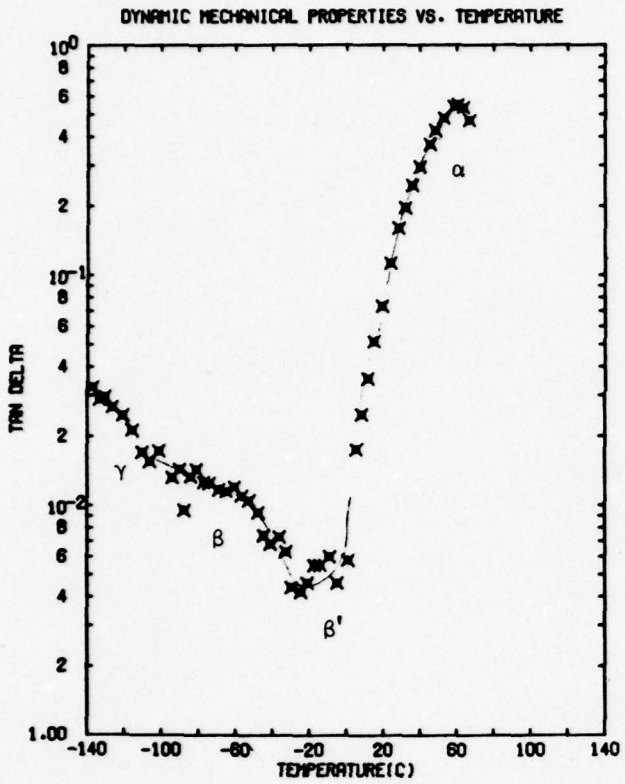

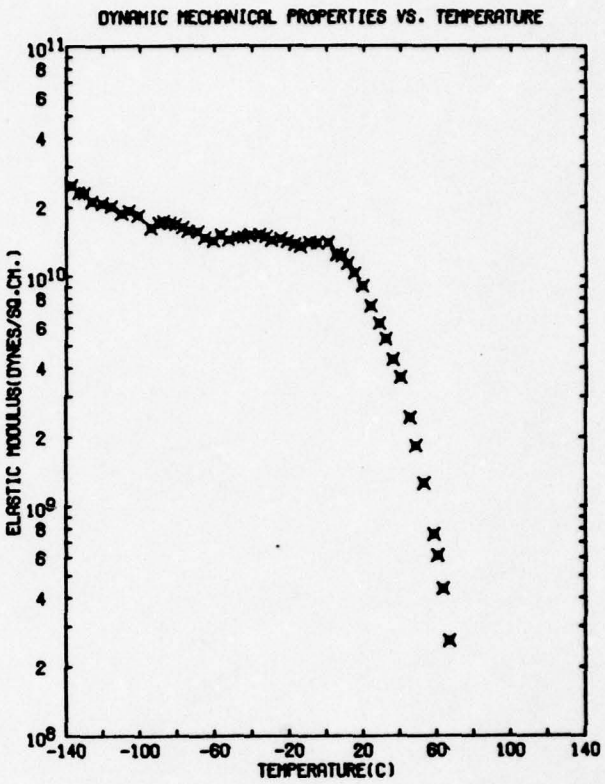

Fig. 3.2.19. Dynamic mechanical properties of paint System VIII as a function of temperature at 11 Hz.

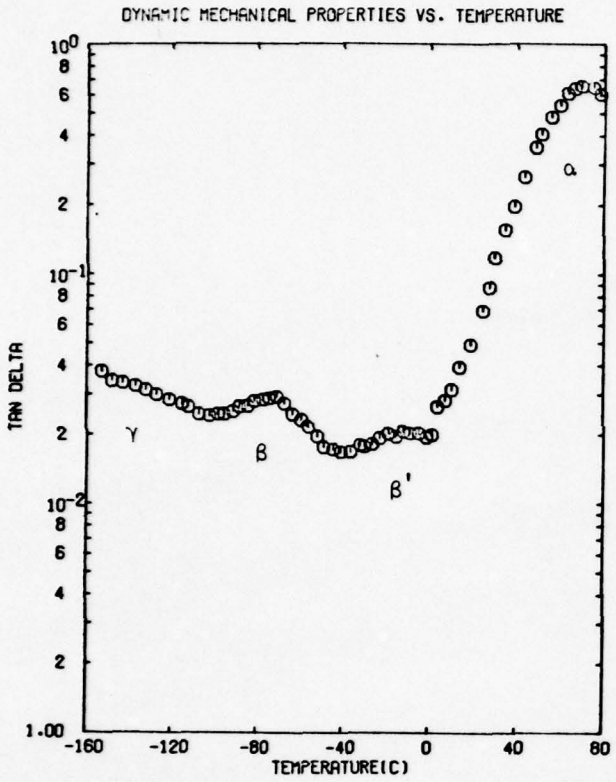

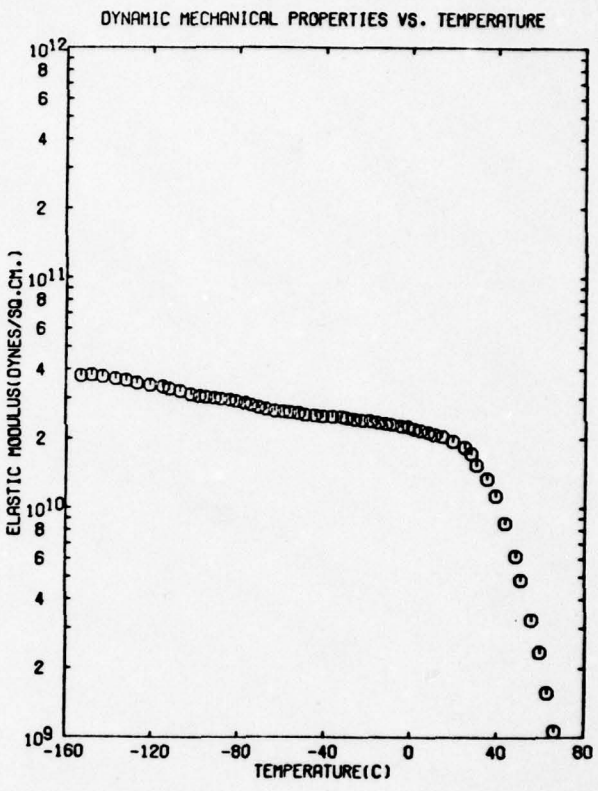

Fig. 3.2.20. Dynamic mechanical properties of paint System VII as a function of temperature at 11 Hz.

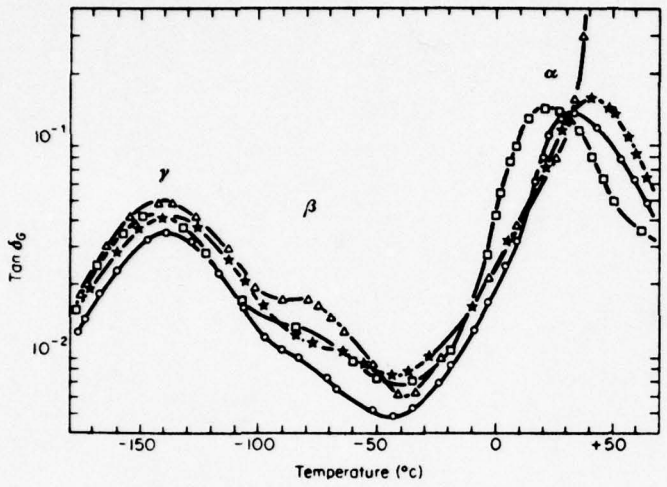

Fig. 3.2.21a. Temperature dependence of tan δ_G at 1 c/s for polyurethanes prepared from hexamethylene diisocyanate and, respectively, 1,4-butanediol (★), 2,5-hexanediol (△), 1,6-hexanediol (○) and 1,10-decanediol (□) (42).

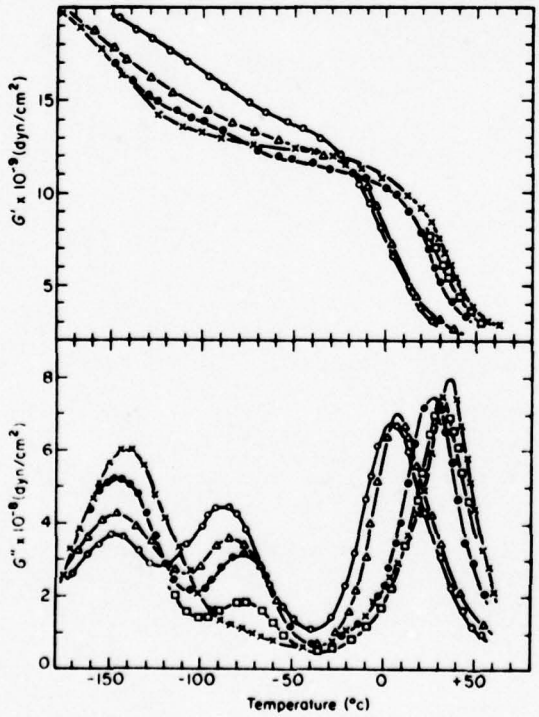

Fig. 3.2.21b. Temperature dependence of G' and G'' at 1 c/s for polyurethane prepared from 1,4-butanediol and 1,6-hexamethylene diisocyanate. Water contents as follows: (x) 0, (□) 3·7, (●) 5·6, (△) 24·5 and (○) 28·8 mole % (43).

The effect of humidity was measured on both polyurethane paints at 22°C. The results are presented in Fig. 3.2.22 for System VIII and in Fig. 3.2.23 for System VII. The modulus was observed to decrease substantially with increased humidity for both systems. In the case of paint System VIII, the 100% relative humidity modulus was 17% of the 0% humidity value, while for System VII it was found to be 40% of the 0% humidity value. This large decrease in modulus is attributed to the breakage of hydrogen bonds by the absorbed moisture, which lessens the interactive attraction forces in these paints. Since the mechanical properties in these paints are strongly dependent on hydrogen bonding, absorbed moisture has a significant effect on the mechanical properties. The increase in loss tangent with increased moisture content indicates the increased chain mobility which results from the breakage of these hydrogen bonds.

Infrared Spectroscopy

The infrared spectra obtained on paint Systems VIII and VII are given as Figs. B-15 and B-16 in Appendix B, respectively. The poor resolution in these spectra resulted from the use of samples which were too thick. Thinner samples are to be made with the hope of obtaining completely resolved spectra. Nevertheless, information on the hydrogen bonding of the N-H groups in these paints was obtained from the N-H stretch peak observed at aoproximately 3370 cm^{-1} in both spectra. According to Hennecker (9), the unbonded N-H stretch absorption occurs at approximately 3450 cm^{-1} while bonded N-H stretch adsorption is at 3300 cm^{-1}. It was concluded from this result that there is extensive hydrogen bonding in these urethane systems.

The infrared has found extensive use for the analysis of various polyurethanes (45, 46) by other investigators. These investigations indicate the usefulness of continued IR work on these paint systems.

Ultraviolet Spectroscopy

As was the case for the infrared, the samples available were too thick to obtain good resolution of the UV absorbance spectrum. Absorption

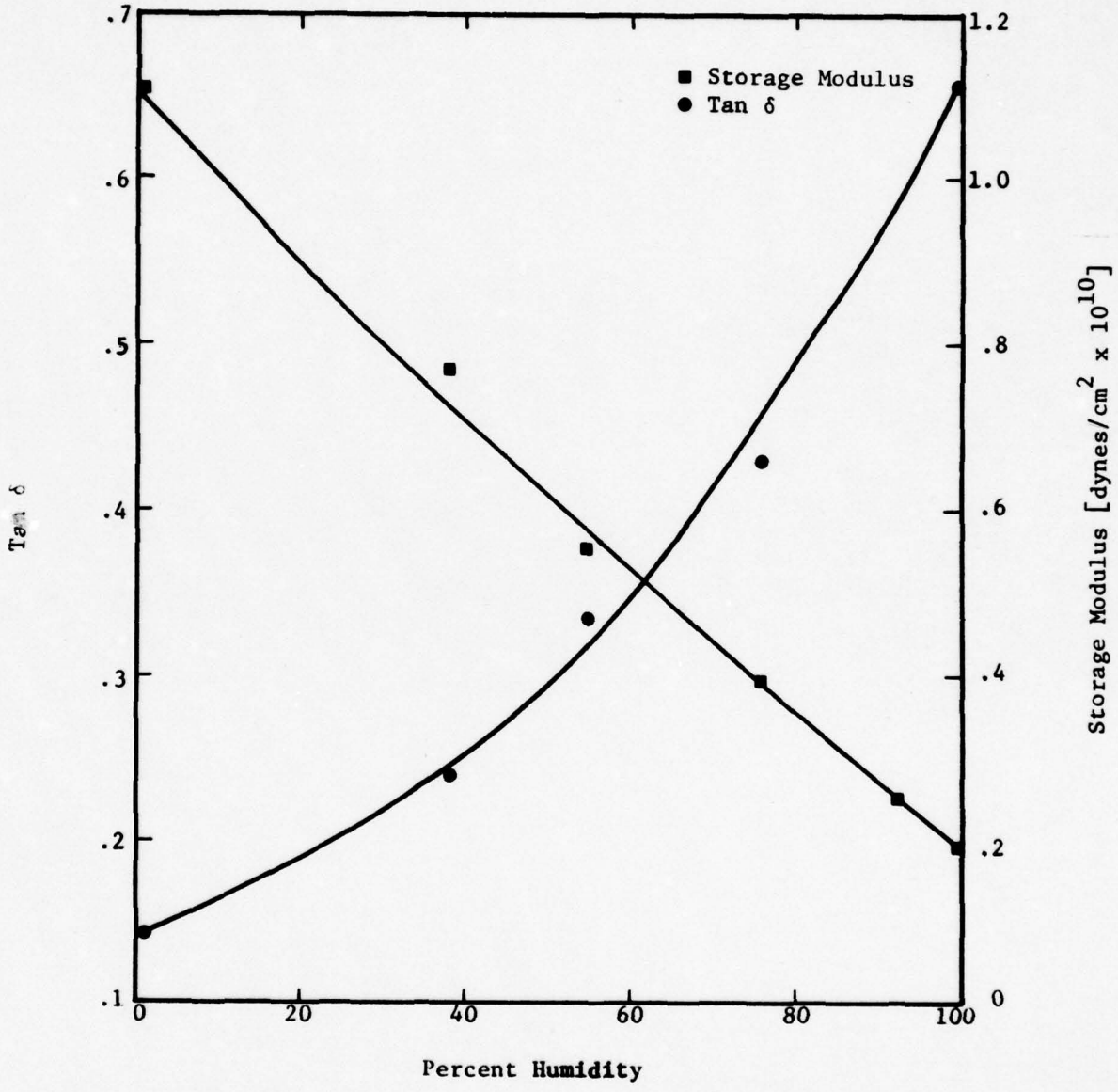

Fig. 3.2.22. Dynamic mechanical properties of paint System VIII as a function of percent relative humidity at 22°C and 11 Hz.

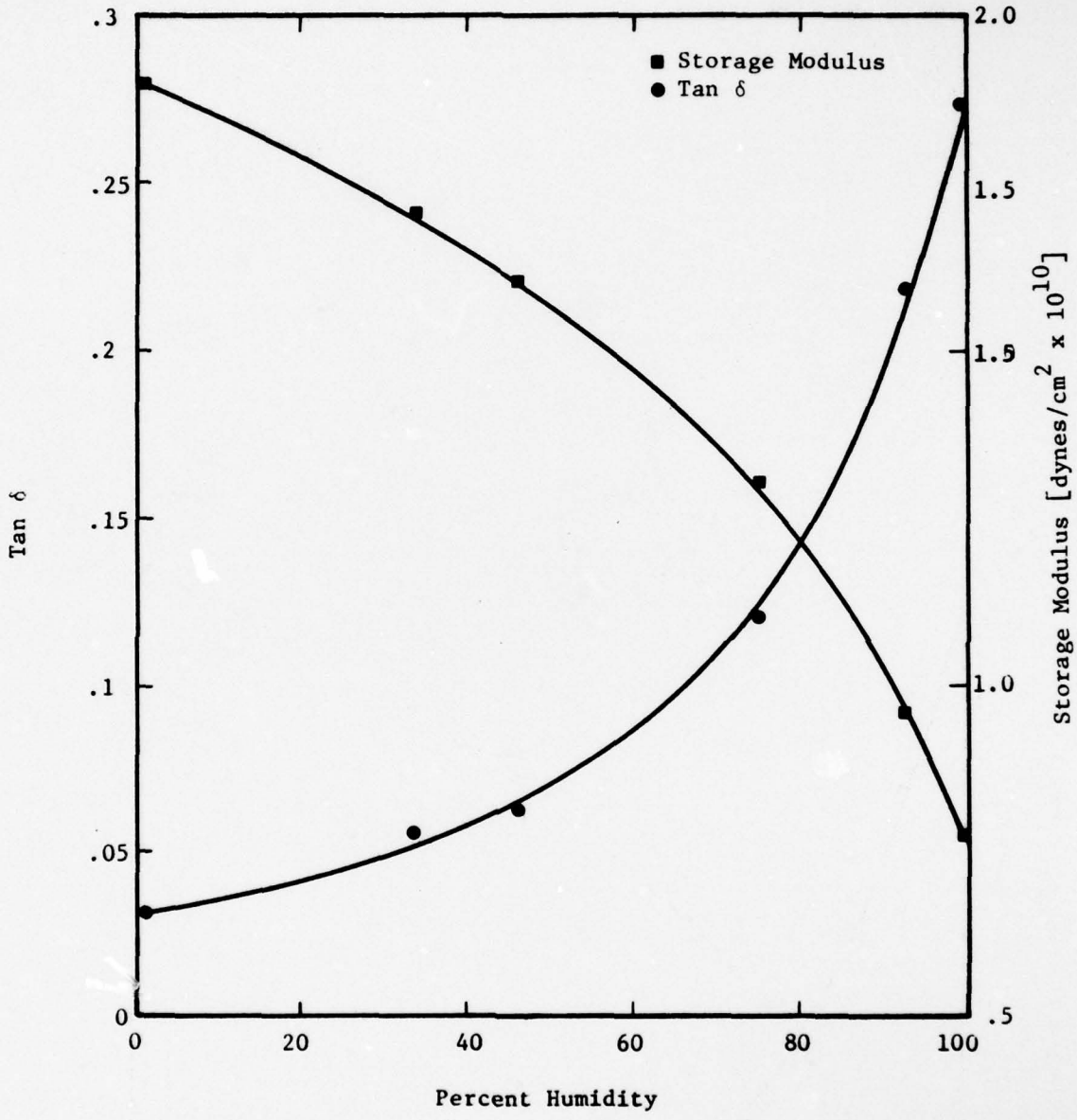

Fig. 3.2.23. Dynamic mechanical properties of paint System VII as a function of percent relative humidity at 22°C and 11 Hz.

spectra similar to the normal VR4 spectrum given in Fig. C-4 in Appendix C were obtained. The results of other investigators (47) who successfully used the UV to characterize photodegradation in a polyurethane system indicates the usefulness of continued work in this area.

3.2.4 Epoxy Systems

System V (A Epoxy)

The chemical structure of this resin is the same as a diglycidyl ether of bisphenol A (48), DGEBA, except that the end groups are phenols and alcohols (1). This resin is a slightly branched amorphous polymer whose molecular weight is high enough that it hardens to form a good surface coating upon solvent evaporation. Further discussion on this resin is given elsewhere (1, 48, 49, 50, 51).

Dynamic Mechanical

In Fig. 3.2.24 the dynamic mechanical properties at 11 Hz are given as a function of temperature. Two peaks were observed in the tan δ vs temperature curve at 98° and -52°C, and are labeled as α and β respectively. The α transition was identified as the glass transition by comparison to the work of Reinking et al., (49). The β transition was attributed to a mobility of the diether linkage as discussed by other authors (49, 52, 53).

The effect of humidity on the dynamic mechanical properties was investigated at 22°C and the results are given in Fig. 3.2.25 The polymer was slightly plasticized by the water with the 100% relative humidity modulus being 85% of the 0% humidity value. The loss tangent was observed to pass through a minimum at approximately 40% relative humidity and then increase slightly with increasing humidity. Overall, the effect of moisture was found to be small in this paint system.

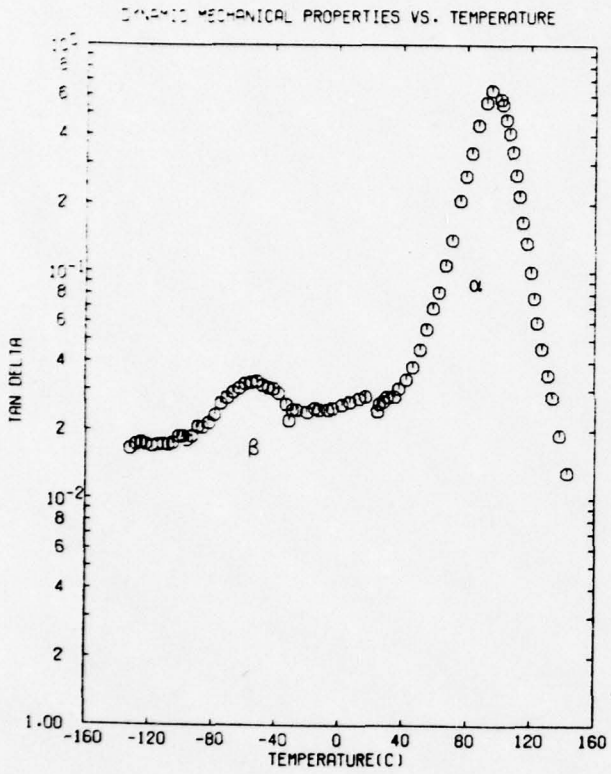

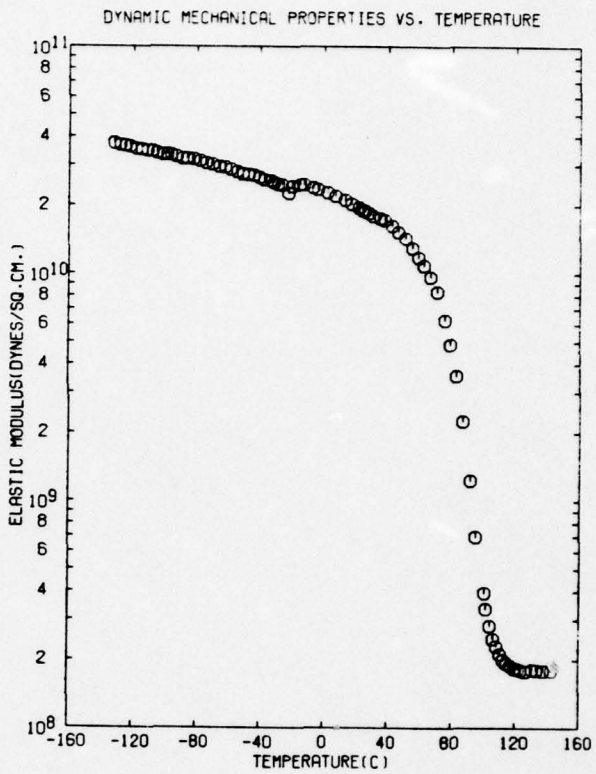

Fig. 3.2.24. Dynamic mechanical properties of paint System V as a function of temperature at 11 Hz.

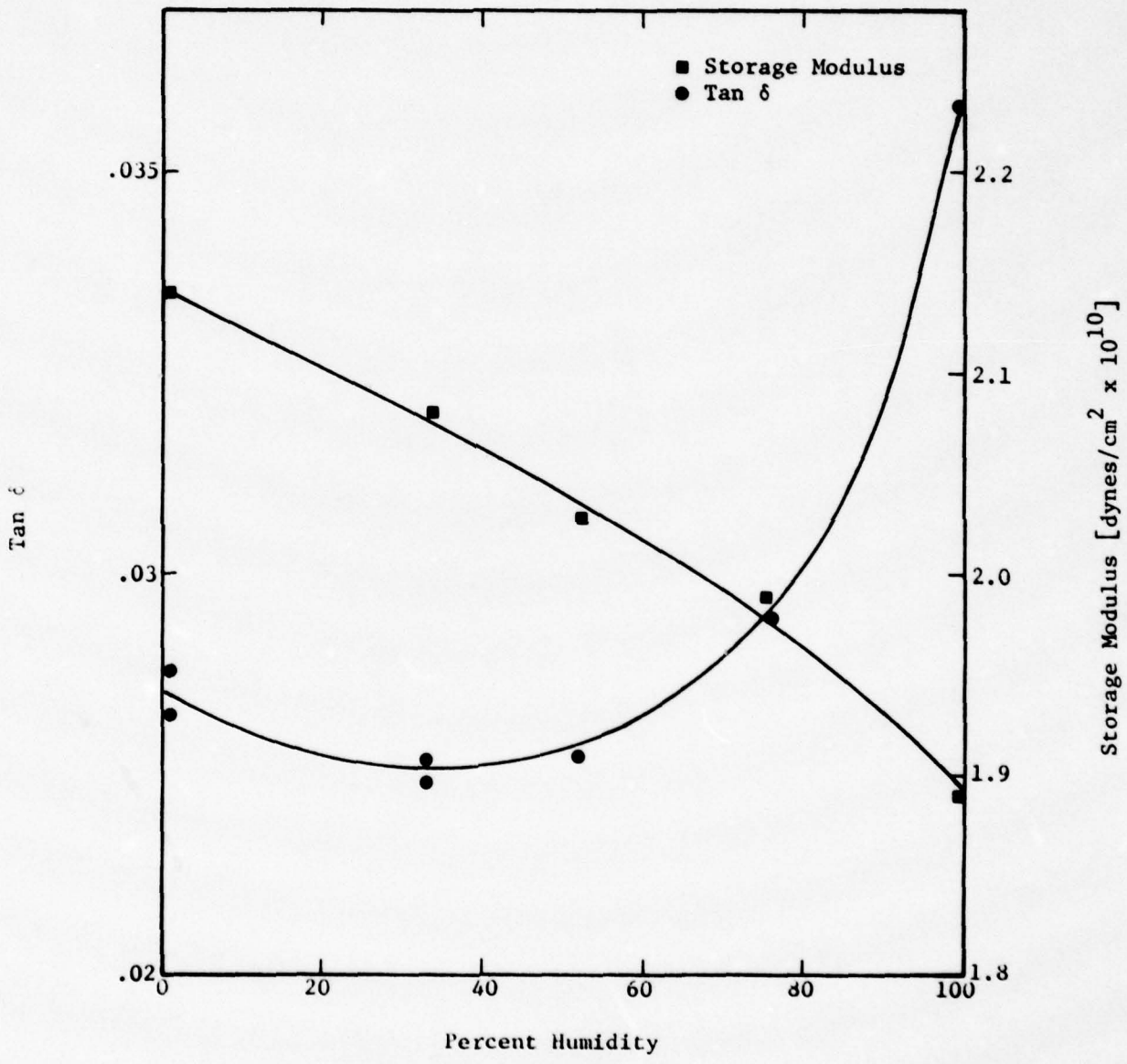

Fig. 3.2.25. Dynamic mechanical properties of paint System V as a function of percent relative humidity at 22°C and 11 Hz.

Infrared Spectroscopy

The infrared spectrum for this resin was obtained from a solvent-cast film and is presented as Fig. B-17 in Appendix B. The spectrum was compared to a spectrum of DGEBA presented by Lee and Neville (50). These spectra were found to be very similar except for two important differences; first, the absorption due to the epoxide ring was not observed, and second, the hydroxyl absorbance was observed to be slightly stronger. These observations are consistent with the fact that the epoxide end groups present in DGEBA effectively have been replaced by phenols and alcohols while the main chain structure remained essentially the same.

Ultraviolet Spectroscopy

The absorbance spectrum obtained on this film is similar to the result presented for VR4 in Fig. C-4 and therefore is not presented. It is hoped that the use of thin films will result in improved resolution of the UV spectrum.

Systems I and VI (E Epoxy and K Epoxy)

Both of these paints are amine-cured epoxides. The cure is acheived by a reaction between the amine and epoxide ring structure, and results in the formation of a highly-regular, three-dimensional network structure. The regularity of the network structure allows it to often be characterized by a single parameter, which gives a measure of either the cross-link density or the molecular weight between cross-links (53). In general, a low molecular weight between cross-links suggests rigidity, while a high value implies a soft, flexible material.

In addition, the properties of the cross-linked resin depend largely on the characteristics of the epoxide and amine curing agent and the conditions under which cure occurs. The epoxide resin used in both paints is Shell Epon 815, which consists of 90% by weight diglycidyl ether of bisphenyl A (DGEBA) and 10% by weight n-butyl ether (1). The difunctionality of the bisphenyl A leads to the cross-linking in this paint system.

Infrared Spectroscopy

The infrared spectrum for this resin was obtained from a solvent-cast film and is presented as Fig. B-17 in Appendix B. The spectrum was compared to a spectrum of DGEBA presented by Lee and Neville (50). These spectra were found to be very similar except for two important differences; first, the absorption due to the epoxide ring was not observed, and second, the hydroxyl absorbance was observed to be slightly stronger. These observations are consistent with the fact that the epoxide end groups present in DGEBA effectively have been replaced by phenols and alcohols while the main chain structure remained essentially the same.

Ultraviolet Spectroscopy

The absorbance spectrum obtained on this film is similar to the result presented for VR4 in Fig. C-4 and therefore is not presented. It is hoped that the use of thin films will result in improved resolution of the UV spectrum.

Systems I and VI (E Epoxy and K Epoxy)

Both of these paints are amine-cured epoxides. The cure is acheived by a reaction between the amine and epoxide ring structure, and results in the formation of a highly-regular, three-dimensional network structure. The regularity of the network structure allows it to often be characterized by a single parameter, which gives a measure of either the cross-link density or the molecular weight between cross-links (53). In general, a low molecular weight between cross-links suggests rigidity, while a high value implies a soft, flexible material.

In addition, the properties of the cross-linked resin depend largely on the characteristics of the epoxide and amine curing agent and the conditions under which cure occurs. The epoxide resin used in both paints is Shell Epon 815, which consists of 90% by weight diglycidyl ether of bisphenyl A (DGEBA) and 10% by weight n-butyl ether (1). The difunctionality of the bisphenyl A leads to the cross-linking in this paint system.

The monofunctionality of the n-butyl ether decreases the cross-linking as a result of its reduced functionality and chain stopping character (50). This results in a decreased viscosity and lower cross-link density (higher molecular weight between cross links).

The amine curing agent used in paint System VI is ethylene diamine, which is a tetrafunctional and cures well at room temperature (53). The amine curing agent in paint System I is a complicated mixture of polyfunctional amine groups (1).

System VI is cured at room temperature and the cure involves interaction with the moisture in the air (1), while the cure for System I is 16 hours at 77°F plus 15 min at 125°F. The rate of cure in System VI falls off rapidly at temperatures below 60°F and/or relative humidities below 30% (54). The increased temperature used to cure System I is expected to lead to a higher degree of cure.

Other important characteristics of the uncured epoxide are the epoxide equivalent, hydroxyl equivalent, and reactivity of the epoxide ring (50). The amine curing agent is also characterized by the amine equivalent weight and the reactivity of the primary and secondary amine hydrogens.

Dynamic Mechanical

Several workers have measured the dynamic mechanical properties of amine cured epoxies (55, 56, 57, 58). The dependence of the transition temperatures and the steepness of the modulus versus temperature curve on the epoxide and curing agent structure have been studied (59, 60). In addition, some relations between dynamic mechanical properties and the molecular weight between cross-links have been suggested (56).

In this work, dynamic mechanical data was obtained at 11 Hz for epoxy System VI and is presented in Fig. 3.2.26. The large relaxation observed in the tan δ vs temperature curve at 66°C was attributed to the material's glass transition by comparison to the work of Kenyon and Nielsen (57). The low temperature of this transition was attributed to a low degree of cross-linking which results due to the presence of the

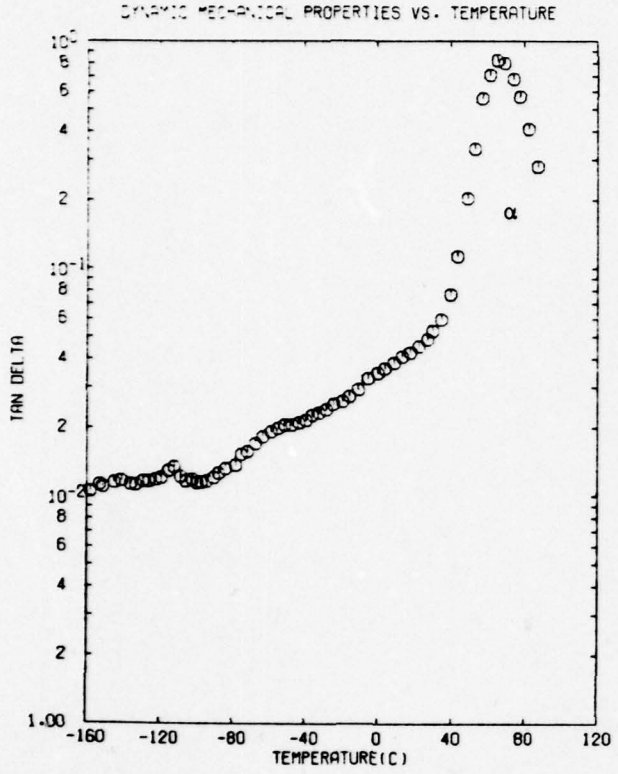

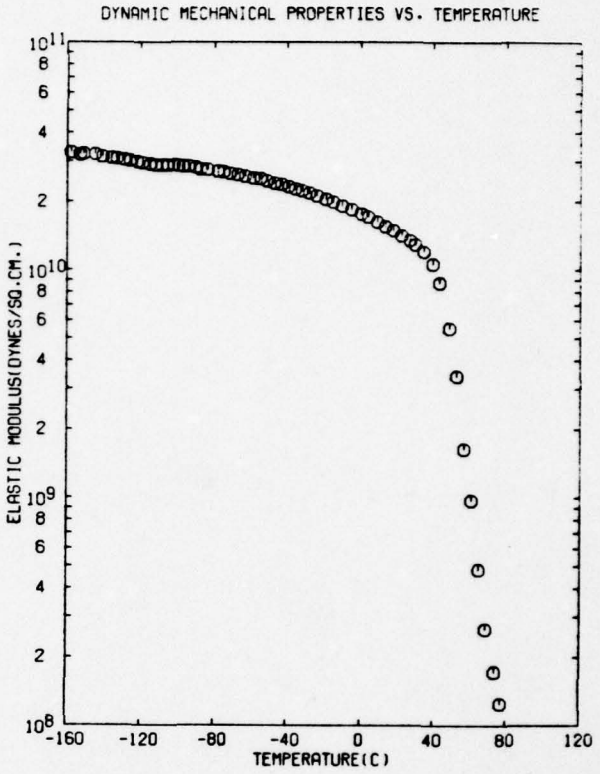

Fig. 3.2.26. Dynamic mechanical properties of paint System VI as a function of temperature at 11 Hz.

n-butyl ether and the room temperature cure. A broad relaxation was also observed over the 80° to 20°C temperature range. At this time the cause of this relaxation is not understood. Dynamic mechanical properties have not been obtained on System I at this time.

Infrared Spectroscopy

Infrared spectra were obtained on the epoxide components and amine curing agents used in these paint systems. These results are presented as Figs. B-18 to 21 in Appendix B. In Fig. B-18 the spectrum for the Epon 815 epoxide is given. Absorption band assignments were made by comparison to the spectrums presented by Lee and Neville (50). The strong absorption at approximately 910 cm^{-1} is characteristic of the epoxide ring structure, while the absorption at and around 1100 cm^{-1} was assigned to the n-butyl glycidyl ether component. In Fig. B-19 the ethylene diamine curing agent used in System VI is given. In Figs. B-20 and B-21 the two components of the polyfunctional amine curing agents used in System I are given. Analysis of these spectra is not complete.

The spectra for the cured epoxy Systems I and VI are given in Figs. B-22 and B-23 respectively. The spectrum for System VI is poorly resolved due to the unavailability of a thin sample. In the spectrum taken on System I, the small epoxide ring absorbance at 910 cm^{-1} indicates the extent of cure. The polymerization of epoxy resins has been studied by monitoring changes in the absorption spectrum (50, 53, 61, 62), and a similar study is planned for this work. In addition, studies on the hydrogen bonding in amine cured epoxy systems have been done (63). Further analysis of these spectra should provide useful information on the structure of these paint systems.

System IX (0 Epoxy)

Dynamic Mechanical

This paint was obtained commercially, and its composition is not known. In Fig. 3.2.27 the dynamic mechanical spectrum obtained at 11 Hz is given. The large relaxation observed was attributed to the material's

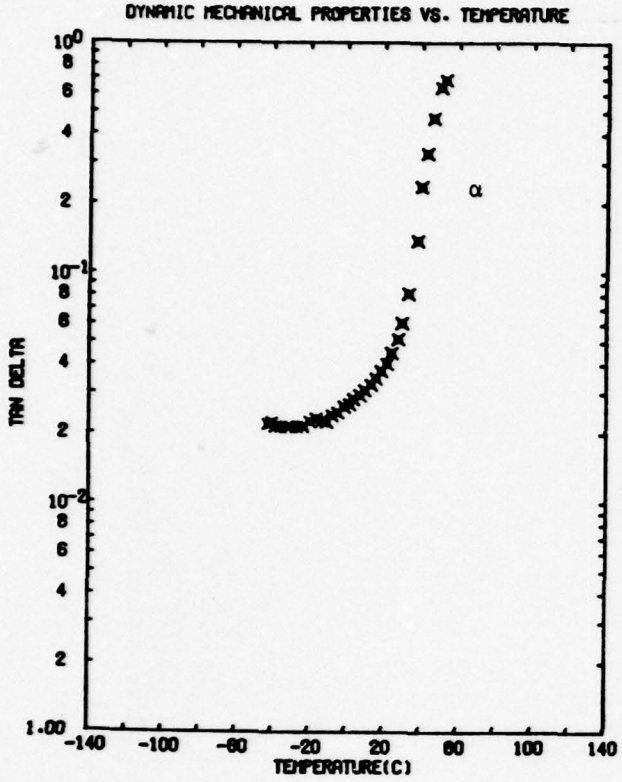

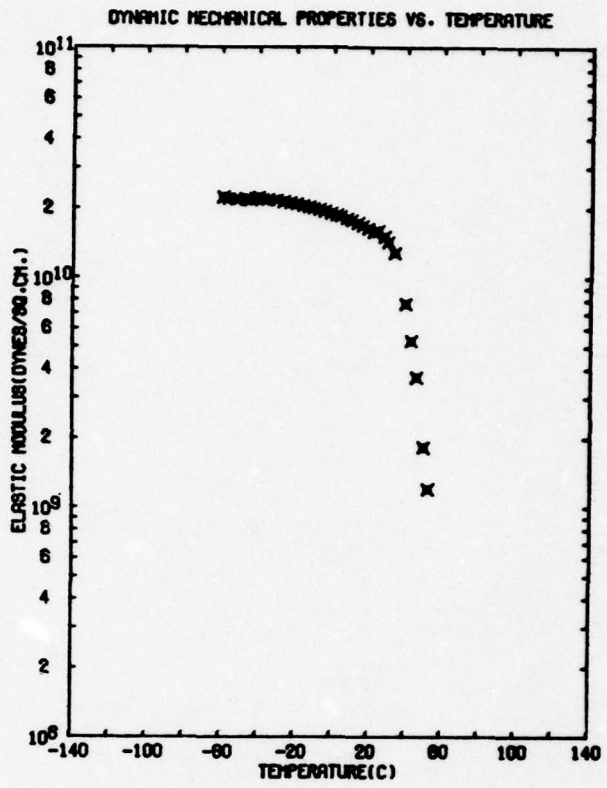

Fig. 3.2.27. Dynamic mechanical properties of paint System IX as a function of temperature at 11 Hz.

glass transition.

3.2.5 Conclusions

The investigation of these nine paint systems has resulted in some structural identification and the measurement of dynamic mechanical properties in different environments. The combination of these and other measurements should lead to an improved understanding and the development of structure property relations for these paints. This information coupled with the diffusion, mathematical modeling, adhesion studies, and x-ray work should lead to a complete understanding of these paint systems.

References (Section 3.2)

1. Letter, Newey and Busso Associates, to Electrochemical Technology Corp., December 11, 1978.
2. Ibid, January 29, 1979.
3. F. W. Billmeyer, Jr., Textbook of Polymer Science, Wiley - Interscience, New York, 1971.
4. Read, Williams, Anelastic and Dielectric Effects in Polymeric Solids, Wiley, 1967.
5. Arnold Wexler and Salvro Hasegawa, J. of Research of the Natl Bur of Stands, 53, No. 1, July, 1954.
6. J. Haslam, H. A. Willis, and D. C. M. Squirrell, Identification and Analysis of Plastics, ILIFFE Books, London, 1972.
7. E. G. Brame, Jr., and J. G. Grasselli, Infrared and Raman Spectroscopy Pt C, Marcel Dekker, Chrc., New York, 1977.
8. D. O. Hummel, Infrared Spectra of Polymers in the Medium and Long Wavelength Regions, J. Wiley & Sons, New York, 1966.
9. J. C. Henneker, Infrared Spectrometry of Industrial Polymers, Academic press, New York, 1967.
10. R. M. Silverstein, G. C. Basslet, and T. C. Morrell, Spectrometric Indentification of Organic Compounds, John Wiley & Sons, New York

11. V. R. Banski et al., Handbook of Analysis of Synthetic Polymers and Plastics, Elles Harwood Ltd., Westgate, England, 1977.

12. Roff and Scott, Fibers, Films, Plastic, and Rublers, Butterworth, London, 1971.

13. R. D. Deanin, Polymer Structure, Properties, and Applications, Cahners Book, 1972.

14. A. F. Fitzhugh and R. N. Crozier, J. Poly. Sci., 8, 225, (1952).

15. R. F. Clash, Jr. and L. M. Rynkiewicz, Ind. Eng. Chem., 36, 279 (1944).

16. Y. Takahashi, J. Appl. Polymer Sci., 5, 468 (1961).

17. Mikhailov, USP Khim, 24, 875 (1955).

18. Aklonis, MacKnight, and Shen, Introduction to Polymer Viscoelasticity, Wiley, 1972.

19. J. D. Ferry, Viscoelastic Properties of Polymer, Wiley, 1970.

20. L. E. Nielsen, Mechanical Properties of Polymers, Reinhold, 1962.

21. Y. Takahashi, J. Appl. Polymer Sci., 5, 468 (1961).

22. T. H. Sutherland and B. L. Funt, J. Polymer Sci., 11, 177 (1953).

23. Veselovshir, Berlomsk Polytech. Inst. USSR, 91, 399 (1956).

24. R. H. Wiley and R. R. Garrett, J. Poly. Sci., 7, 121-123 (1951).

25. N. G. Mcrum, B. E. Read, and G. Williams, Anelastic and Dielectric Effects in Polymer Science, Wiley, 1967.

26. M. Takayanagi, Mem. Fac. Eng., Kyushu Univ., 23, 1 (1963).

27. A. Elliot, Infrared Spectra and Structure of Organic Long Chain Polymers, St. Martians Press, New York, 1969.

28. D. W. Van Krevelen, Properties of Polymers, their Estimation and Correlation with Chemical Structure, Elsevier Scientific, New York, 1976.

29. H. Sasabe and C. Moynihan, J. Poly. Sci. Phys. Ed., 16, 1447-1457 (1978).

30. F. Wurstlin, Z. Kolloid,

31. G. Pezzin, J. Appl. Poly. Sci., 11, 2553-2566 (1967).

32. V. Heidingsfield, J. Zelinger, and V. Kuska, J. Appl. Poly. Sci., 15, 2446 (1971).

33. C. West and S. Copper, J. Poly. Sci. Poly. Sym., 60, 127-150 (1970).

34. Infrared Spectroscopy. Its Use in the Coatings Industry, Federation of Societies for Paint Technology, Philadelphia, 1969.

35. D. P. Wyman, J. Appl. Poly. Sci., 11, 1439-1448 (1967).

36. J. H. Saunders and K. C. Frisch, Polyurethanes - Chemistry and Technology, Wiley - Interscience, New York, 1962.

37. R. A. Assink, J. Poly. Sci. Phys. Ed. 15, 59-69 (1977).

38. S. L. Samuels and G. L. Wilkes, J. Poly. Sci. Phys. Ed., 11, 807 (1973).

39. W. Dzierza, J. Appl. Poly. Sci., 22, 1331-1342 (1978).

40. R. A. Bieneman, J. Paint. Tech., 43, 92-98 (1971).

41. E. N. Doyle, The Development and Use of Polyurethane Products, McGraw-Hill, New York, 1971.

42. H. Jacobs and E. Jenkel, Makronel Chem., 43, 132 (1961).

43. H. Jacobs and E. Jenkel, Makronel Chem., 47, 72 (1961).

44. J. D. Keenan, M.S. Thesis, University of Washington, 1979.

45. J. C. West and S. L. Cooper, J. Poly. Sci. Poly. Symp., 60, 127-150 (1977).

46. W. J. MacKnight and M. Yang, J. Poly. Sci. Symp., 42, 817-832 (1973).

47. E. L. Cheu and Z. Osawa, J. A-pl. Poly. Sci., 19, 2947-2959 (1975).

48. W. G. Potter, Epoxide Resins, Springer-Verlag, New York, 1970.

49. N. H. Reinking, A. E. Barnabeo, and W. J. Hale, J. Appl. Poly. Sci., 7, 2135-2144 (1963).

50. H. Lee and K. Neville, Handbook of Epoxy Resins, McGraw-Hill, New York, 1967.

51. J. A. Brydson, Plastic Materials, Van Nostrand Reinhold, New York, 1970.

52. E. Cuddihy and J. Moacanin, Advan. Chem. Ser., 192, 96-107 (1970).

53. C. A. May and Y. Tanaka, Epoxy Resins Chemistry and Technology, Marcel Dekker, New York, 1973.

54. "Amine-cured EPON Resin Coatings," Polymers Division, Shell Chemical Company, SC: 71-11.

55. D. E. Kline, J. Polymer Sci., 47, 237 (1960).

56. T. Murayama and J. P. Bell, J. Poly. Sci. Pt A-2, 8, 437-445 (1970).

57. A. S. Kenyon and E. Nielsen, J. Macromol, Sci.-CHEM A3, 2, 275-295 (1969).

58. J. P. Bell, J. Poly. Sci. Pt A-2, 6, 417-436 (1970).

59. T. K. Kwei, J. Poly. Sci. A-2, 4, 943 (1966).

60. F. R. Dammont and T. K. Kwei, J. Poly. Sci. A-3, 5, 5, (1967).

61. C. E. Feazel and E. A. Verchot, J. Poly. Sci., 25, 351 (1957).

62. J. Felgin, D. M. Longnecker, and I. Pether, SPE. Trans., 5, 39 (1965).

63. J. G. Williams and O. Delatyck, J. Poly. Sci., Pt A-2, 8, 295-304 (1970).

3.3 Transport and Related Properties

The permeability of water through vinyl resins, VR3 and VR4, has been measured. The permeability has been shown to be a strong function of temperature in Fig. 3.3.1 from 21°C to 42°C. Heating above 40°C has been shown to produce permanent changes in VR4. These studies are ongoing, and without the complimentary knowledge of water solubility, only general conclusions can be drawn from permeability data. These data are consistent, however, with the concept that the physical structure of the vinyl resins is rapidly changing with temperature in the region between 20°C and 40°C. This is expected because VR4 exhibits a glass transition just above 40°C. It is likely, therefore, that the permeability, as well as both its components (solubility and diffusivity) are strong functions of temperature in this region. This concept is further supported by Bell (1-3) who has proposed the following formula relating the diffusivity of a dye through polymers:

$$\frac{D}{RT} = AE''^{B} \qquad (1)$$

where A and B are constants, and E" is the elastic loss modulus of the polymer, easily obtained by dynamic mechanical measurements. The loss modulus of VR4 as a function of temperature is shown in Fig. 3.2.2. On the basis of this preliminary evidence, it appears that, after obtaining solubility data, the permeability results can be correlated with dynamic mechanical measurements.

The ionic capacity of paint films is defined as the moles of counter-ions in a specified mass or volume of material. The ionic capacities of the paints under study here are unknown but can be expected to be small (4-7). An attempt to measure the ionic capacity of K epoxy and VR3 vinyl resin has been made. The method employed standard acid-based titration methods and was largely unsuccessful. The results are presented in Tables 3.3.1 and 3.3.2. Several problems were encountered while performing the experiments including interference from the ionic capacity of the glass vessels in which the titrations were performed. Even though no reliable quantitative results were obtained, one valid observation was

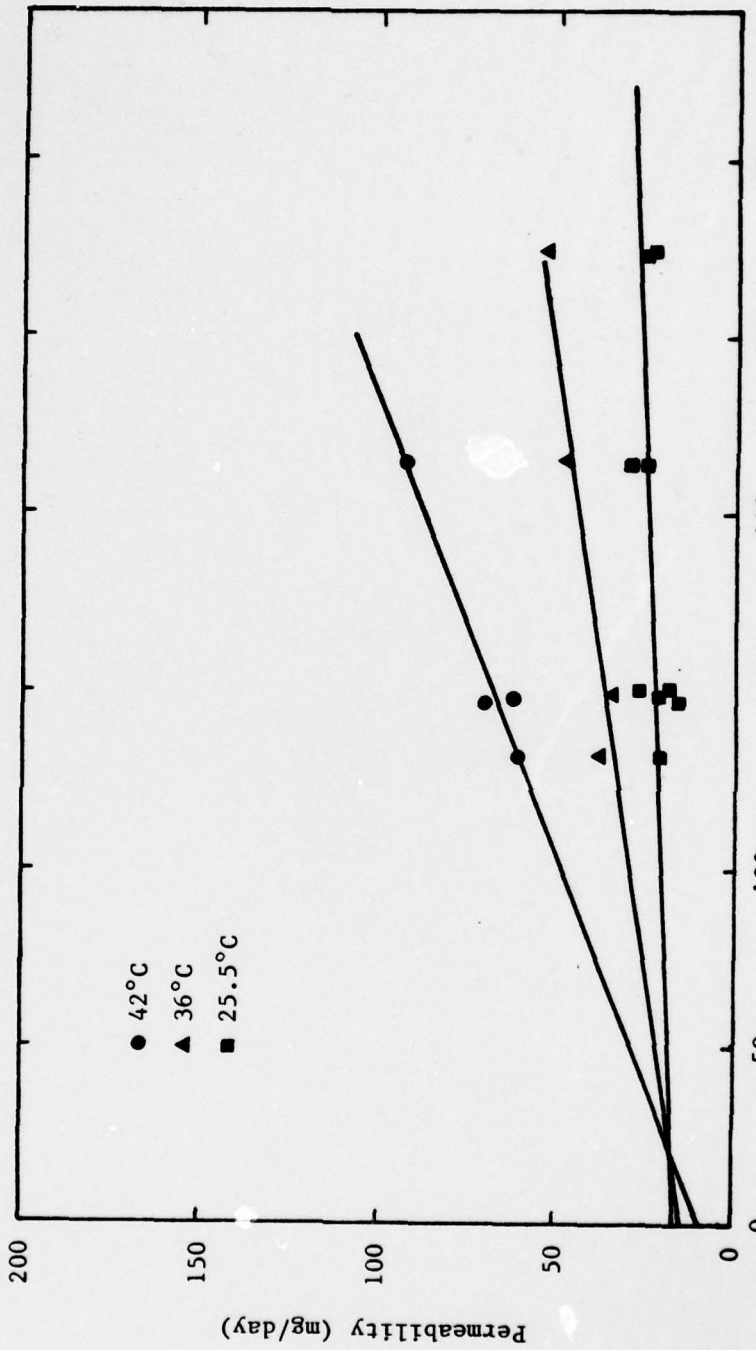

Fig. 3.3.1. VR4, water permeability vs reciprocal thickness.

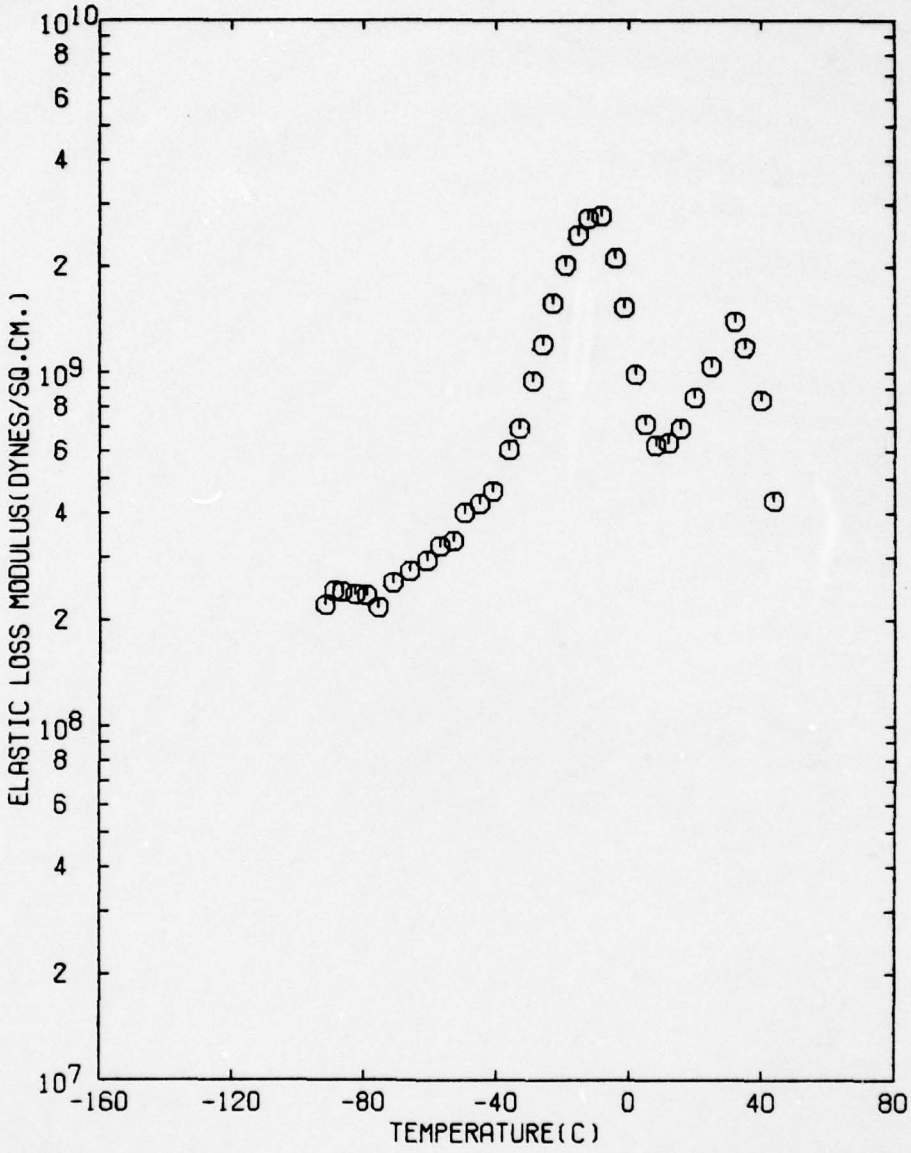

Fig. 3.3.2. Elastic loss modulus vs temperature for VR4.

Table 3.3.1

Ion Exchange Capacity meq/g*

Exchange Solution pH	Glass (meq/cm^2)	VR3 with TCP	VR3 (repeat) with TCP	VR3 without TCP	K Epoxy
13	†	0.1119	0.0903	0.1190	0.04490
		±123%	±57%	±38%	±92%
12	6.979×10^{-6}	0.000	0.000	0.000	0.07866
	±1372%	±0.082	±0.122	±0.043	±11%
11	†	0.00426	†	0.000	0.00090
		±11%		±0.010	±79%

* Ionic capacitance calculated as meq (measured)/wt. (paint).

† No experiment attempted.

Table 3.3.2

Ion Exchange Capacity (meq/g)*

Exchange Solution pH	Glass (meq/cm^2)	VR3 with TCP	VR3 (repeat) with TCP	VR3 without TCP	K Epoxy
1.0	0.0000345	0.2773	0.0897	0.000	0.1064
	±800%	±48%	±276%	±0.055	±82%
2.0	0.0007818	0.00258	0.00687	0.000	0.000
	±27%	±1997%	±774%	±0.122	±0.031
3.0	0.0000614	0.00279	0.00129	0.000	0.00079
	±6%	±121%	±432%	±0.005	±79%

*Ionic capacity calculated as [meq (measured) - meq(glass)]/wt. (paint).

recorded; the ionic capacitance of these materials can be strongly dependent on minor components. Tables 3.3.1 and 3.3.2 show that this was the case for VR3 for which the major portion of the ionic capacitance was traced to the plasticizing agent, tricresyl phosphate (TCP). The probability exists that other paints will display similar behavior and that the minor component composition will be found to have a major effect on the transport properties. Further investigation of this subject is planned.

References (Section 3.3)

1. J. P. Bell, J. Appl. Polymer Sci., 12, 627 (1968).
2. J. H. Dumbleton, J. P. Bell, and T. Murayama, J. Appl. Polymer Sci., 12, 2491-2508 (1968).
3. J. P. Bell, T. Murayama, J. Appl. Polymer Sci., 12, 1795-1799 (1968).
4. W. U. Malik and L. Aggarwal, J. Oil Color Chem. Assoc., 57, 131 (1974).
5. U. Ulvarsson, M. L. Khullar, and E. Wahlin, J. Oil Color Chem. Assoc., 50, 254 (1967).
6. U. Ulfvarson and M. Khullar, J. Oil Color Chem. Assoc., 54, 604 (1971).
7. M. L. Khullar and U. Ulfvarson, IX FATIPEC Congress, Sect. 3, 165 (1968).

3.4 Small Angle X-ray Scattering (SAXS)

The SAXS experiment is done by examining the scattering of monochromatic, well-collimated x-rays in a narrow angular region (up to$\sim$100 mrad) near the incident beam direction. As in the familiar scattering of visible light by particles, there is scattering and a halo effect around the incident beam. At these small angles the x-ray scattering entities are 10-100 Å in size and depend on the external dimension of the scatterer, not its internal structure. The sample is assumed to be approximately homogeneous in composition with scattering entities randomly dispersed within it. The SAXS is sensitive only to the difference in electron density between the matrix and the scatterers so the scatterer can be a void as well as a particulate inclusion.

The scattering intensity (1) is

$$I(h) = N\Delta\rho^2\nu^2 \exp\left(\frac{-h^2 r_g^2}{3}\right) \tag{1}$$

where

$$h = \frac{4\pi}{\lambda} \sin \varepsilon/2 \tag{2}$$

and N = number density of scatterers

$\Delta\rho$ = electron density difference between scatterers and matrix

ν = volume of scatterer

r_g = radius of gyration of scatterer

λ = x-ray wavelength = 1.54 Å in this case

ε = scattering angle

h is called the scattering vector

The size of the scattering entities may be estimated with a Guinier plot (1), $\ell n\ I(h)$ vs h^2, where r_g can be determined from the slope.

Experimental Plan

Five samples of paint were formulated and treated in various ways in order to distinguish different possibilities in the x-ray scattering

experiment. These are shown in Table 3.4.1. Each paint was examined as freshly prepared (D), after aging in H_2O for 18 days (C), after aging in 5 molar NaCl solution for 18 days (B), and after counter-current diffusion of Ag^+: Sn^{++} (A). Since the scattering entity depends only on the difference in electron density between scatterer and matrix, these treatments could have the following effects on the scattering pattern. If an unconnected void network was present in the fresh paint, the various treatments could open up the voids to make them scatter more. Particularly the diffusion of Ag^+ and Sn^{++} into the voids to precipitate Ag would make them more visible. Since the paints are primarily hydrocarbons, the presence of NaCl in the voids would result in more scattering, or conversely, filling the voids with H_2O should cause less scattering unless there was some sort of structural rearrangement of the molecules in the paint. All of these effects are apparent in the data to be discussed.

Experimental Results

The paint samples were examined on the Oak Ridge National Laboratory 10 meter SAXS camera (2, 3) which includes a 6 kW rotating anode x-ray generator (Cu tube), a pyrolytic-graphite, incident-beam monochrometer, pinhole collimatron, a two-dimensional position-sensitive proportional counter, and an on-line minicomputer for data acquisition and analysis. The paint samples were folded to the approximate thickness ($\mu x \approx 1/e$) and inserted into the x-ray beam in a holder in which the paint could be maintained either dry or wet. The scattering curves were corrected for background scattering from the sample holder, spatial sensitivity of the detector, and photo electric absorption. The SAXS pattern from a typical paint as obtained directly with the detector is shown in Fig.3.4.1. The iso-intensity contours are centered around the primary beam stop. The essentially circular pattern shows the scattering to be isotropic, as expected.

The scattering intensity as a function of scattering angle, ε, was obtained by performing a rectangular-to-polar coordinate transformation and integrating the azimuthal angle over 2π. These integrated intensities were normalized to the same relative intensity scale by

Table 3.4.1

Description of Paint Samples

O PUR		N PUR		VR3		VR4		A Epoxy		Conditions*
Painted 12/08/78		Painted 4/11/79		Painted 3/30/79		Painted 1/11/79		Painted 3/30/79		
1A	#1	2A	#2	3A	#3	4A	#4	5A	#3	Ag+/Sn++
1.39 mils		1.09 mils		2.87 mils		2.98 mils		1.05 mils		$AgNO_3$ ≈ 1.6M ≈ SnCl
1B	#1	2B	#2	3B	#3	4B	#4	5B	#3	5M NaCl soln.
1.22 mils		1.26 mils		2.12 mils		2.12 mils		0.84 mils		
1C	#1	2C	#2	3C	#3	4C	#4	5C	#3	H_2O
0.9 mils		0.89 mils		1.99 mils		2.45 mils		0.71 mils		
1D	#4	2D	#2	3D	#3	4D	#4	5D	#3	Fresh membranes
6.71 mils		1.11 mils		2.73 mils		1.66 mils		0.86 mils		

* Membranes A, B, and C were soaked in the indicated solution for 18 days beginning 5/7/79.

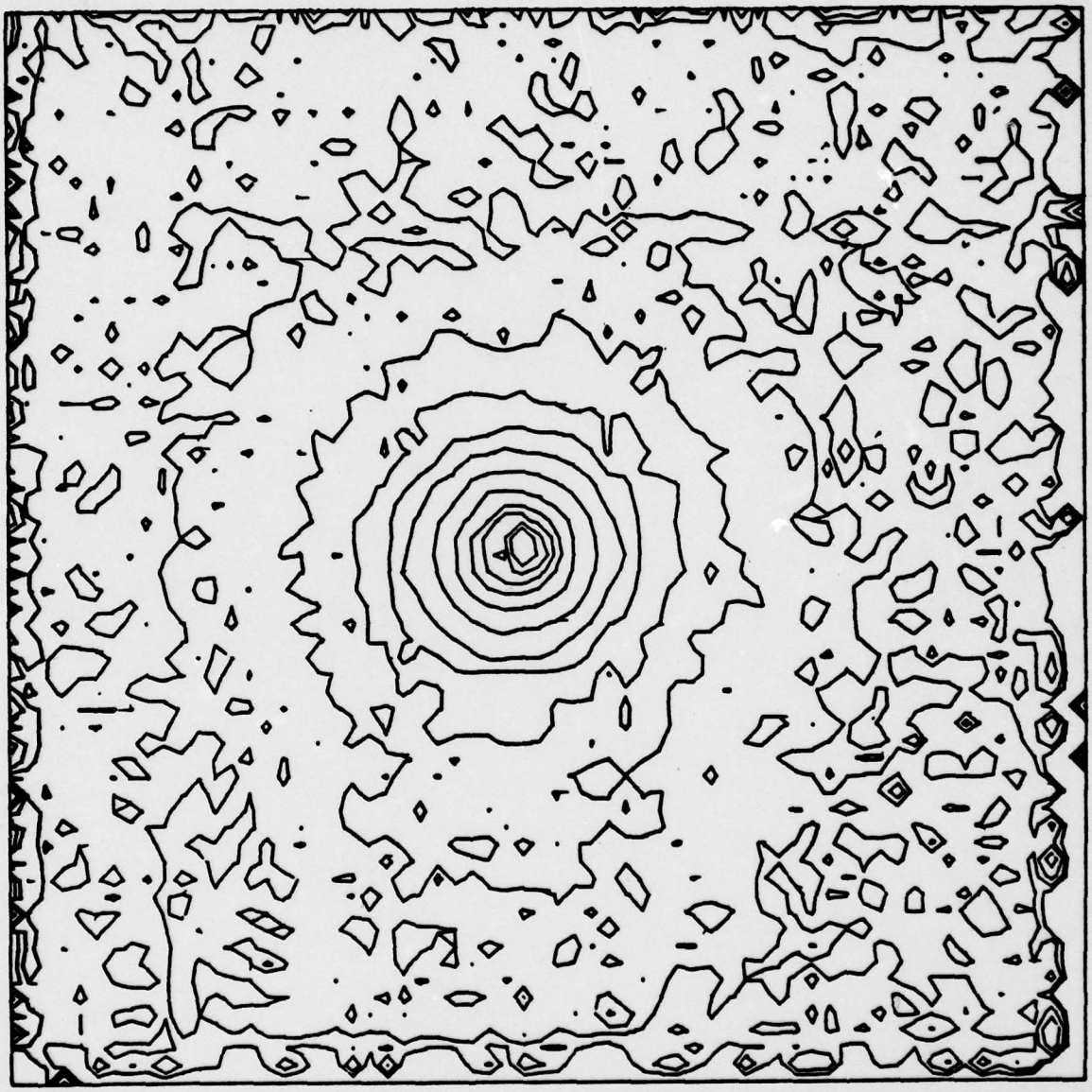

Fig. 3.4.1. Two-dimensional isointensity contour plot of a typical paint.

$$I(h)_{relative} = I(h)_{integrated}/I(mon) \times T \times \ell nT$$

where I(mon) is the measured count from a monitor detector which samples the indident beam, and T is the measured transmission of the individual sample. This procedure removed the effect of different counting times and different sample thicknesses. The scattering from the individual paint samples are shown in Figs. 3.4.2A-K, all plotted relative intensity I(h) vs ε in milliradians. In Fig. 3.4.2A scattering is compared for the fresh paint samples. Over most of the scattering range they fall into two groups: 3D and 4C are very low in scattering while 1D, 2D, and especially 5D (the epoxy) scatter more intensely. However, all are weak scatterers compared to many common materials (3). In Fig. 3.4.2B the effects of the aging treatments are shown (all examined dry). Although the data for the fresh paint, 4D, were faulty, the aging in H_2O, salt water, and Ag^+/Sn^{++} each increased the scattering. This is consistent with the idea that H_2O opens voids, NaCl is retained within the voids and scatters more, and finally, diffusion of Ag^+/Sn^{++} causes even more intense scattering. The effect of the Ag^+/Sn^{++} diffusion was largest on paint #1 shown in Fig. 3.4.2C. This is a large effect and plainly makes the x-ray scattering entity more visible. This data is examined later to determine the scatterer size. A similar, but diminished effect is shown in Figs. 3.4.2D and 3.4.2E for paints #2 and 3. Note that in Figs. 3.4.2D and 3.4.2E and scattering from the Ag^+/Sn^{++} decorated paints (2D and 3D) have different shapes compared with the fresh paint. In Fig. 3.4.2D the scattering is highest at the low and high angles overlapping in the middle, suggesting filling large and small voids, respectively. In Fig. 3.4.2E the curves overlap on the ends with increased scattering in the middle region, suggesting a medium-sized void. The scattering from wet samples as in the aging bath is shown in Fig. 3.4.2F, G, H, I, and J. The wet, aged in salt water samples are each shown compared with the scattering from the fresh paint (except for paint 4D which wasn't available). In some, the wet sample scatters more, in others, less. This is due to the combined and competing effects of H_2O and NaCl within the voids. Since H_2O has approximately the same electron density as the paints, it would make them scatter less while NaCl would increase scattering. There is a possibility that this effect could be developed into a technique to actually measure NaCl concentration

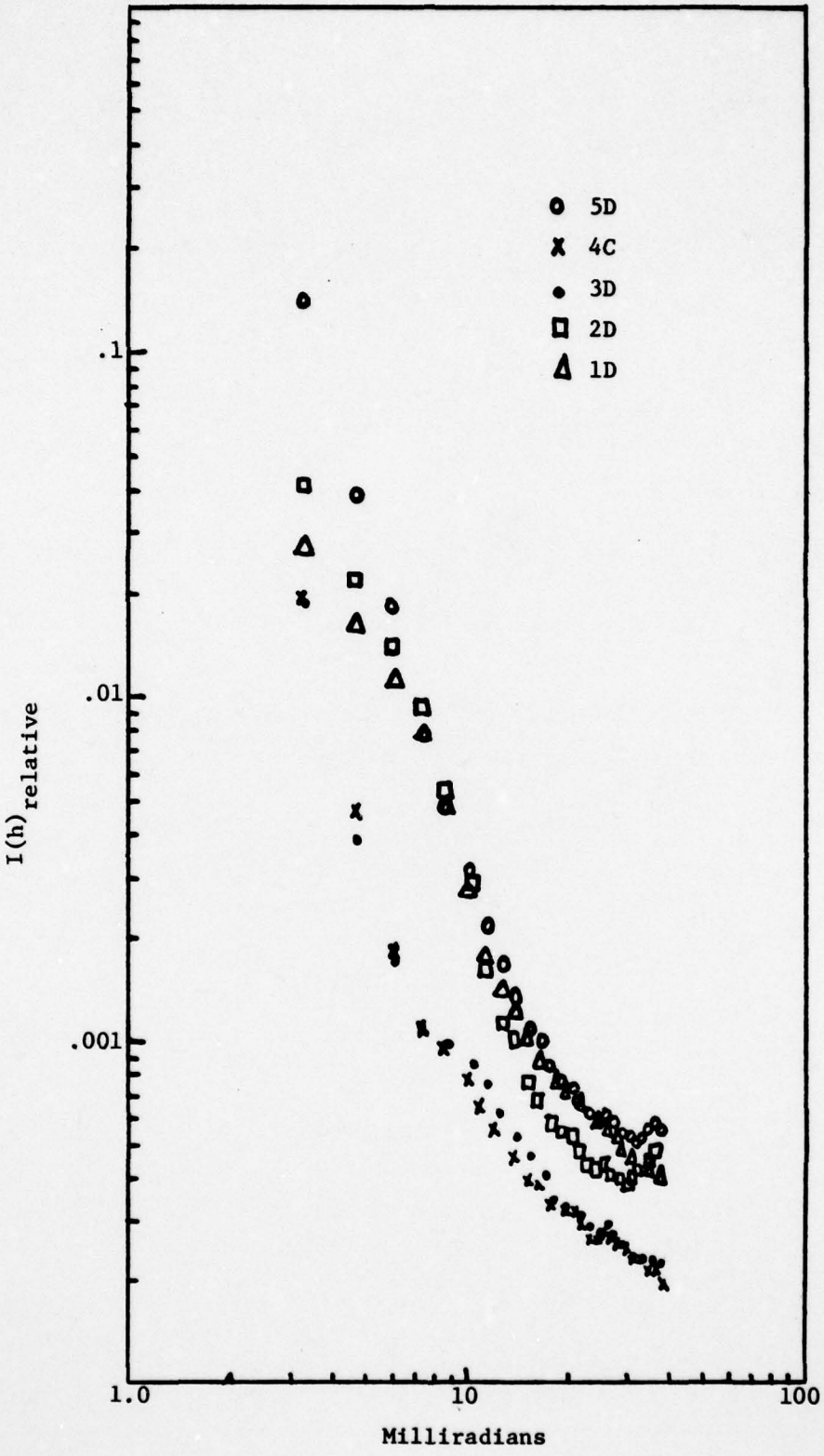

Fig. 3.4.2A. Comparison of scattering from fresh paint samples (except for paint 4D where the data was bad so 4C is shown for comparison).

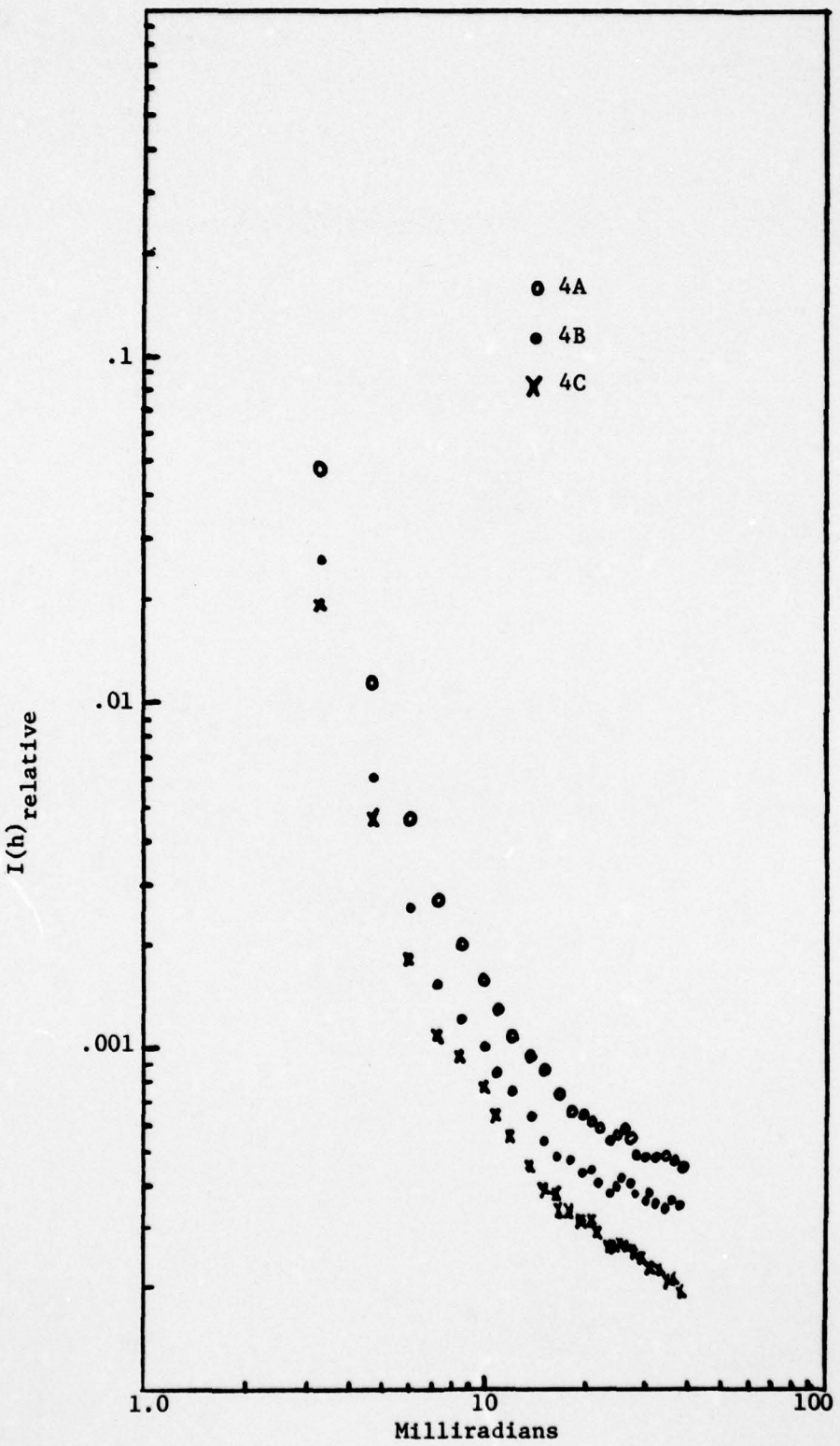

Fig. 3.4.2B. The effect of different aging treatments on the x-ray scatterers in paints. The data from 4D, the fresh paint, was faulty, but the comparison of 4C, aged in H_2O; 4B, aged in salt water; and 4A, diffused with Sn/Ag show a general scattering increase.

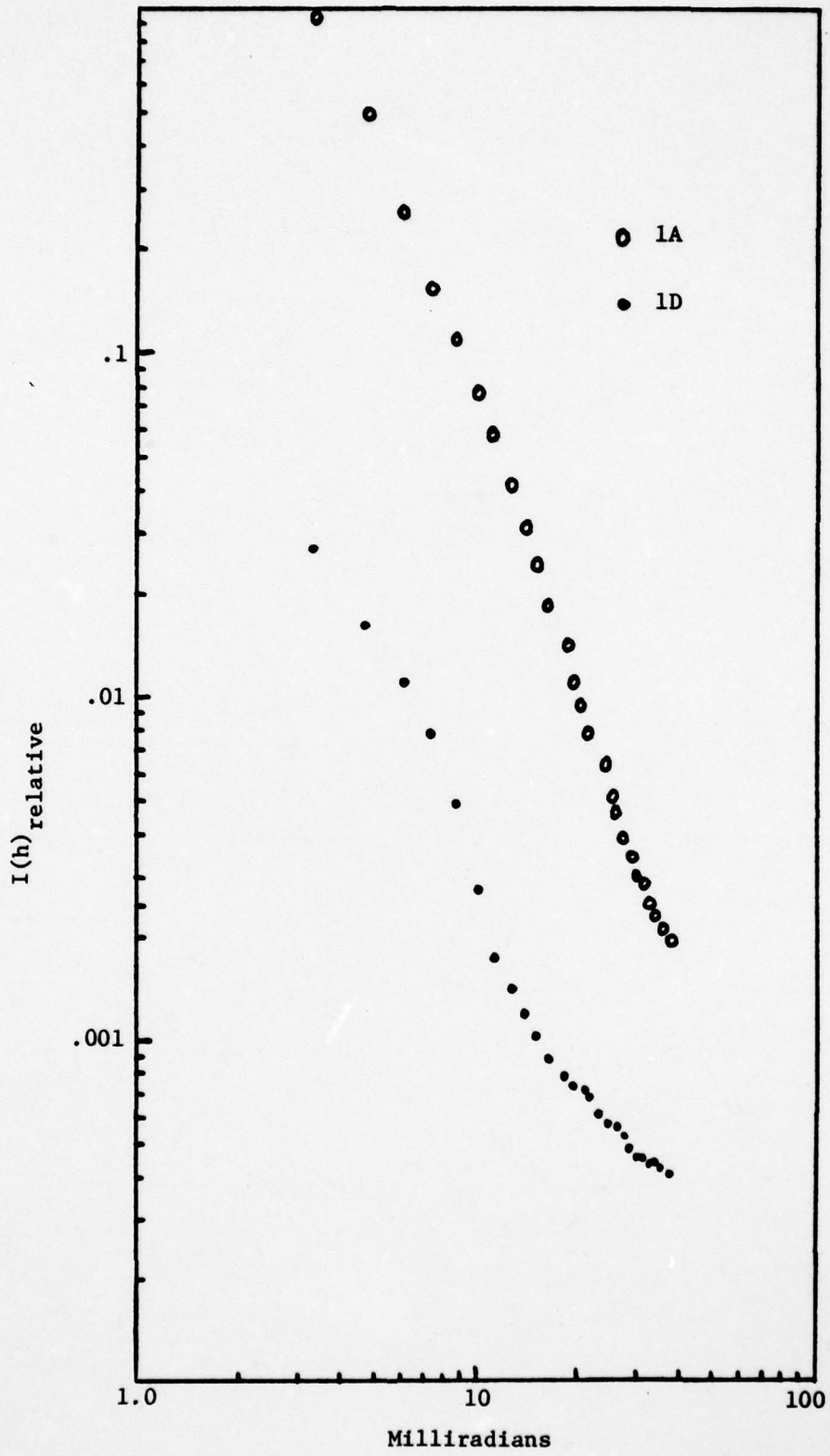

Fig. 3.4.2C. Comparison of fresh paint (1D) and after Ag/Sn diffusion (1A).

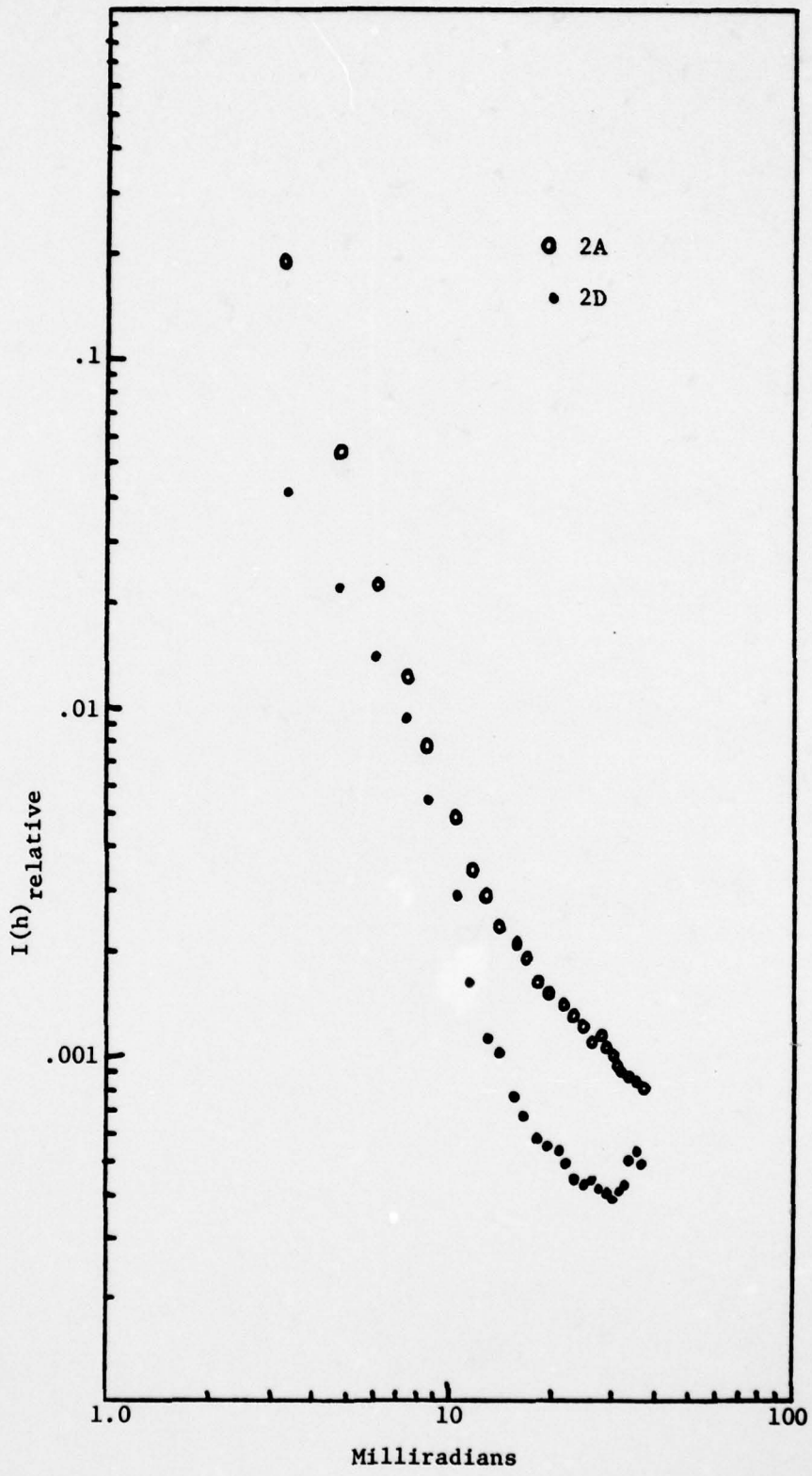

Fig. 3.4.2D. Comparison of fresh paint (2D) and Ag/Sn diffused (2A) paint samples.

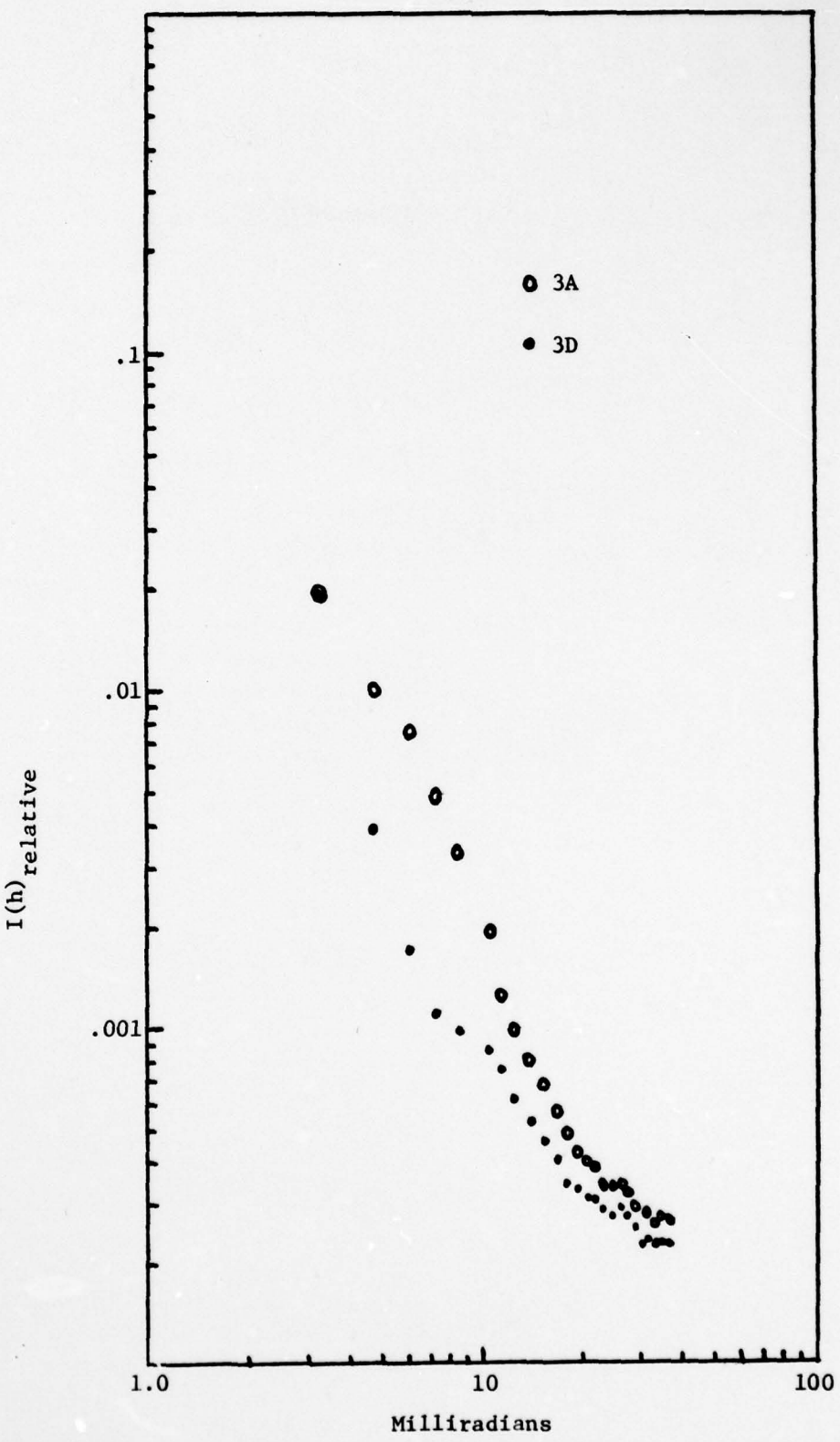

Fig. 3.4.2E. Comparison of fresh paint (3D) and Ag/Sn diffused (3A) paint samples.

AD-A080 960 ELECTROCHEMICAL TECHNOLOGY CORP SEATTLE WASH F/G 11/3
DETERMINATION OF THE EFFECT OF COMPOSITION, STRUCTURE AND ELECT--ETC(U)
DEC 79 T R BECK N00014-79-C-0021

UNCLASSIFIED NL

2 OF 2
AD-
A080960

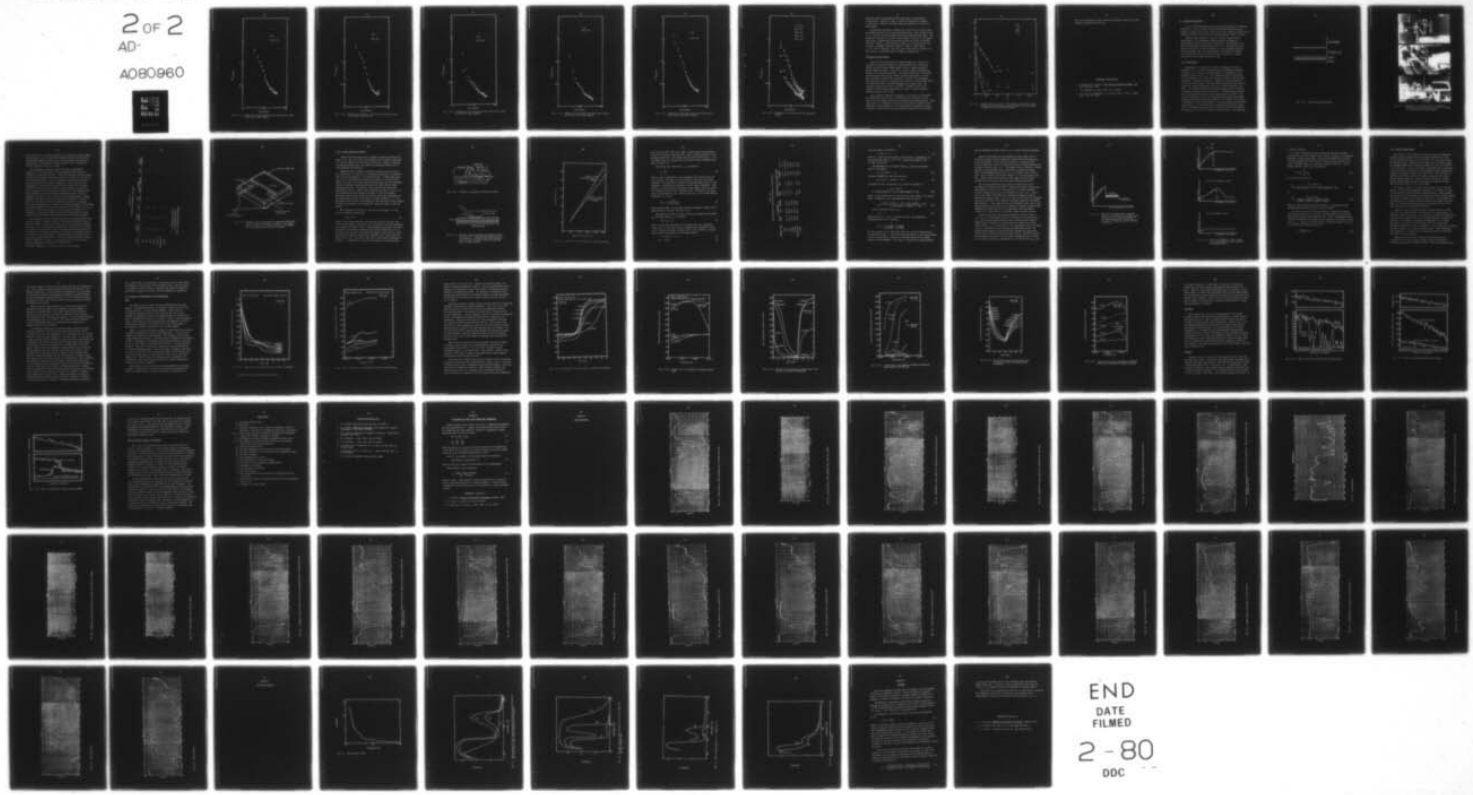

END
DATE FILMED
2-80
DDC

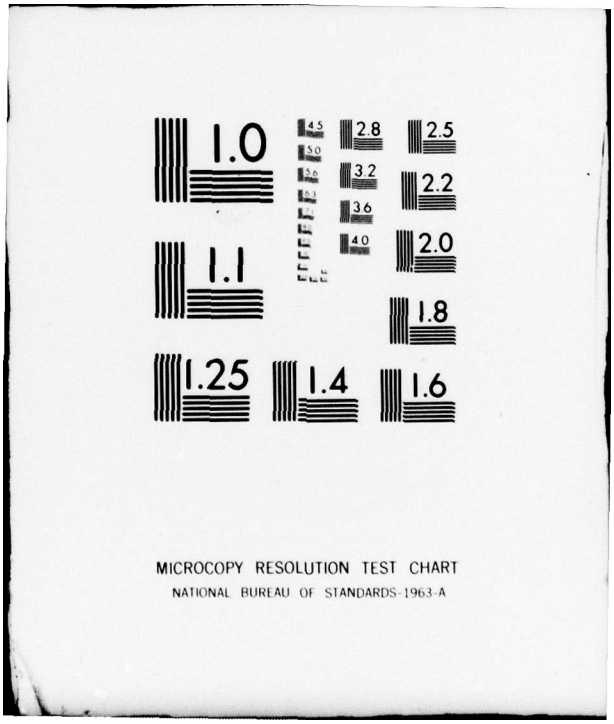
1.0
1.1
1.25
1.4
1.6
2.0
2.2
2.5
2.8
3.2
3.6
4.0
4.5
5.0
5.6
MICROCOPY RESOLUTION TEST CHART
NATIONAL BUREAU OF STANDARDS-1963-A

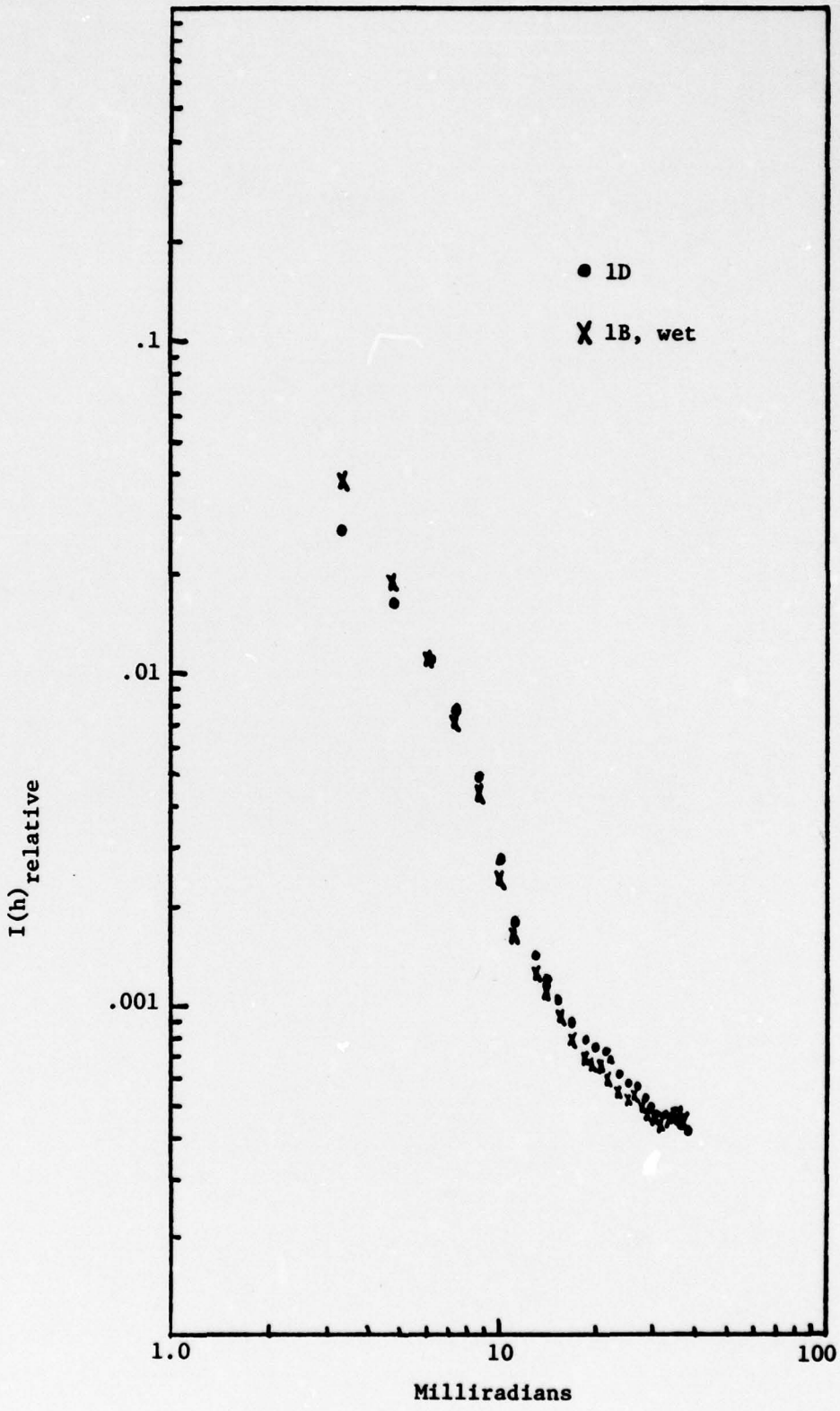

Fig. 3.4.2F. Comparison of scattering from fresh paint and wet, aged in salt water paint samples.

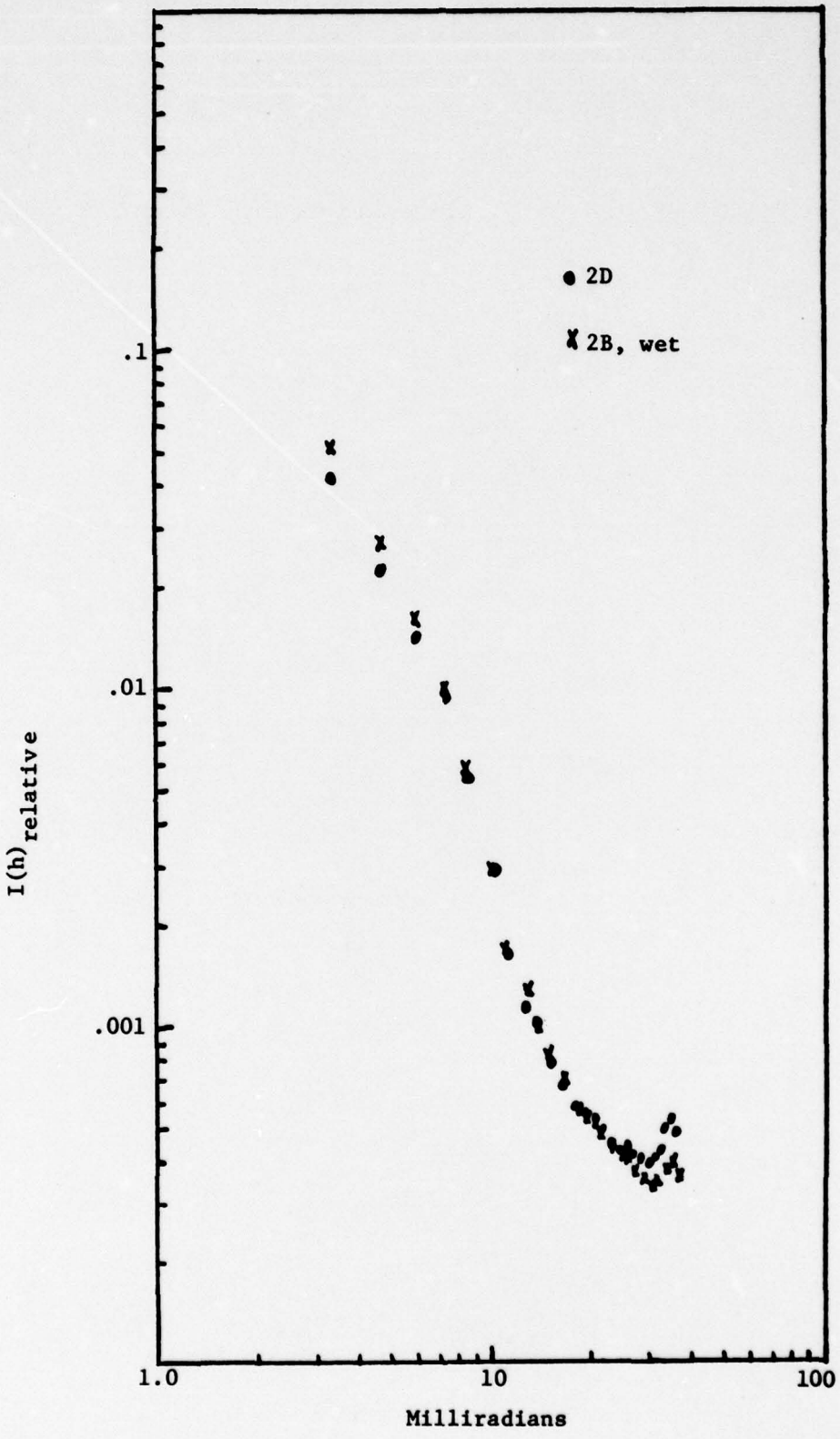

Fig. 3.4.2G. Comparison of scattering from fresh paint and wet, aged in salt water paint samples.

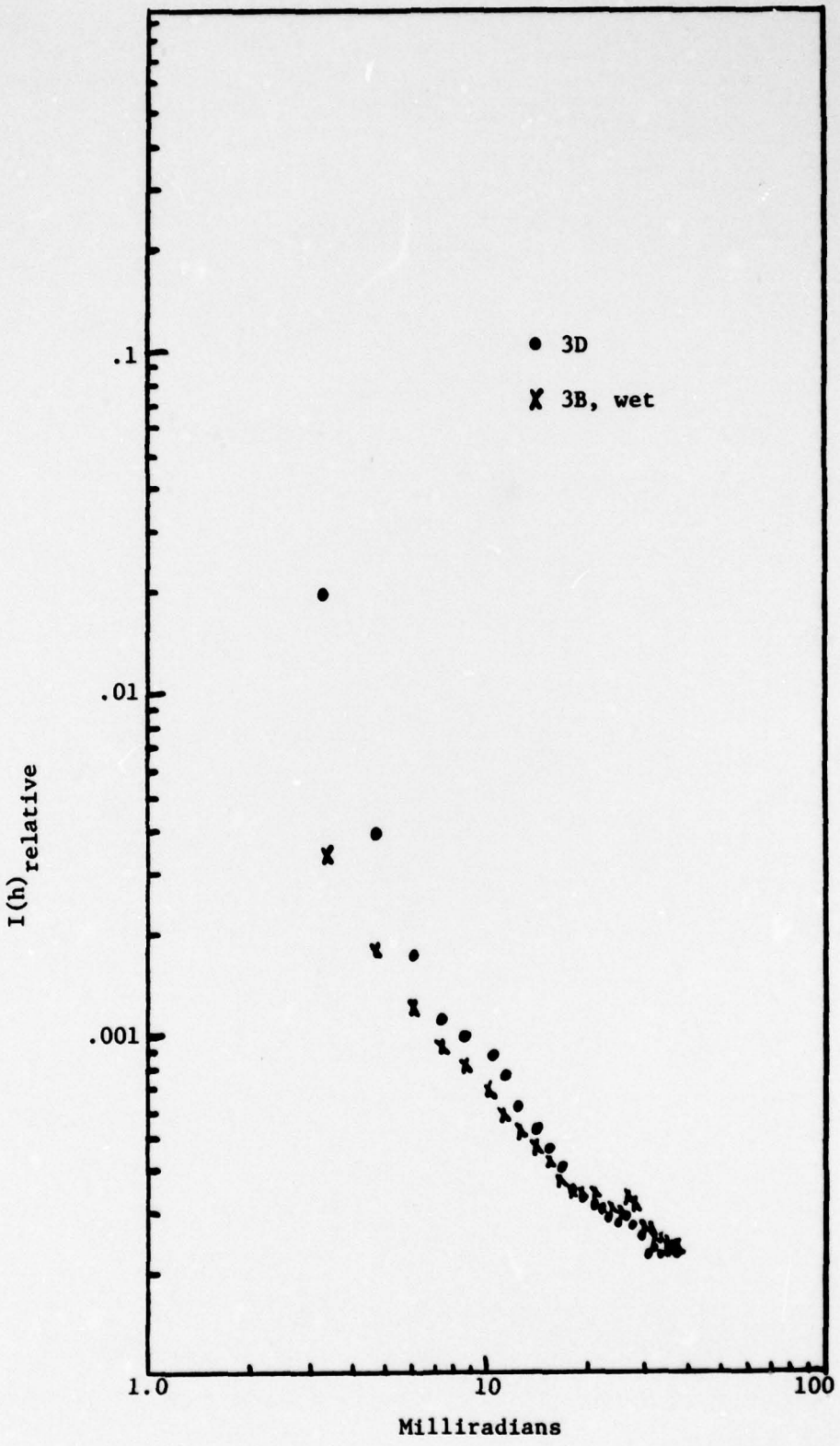

Fig. 3.4.2H. Comparison of scattering from fresh paint and wet, aged in salt water paint samples.

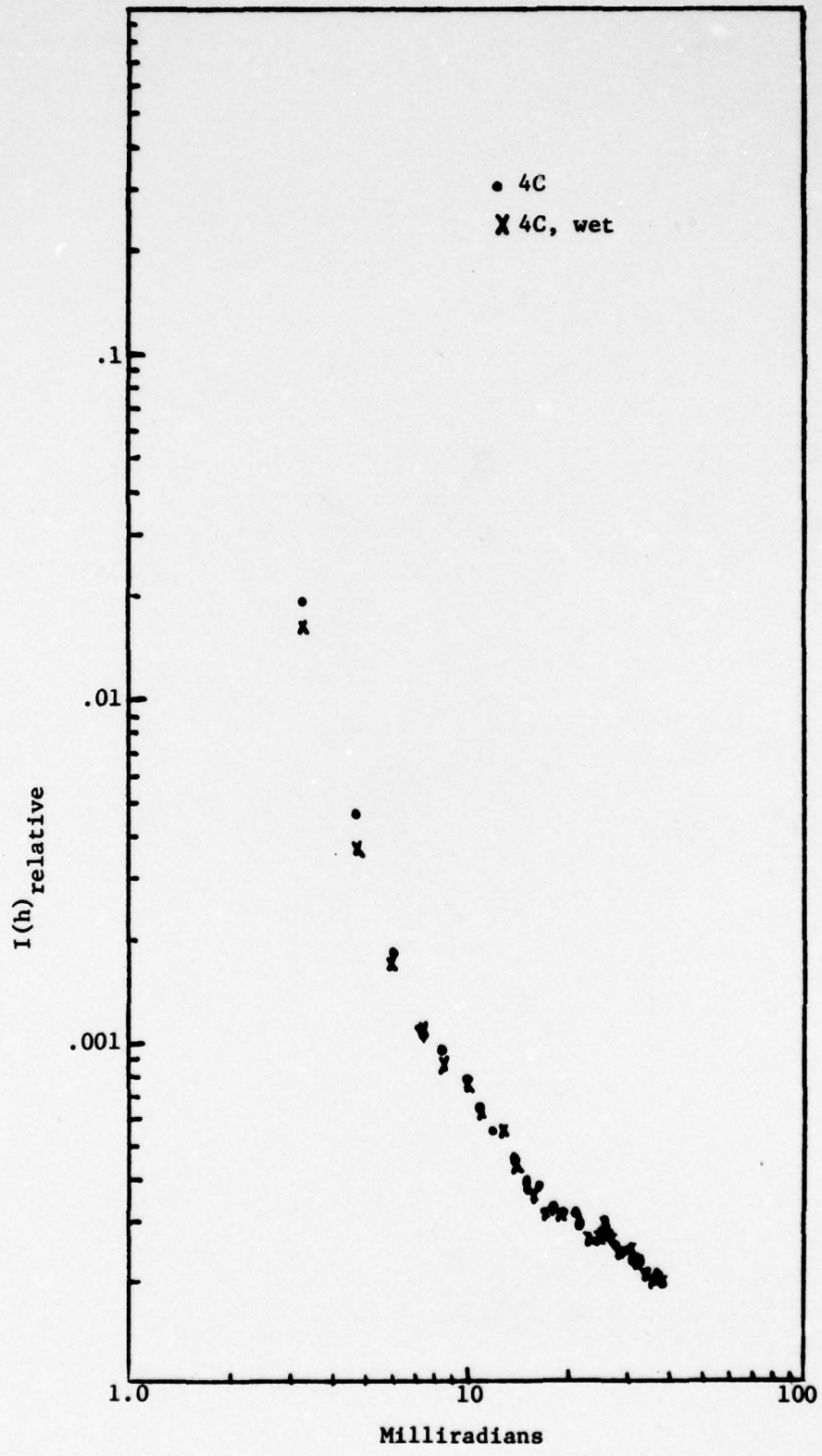

Fig. 3.4.2I. Comparison of scattering from fresh paint and wet, aged in salt water paint samples.

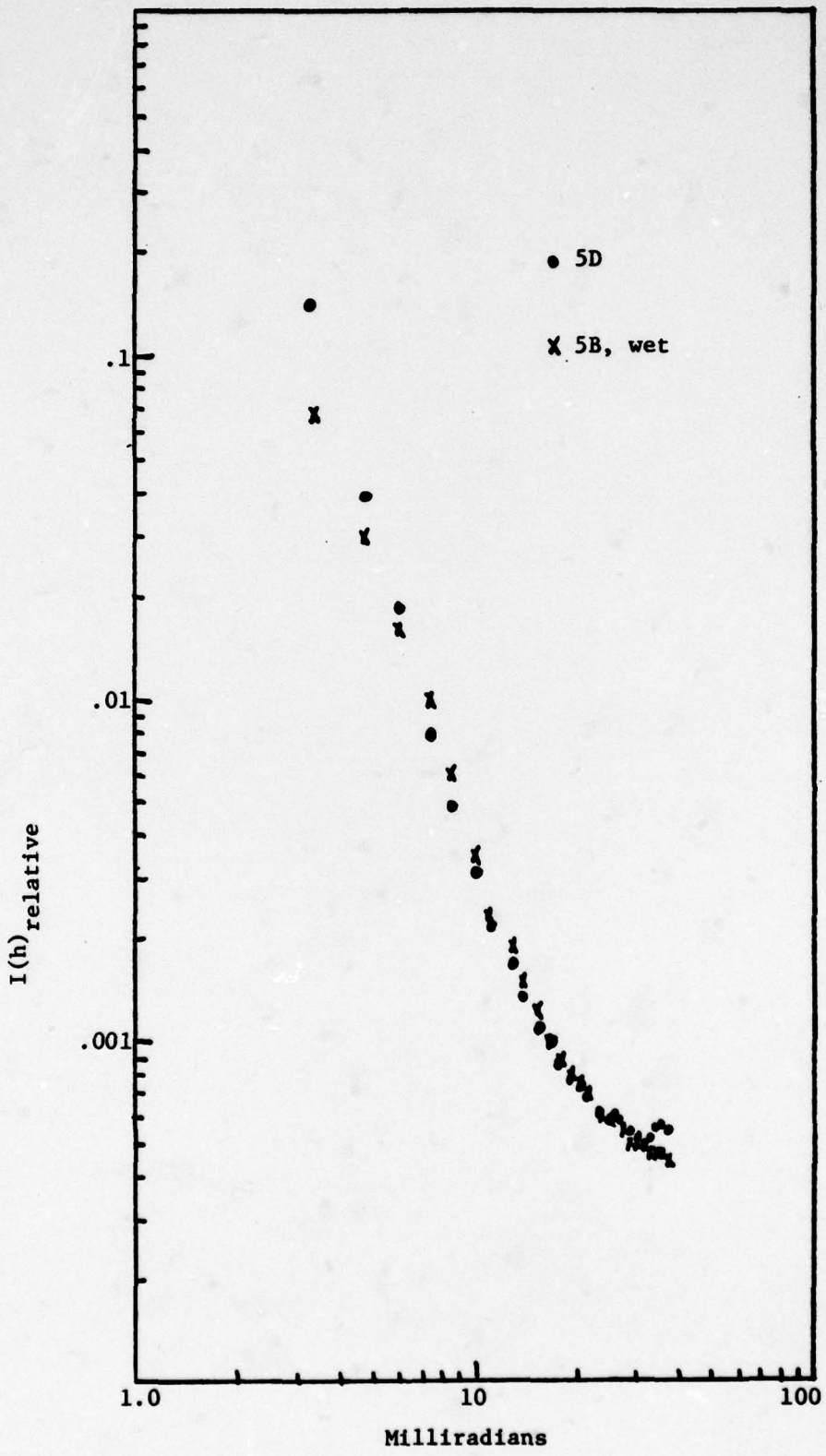

Fig. 3.4.2J. Comparison of scattering from fresh paint and wet, aged in salt water paint samples.

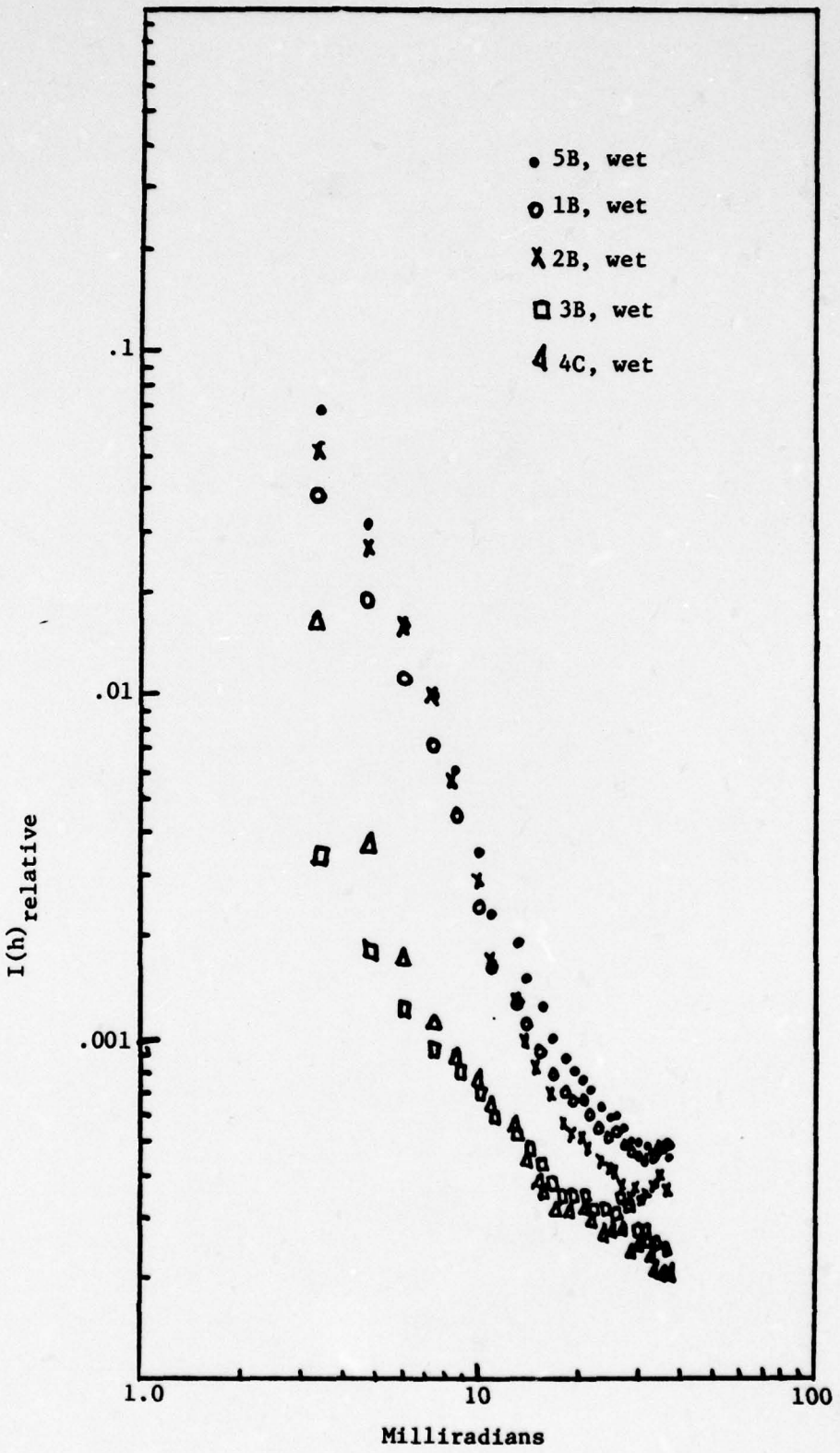

Fig. 3.4.2K. Comparison of scattering from wet, aged paint samples.

within the voids by preparing carefully-aged paints in varying NaCl concentrations. Finally, in Fig. 3.4.2K the wet samples are compared to each other. Basically, the same trends are observed as for the dry, fresh paints.

As mentioned previously, a Guinier plot of ℓn I(h) vs h^2 can be used to estimate the size of the x-ray scattering regions. This is done in Fig. 3.4.3. The data from the strongest and weakest scatterers are shown. The rationale of the plot is to pick a linear region of the plot in the region where there is appreciable x-ray scattering (the left side) and evaluate the slope. There is a distribution in sizes in all the data so that the technique is somewhat arbitrary; however, a range of sizes between r_g = 15 - 30Å is indicated. Note that this is the radius of gyration and may indicate a considerably smaller diameter, elongated void.

Discussion and Conclusions

These data have demonstrated that SAXS examination of paints is a sensitive and feasible technique for characterizing them. Scattering differences were observed between similar paints, larger differences between dissimilar paints. The effects of various aging treatments was evident in the scattering patterns. The general effect was for increased scattering after aging in H_2O, another increase after aging in 5 molar NaCl and another increase after diffusion of Ag^+/Sn^{++} into the paints. The scattering results are consistent with a model of a void network within the fresh paint which is increased (opened up) by aging in H_2O. The increased scattering after NaCl or Ag^+/Sn^{++} treatment is due to the presence of these heavier atoms within the voids. The size (radius of gyration) appears to be 15-30 Å.

This relatively superficial examination of the data can be extended with considerably more effort to determine the total internal surface area of the void network and the size distribution of scattering voids. There should also be a consistency in the void characteristics modulated by the different electron densities of each paint through the sequence of aging treatments. Given the size and electrochemical properties of the various

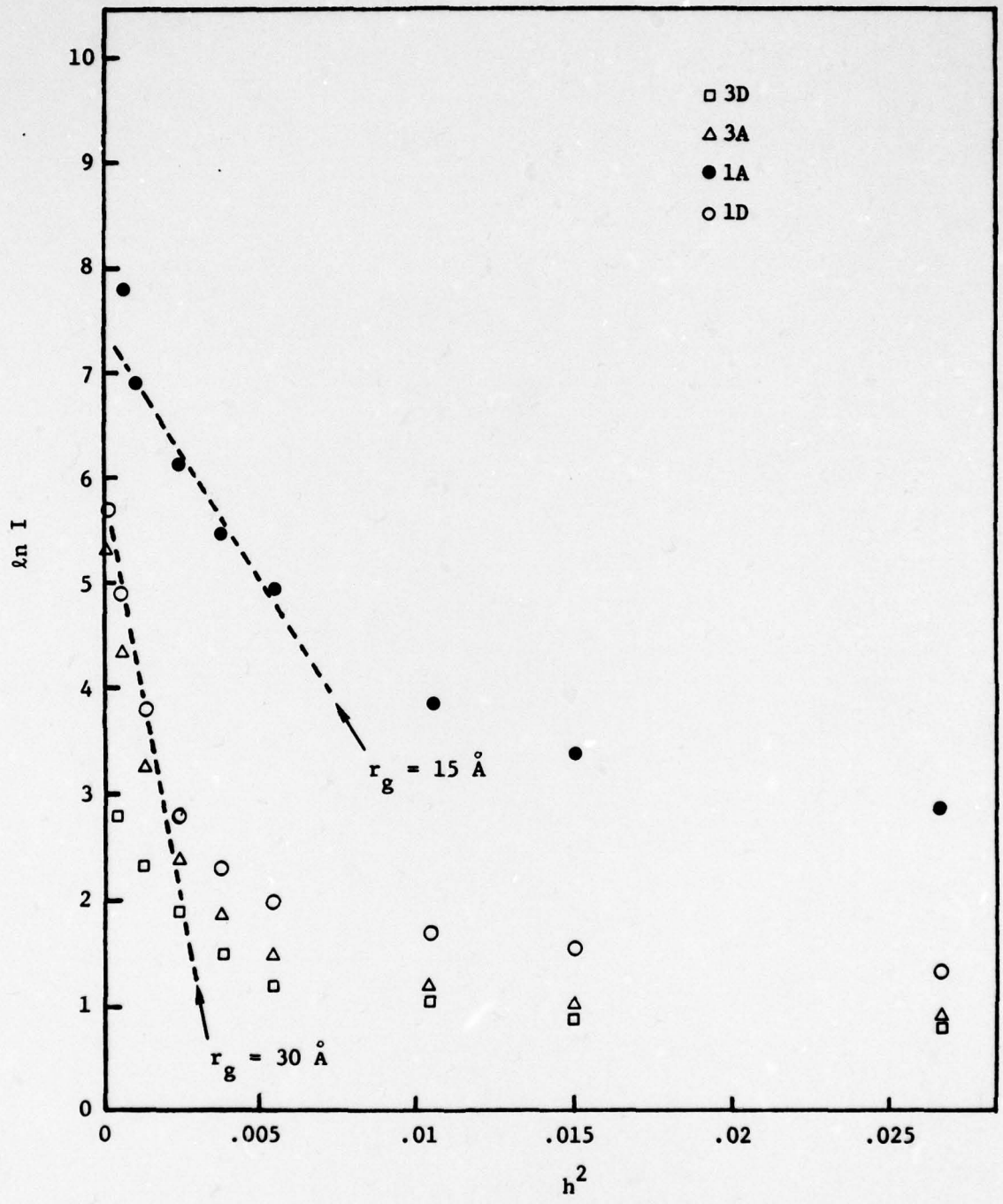

Fig. 3.4.3. Guinier plot of ℓn I vs h^2. The slopes in the region of most intense x-ray scattering were used to evaluate r_g, the radius of gyration of the scattering entities.

ions, some information could be derived concerning the sizes of the void openings contrasted with void size.

References (Section 3.4)

1. A. Guinier and G. Fournet, Small Angle Scattering of X-rays, John Wiley, New York, 1955.

2. R. W. Hendricks, J. Appl. Cryst. 11, 15 (1978).

3. J. S. Lin, R. W. Hendricks, L. A. Harris, and C. S. Yust, J. Appl. Cryst., 11, 621 (1978).

3.5 Adhesion Measurements

Iron is a structural metal that is nearly always painted for corrosion protection. It is, of course, the principal structural metal for Navy vessels. An oxide scale or rust forms on iron, but, except for the so-called weathering steels, the oxide is not protective against further corrosion.

Because cleaned surfaces of iron very rapidly form oxide skins upon exposure to the atmosphere, applied protective coatings are always bonded to oxide rather than to base metal. The structure of the metal coating system is illustrated in Fig. 3.5.1. Sometimes the metal surface is treated to obtain a phosphate or other conversion coating to which the polymer paint film better adheres. Any studies of adhesion on iron must take into account that the paint is bonded to a surface layer of some type rather than metallic iron.

3.5.1 Experimental

Experiments were performed to measure the adhesion of various coatings on iron. A machine, patterned after the Hesiometer described by Asbeck (1, 2), was built to measure adhesion. Photographs of the machine are shown in Fig. 3.5.2. The results obtained by this machine can be reproduced, for a single test speciman, at better than 95% reproducibility. The machine consists of a sharp steel knife suspended on four vertical leaf springs. The knife edge is pushed along the interface between the coating and substrate and cuts or peels the paint off the metal. The horizontal deflection of the knife against the leaf springs is measured and converted to cutting force. A thickness gauge measures the coating thickness adjacent to the cutting edge of the knife. Both the knife deflection and the coating thickness are measured with linear variable differential transformers (LVDT's). The position of the knife is measured by a linear potentiometer. The output signals from the hesiometer, LVDT's, and potentiometer were recorded as cutting force versus position, thickness versus position, and cutting force versus thickness. The coating was pre-cut with a scalpel along both sides of the hesiometer

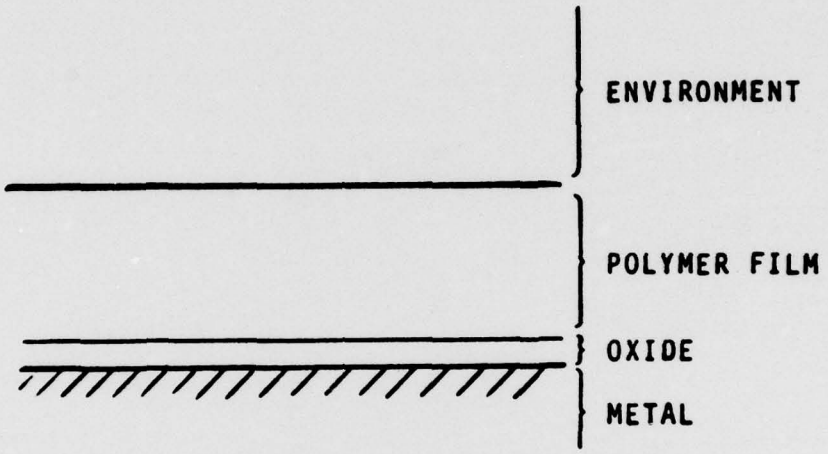

Fig. 3.5.1. Metal-oxide-coating system.

c

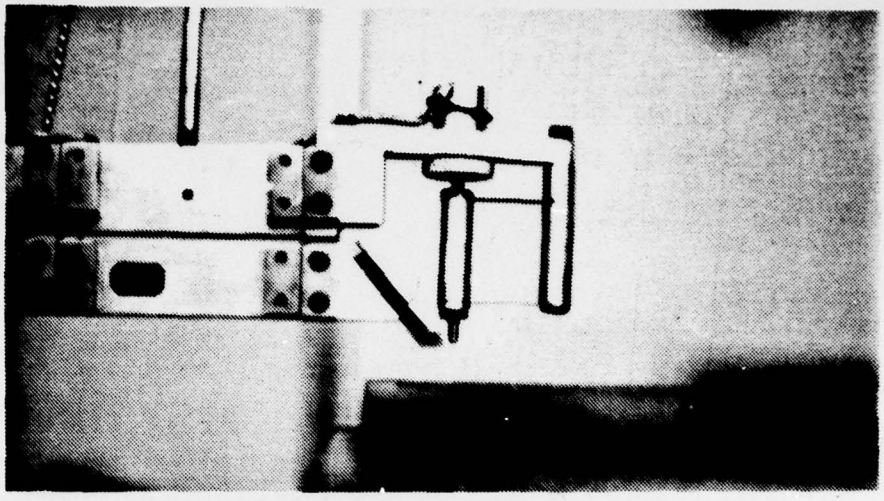

b

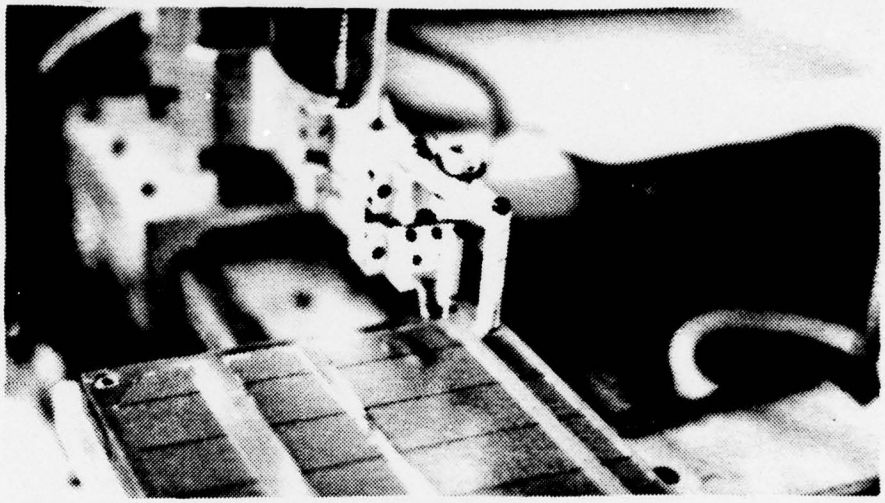

a

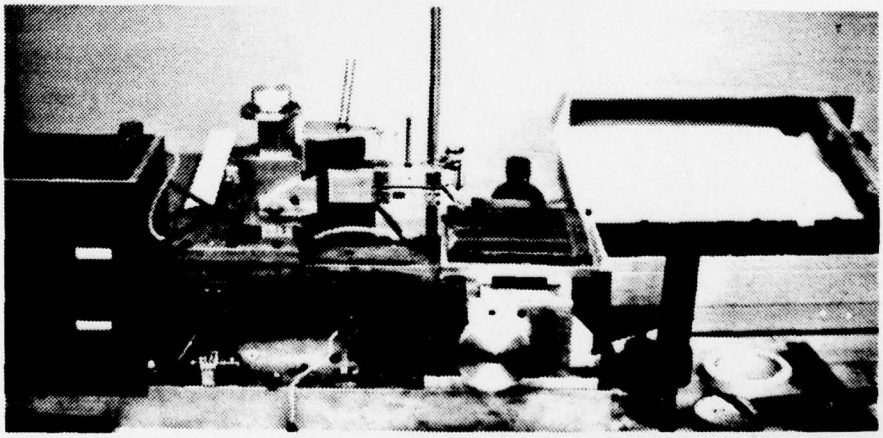

Fig. 3.5.2. Hesiometer: a. overall view; b. cutting head and steel plate with cuts on paint film; c. closeup of cutting head and thickness gauge.

knife width (¼ in.) to prevent peeling of the coating in the edge regions. A total weight of up to 933 grams (including the weight of the arm) was placed on the knife in order to keep it moving between the coating and the substrate. The knife has a forward velocity of 12.5 in./min and travels a distance of about 3.5 inches.

The experimental procedure involves painting a wedge-shaped coating onto a flat steel plate (coating thickness varied from about 0.0005 in. to more than 0.005 in.). After the coating has dried the plate is bolted to the hesiometer and the coating is cut into ¼ in. wide strips as previously described. About five reference position lines are then drawn on the paint surface with a marking pen. These lines are drawn perpendicular to the direction of knife travel and are used to measure the length of the paint strips before and after removal. A section of paint at one end of the test speciman is removed so the hesiometer knife begins sliding on the metal before encountering the paint. When the hesiometer is turned on, the cutting force (knife displacement), coating thickness, and knife position are simultaneously recorded. As shown in Fig. 3.5.7 (see surface energy calculations) the slope of the cutting force versus thickness curve is related to the shear strength of the coating, and at the transition from cutting to peeling (3) the cutting force ($F_{c,cr}$)* is related to the surface energy of the coating metal interface. By studying the surface energy (adhesion) under varying conditions we hope to discover relationships between adhesion and the corrosion mechanism.

The parameters affecting adhesion which have been investigated in this study are: types of coating, the short- and long-time exposure effects of moisture, methanol, aqueous electrolyte, and anodic and cathodic currents (see Table 3.5.1). For short-time experiments on the effects of solutions, the coating was covered with a paper towel which had been saturated with the liquid. For long-time experiments on the effects of solutions, and for all electric current experiments, a barrier was built around part of the plate with silicone rubber (Fig. 3.5.3) and the resultant well was filled with the appropriate solution. The remaining portion of the plate was used as a reference for comparison of cutting force.

---

* A table of nomenclature is given at the end of this section.

Table 3.5.1

Hesiometer Experiments Attempted

Paint	Friction Coeff.	Surface Energy	Water	NaCl Soln.	Current		MeOH	Solvent Cleaning
					Anodic	Cathodic		
VR2	-	-						
VR3	X	X	X	X	-	-	X	-
VR4	X	X						
E Epoxy	X	X	X				X	
K Epoxy	X	X		-		-		
Methacrylate	X	X	X	-	-	-	-	
N PUR	-	-						

X = Satisfactory Results

- = Preliminary Results

Blank = No Experiment Attempted

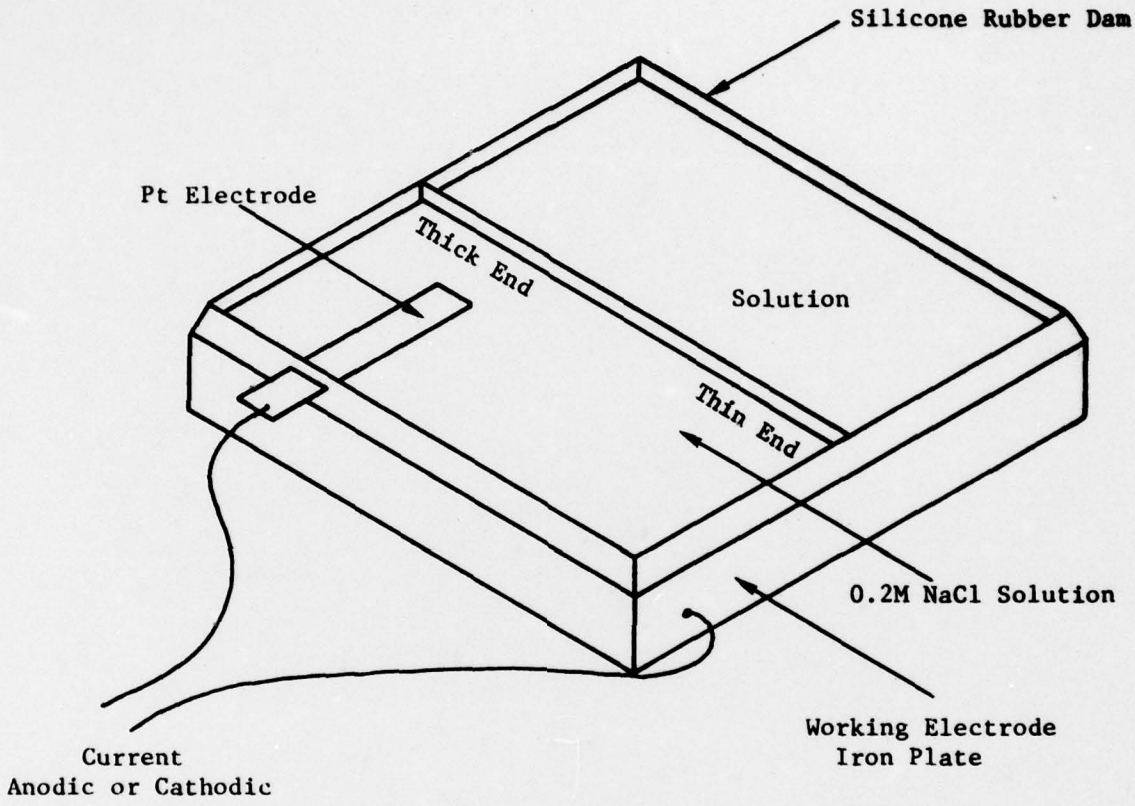

Fig. 3.5.3. Hesiometer plate as prepared for experiments testing the effects of anodic and cathodic currents. Two solution wells are shown: the left, in which current was passed, and the right, which was used as a reference.

3.5.2 Surface Energy Calculation

Several theories concerning the orthogonal cutting of materials are known (4-7). One of the first was proposed in the mid 1940's by Merchant (4,5) and was adapted to paint films by Asbeck (8). Asbeck's techniques are employed because none of the other more elaborate theories offer a clear advantage over Merchant's.

Merchant's theory attempts to describe the force vector acting on the cutting tool as a function of the physical properties of the material being cut and the geometry of the cutting process. A single shear plane, Fig. 3.5.4, is proposed which separates two regions of the paint film. Material in front of the knife, below the shear plane, has not experienced plastic deformation, whereas material above the shear plane has been permanently deformed. The Merchant theory proposes that this plastic deformation occurs in a single plane defined by the angle ϕ in Fig. 3.5.4. This assumption has been checked by Merchant for only one polymeric material (celluloid), but Asbeck has used the same theory extensively and has claimed great success in applying it to paint polymers (1, 2, 3, 8). The present work is based on the supposition that the theory is well founded for paint type polymers, and no additional checks were made to test that premise.

The coefficient of friction, μ, and the friction angle, τ, in Fig. 3.5.4, are defined by Asbeck (8),

$$\mu = \frac{F}{W} = \tan \tau \qquad (1)$$

where F is the force required to slide the knife across the paint, and W is the total weight on the knife. The coefficient of friction is obtained by recording the friction force, F, while changing the weight on the knife, as the heel of the knife is sliding on the coating surface (Fig. 3.5.5). Two plots of the friction force versus the weight of the knife for a vinyl chloride -vinyl acetate- vinyl alcohol copolymer resin coating (VR3) are shown in Fig. 3.5.6. The slope of each plot is the average coefficient of friction, μ. Although the correlation coefficients for each individual

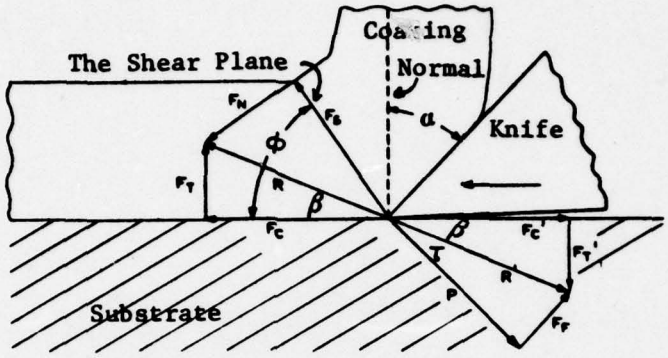

Fig. 3.5.4. Merchant's orthogonal cutting force vectors.

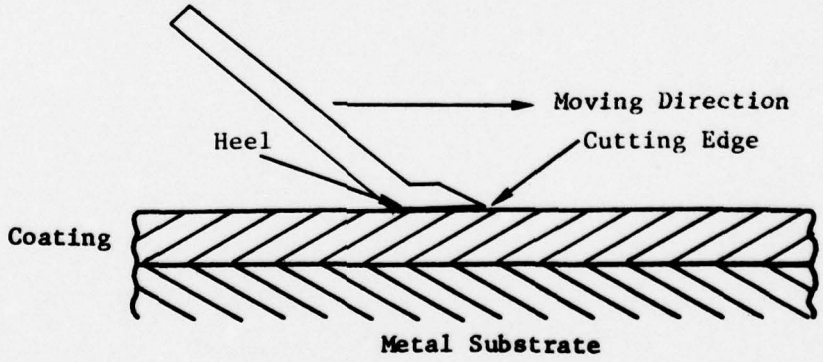

Fig. 3.5.5. The most consistent method of measuring friction coefficient (μ). The horizontal sliding force (F) is recorded as a function of the total vertical force (w) while the knife slides over the paint surface without cutting.

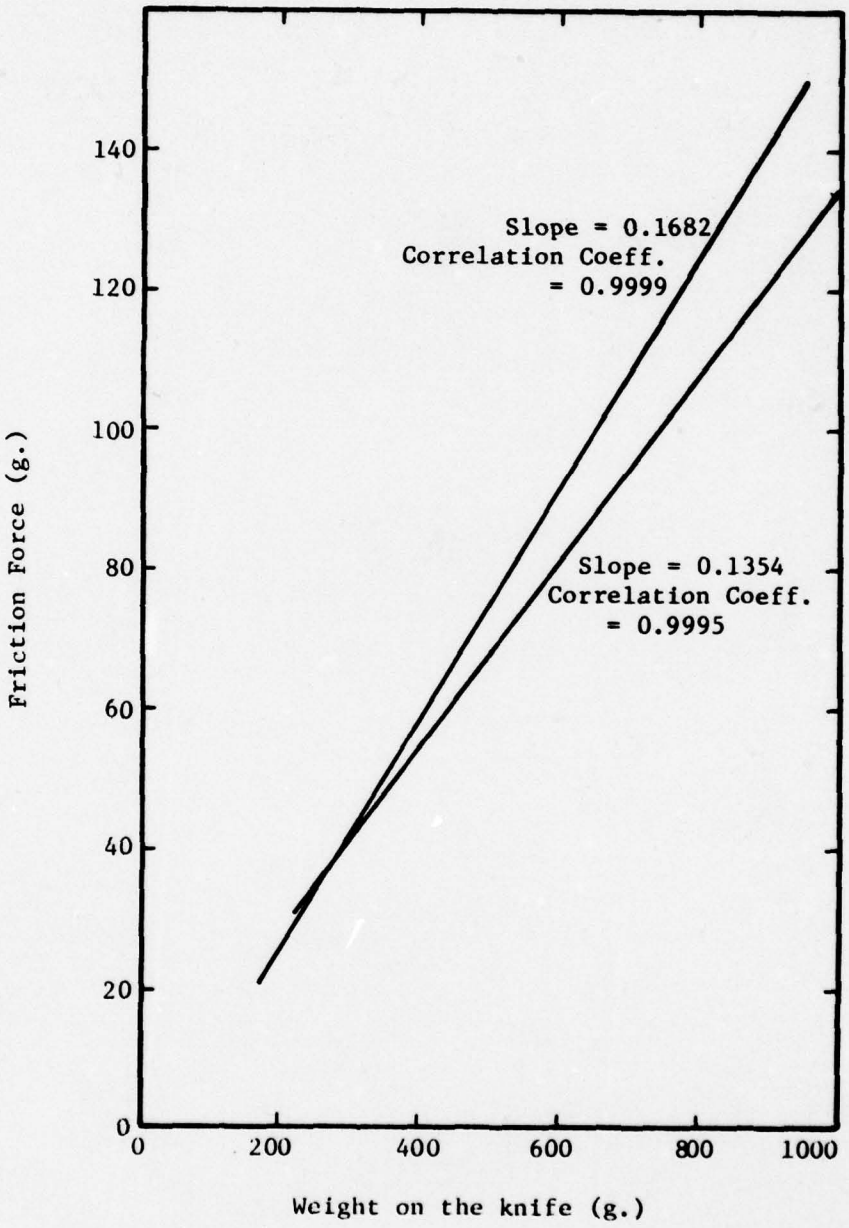

Fig. 3.5.6. The plot of the coefficient of friction for VR3.

plot are better than 0.999, the slopes of plots obtained from different areas of the coating varied about 20%. This is typical behavior for the coatings studied here. The average values of the friction angle, τ, for the various types of coatings used in the surface energy calculation are shown in Table 3.5.2.

The coating chip length ratio, r_L, is defined by

$$r_L = \frac{L_2}{L_1} \tag{2}$$

where L_1 and L_2 respectively are the lengths of the coating before and after removal. The value of L_2 was observed to vary with the coating thickness. This represents a change in the Merchant shear angle, ϕ, with thickness, a condition not discussed by either Asbeck or Merchant. Best values of L_2 were obtained by measuring a small segment (about 1.5 cm) of the coating at the thin end of the paint strip. The angle of the shear plane, ϕ, with respect to the substrate (see Fig. 3.5.4) has been derived by Merchant (4, 5) to be

$$\tan \phi = \frac{r_L \cos \alpha}{(1 - r_L \sin \alpha)} \tag{3}$$

where the rake angle α is the angle between the substrate normal and the upper surface of the knife (see Fig. 3.5.4).

Many materials exhibit a linear relationship between shear strength, S_s', and normal stress, S_n, as follows:

$$S_s' = S_o + k\, S_n \tag{4}$$

where S_o is the shear strength of the coating under zero compressive stress, and k is the slope of shear strength versus compressive stress curve. Moreover, Merchant has shown that for such materials a relation exists between the constant k and the shear angle ϕ:

$$k = \cot(2\phi + \tau - \alpha) \tag{5}$$

$$\text{or } k = \cot(C) \tag{6}$$

Table 3.5.2

Characteristic Surface Free Energy for Various Paint

Type of Paint	C (degrees)			Surface Energy (erg/cm^2 x 10^5)			
	High	Low	Average	High	Low	Average	τ
VR2				27.51		24.44	7.41
VR3	94.22	82.46	88.65	12.77	7.17	10.27	10.67/8.12
VR4	91.11	89.09	90.4	18.53	12.95	16.18	15.09
E Epoxy	87.99	78.22	83.10	7.64	6.95	7.30	11.86
K Epoxy	84.42	81.23	82.83	-	-	9.46	8.23
Methacrylate	95.61	81.40	90.38	34.56	6.57	15.19	8.05
N PUR				6.00	5.01	5.50	17.11

where the angle C is defined as:

$$C = 2\phi + \tau - \alpha \tag{7}$$

Since C, τ, and α are all constant, ϕ must be also. Furthermore, for the special case where k = 0, C = 90°. Asbeck has assumed C = 90° for most of his work.

The expression for the normal stress, S_n, acting on the shear plane, ϕ, is given by

$$S_n = S_s' \tan(\phi + \tau - \alpha) \tag{8}$$

The shear strength, S_s', has been derived as

$$S_s' = S_o/[1 - k \tan(\phi + \tau - \alpha)] \tag{9}$$

An equation for the cutting force, F_c, derived by Merchant is

$$F_c = \frac{S_o \, t \, w \, \cos(\tau-\alpha)}{[\sin \phi \cos(\phi + \tau - \alpha) - k \sin \phi \sin(\phi + \tau - \alpha)]} \tag{10}$$

where t is the thickness of the coating and w is the width of the coating strip. Elimination of S_o using Equations 9 and 10 leads to

$$S_s' = \frac{F_c \, [\sin \phi \cos(\phi + \tau - \alpha) - k \sin \phi \sin(\phi + \tau - \alpha)]}{t \, w \, \cos(\tau-\alpha)[1 - k \tan(\phi + \tau - \alpha)]} \tag{11}$$

Beta is defined as (Fig. 3.5.4)

$$\beta = \alpha - \tau \tag{12}$$

Substitution for ϕ, τ, and α in terms of β and C, and simplifying trigonometrically, Eq. 11 becomes

$$S_s' = \frac{F_c}{t \, w \, \left[\tan\left(\frac{C-\beta}{2}\right) + \cot\left(\frac{C+\beta}{2}\right)\right]} \tag{13}$$

All the variables on the right hand side of Eq. 13 can be obtained from the experimental data. τ and ϕ are calculated from Eq. 1 and 3 respectively. α and w are the physical constants of the knife which can be obtained directly from measurements. The output of cutting force versus thickness

from the hesiometer provides values of F_c at various coating thicknesses, t.

Asbeck (3) has shown that the mechanism of paint removal can be expected to change from the cutting mode, quantitatively discussed here, to the peeling mode. Also according to Asbeck, it is expected that, in the cutting mode, a plot of cutting force versus coating thickness will be linear as shown in Fig. 3.5.7. The removal force is reported to change abruptly at the transition from cutting mode to cracking or peeling mode, and the maximum cutting force, $F_{c,cr}$, occurring at this critical point, can be related to the surface energy, T, of the paint–metal interface. Asbeck claims these results are very common, but the results obtained from this study do not reveal these same characteristics.

The present experiments, when plotted as removal force versus thickness, are different from Asbeck's examples and depend on paint type. Some examples of cutting force data as well as the present proposed critical cutting force, $F_{c,cr}$, are illustrated in Fig. 3.5.8. A rapid drop in the removal force where the cutting mode changes to peeling mode cannot always be found. Only in the case of soft epoxy (not throughly cured) was the removal force observed to decrease sharply at the peeling mode transition. Later, when the epoxy was completely cured, the coating became brittle, and the removal force reduced to a minimal constant value. Experience has shown that all the coatings which have been studied require ten to thirty days for the surface energy to become constant.

Asbeck has derived a relationship between the critical cutting force, $F_{c,cr}$, and the surface energy of the paint, but the evaluation of $F_{c,cr}$ is not always simple because no sharp transition from cutting to peeling exists. Because of the difficulties in choosing the critical cutting force, $F_{c,cr}$, and variations in the measurement of the chip length ratio, r_L, some form of curve smoothing was deemed appropriate. The method chosen consisted of fitting the best straight line through the initial cutting force versus paint thickness curves. The point at which this straight line deviates from the actual experimental data is chosen as the critical point and is represented by a critical force, $F_{c,cr}$, and

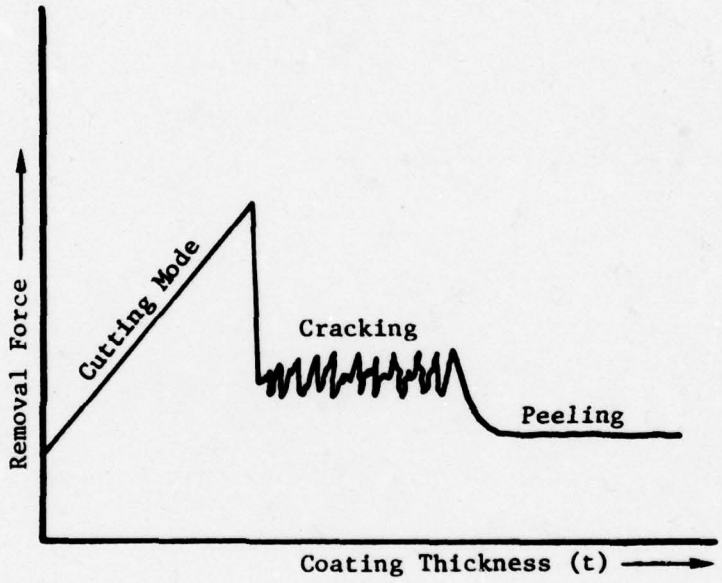

Fig. 3.5.7. Qualitative representation of Asbecks adaption of Merchants theory showing total cutting force vs coating thickness, and the transition from the cutting mode through an intermediate region (cracking) to peeling.

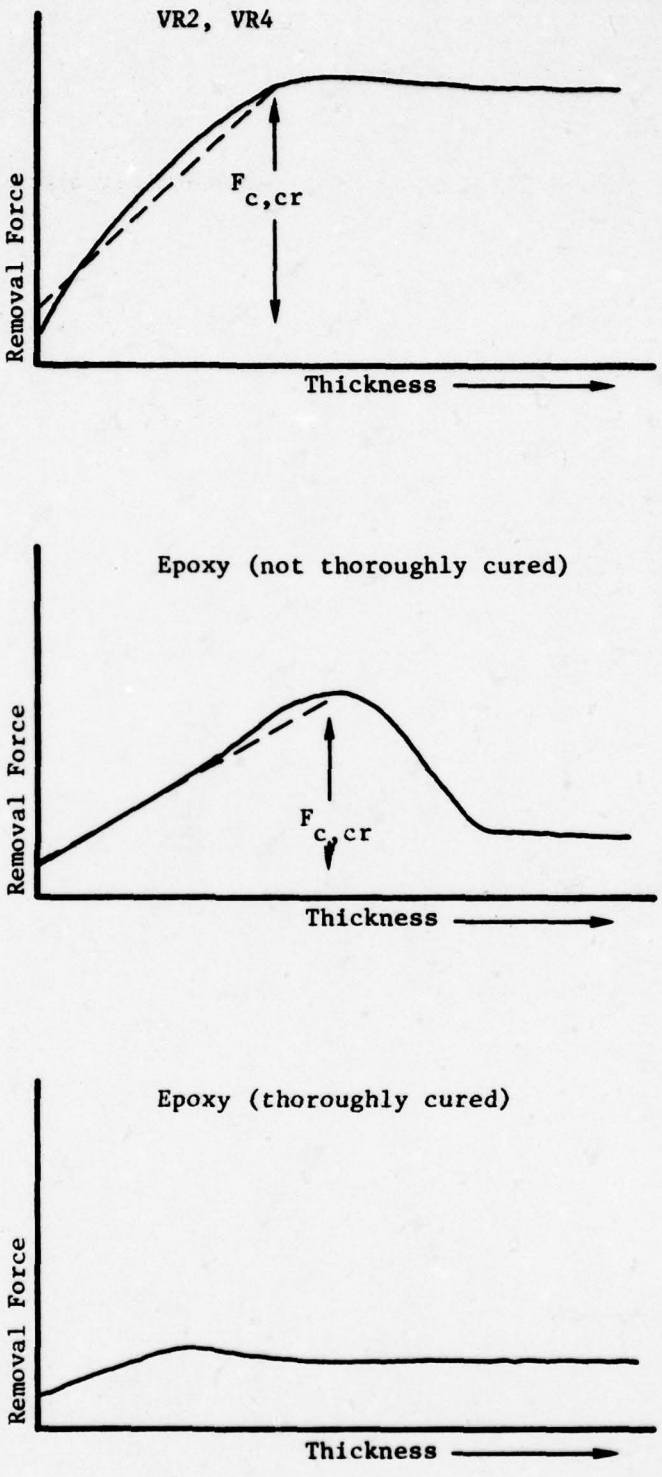

Fig. 3.5.8. Qualitative examples of total cutting force vs thickness for three recently investigated paints.

a critical thickness.

In order to establish the best straight line through the initial portion of the force vs thickness curve, values of S_s' and S_n are calculated using Eqs. 13 and 8 respectively. These stress variables are evaluated at several thicknesses in what appears to be the initial portion of the curve. Intercept values, S_{oi}, are then calculated, using Eq. 4, and an average intercept value, $\overline{S}_o$, is obtained as

$$\overline{S}_o = \frac{1}{N} \sum_{i=1}^{N} S_{oi} \tag{14}$$

Eq. 10 can now be written as

$$\frac{F_c}{t} = \frac{\overline{S_o}\ w \cos(\tau-\alpha)}{[\sin\phi \cos(\phi + \tau - \alpha) - k \sin\phi \sin(\phi + \tau - \alpha)]} \tag{15}$$

or,

$$\frac{F_c}{t} = \frac{\overline{S_o}\ w \cos(-\beta)}{\sin\left(\frac{C+\beta}{2}\right) \cos\left(\frac{C-\beta}{2}\right) - k \sin\left(\frac{C+\beta}{2}\right) \sin\left(\frac{C-\beta}{2}\right)} \tag{16}$$

where F_c/t is the average slope from the plot of cutting force versus thickness which has been recorded on the XY recorder.

In order to calculate the surface energy, a straight line having a slope calculated by Eq. 16 is fitted to the experimental data plotted as cutting force versus coating thickness (Fig. 3.5.8). The maximum cutting force that intercepts the straight line is considered the critical cutting force, $F_{c,cr}$. Finally, the characteristic surface free energy, T, is calculated using the following equation (3).

$$T = \frac{3}{2} \frac{F_{c,cr}}{w} \tan\beta \tag{17}$$

3.5.3 Surface Energy Results

The results of the characteristic surface free energy experiments obtained from seven types of paint are listed in Table 3.5.2. The surface energies varied from 5 x 10^5 erg/cm^2 to 34 x 10^5 erg/cm^2 among the coatings listed. These results are higher than the surface energy for polymethyl methacrylate reported by Asbeck (3) (1.3 x 10^5 erg/cm^2 to 5.3 x 10^5 erg/cm^2). Since a full range of experiments was not performed on VR2 and N PUR, the reported surface energies for these coatings were obtained by assuming the angle C was equal to 90°. This fact may be important since these two paints represent the high and low values of surface energy respectively. Except for VR2 and N PUR, the average surface energies among the other five paints are reasonably constant. They only vary by about 5 x 10^5 erg/cm^2 (40%).

The results in Table 3.5.2 show a fairly large scatter in surface energy. A more detailed examination shows this to be largely the result of variations in C between different substrate plates. Asbeck assumed that C equals 90° which eliminates some scatter in surface energy; however, it implies a constant shear strength for the paint. In reviewing Eq. 7, the variation of C is mainly caused by changes in the angle of the shear plane, ϕ. The inaccuracy associated with calculating ϕ is one of the major difficulties encountered in this study.

Equation 16 clearly supports Asbecks contention that the cutting force (F_c) is a linear function of thickness in the cutting region. As discussed previously (see Fig. 3.5.8) this has not always been observed in practice, and it appears likely that the shear angle ϕ is a function of thickness. This feature is contained in Rubenstein's (6, 7) theory, but overall the scatter in surface energy (T) is not reduced when Rubenstein's analysis is used. Furthermore, if ϕ is a function of thickness, the shear strength is not linear in normal stress. After considering these problems, it is clear that much opportunity exists for improving the theory of cutting polymers.

Despite the fact that some problems were encountered during evaluation of the surface energy, results obtained using blades of different angle (α) gave consistent results. This is encouraging because

the surface energy is a property of the metal-substrate-paint combination only. The consistent results indicate that even if the accuracy of the method is questioned, a relative measure of adhesion (T) can be obtained. On this basis, a series of experiments was designed to establish effects of various conditions (passage of current, etc.) on the measured adhesion. The effects of water, salt solution (NaCl), anodic and cathodic currents, and methanol were studied.

When the surface energy (adhesion) of a single test speciman was evaluated at different points on the substrate, quite reproducible results were obtained (±20%). When these surface energy values were compared to those obtained from different substrate blocks (same-type iron substrate) wider variations were observed. In the experiments testing the environmental effects, one-half of the substrate block was exposed to the new environment while the remaining half was maintained at a standard condition as a reference.

An additional complication is encountered when evaluating adhesion under wet conditions. For reasons which will become obvious, time is a critical factor in these experiments. Eq. 16 indicates that the cutting force is a function of paint thickness, t, and blade angle, α. The critical cutting force and critical thickness are thus functions of blade angle, and a transition from cutting to peeling is not always observed for a given blade angle and thickness variation (thin to thick sides of the paint wedge). Under normal, dry conditions, several blades can be tested, and the ones producing the best results can be chosen and compared. Under nonsteady-state conditions, the time required to find the appropriate blade was considerably longer than the time constant for adhesion change. Thus cutting force, not surface energy, was recorded under these conditions. The measured cutting force is not related to the surface energy except at the cutting-to-peeling transition. Most of the cutting forces measured under wet conditions are much lower than those obtained on dry samples. If it is assumed that this means the wet samples are peeling, the transition from cutting to peeling must have occurred, for a given α, at smaller paint thicknesses in the wet tests. Ignoring the change in mechanical properties caused by solvent swelling, this fact indicates a decreased surface energy under wet conditions. Although the mechanical properties

have a direct effect on the measured cutting force, most of these paints are designed to exclude water from the polymer matrix. They thus swell only slightly in polar solvents. Consequently the change in mechanical properties is expected to be small, and the assumption is reasonable.

3.5.4 Effect of Environments on Coating Adhesion

Water

The effects of water on VR3, E epoxy, and methacrylate have been studied. Qualitatively speaking, the presence of water on any of these coatings partially or totally destoys adhesion. Usually when the coatings were exposed to water for more than one hour, the coating changed from transparent to white, and simultaneously the cutting force, which corresponds only indirectly to adhesion, reached a constant minimum value. Upon drying, the coating regained its clear appearance, and the cutting force returned to its original value. The friction angle, τ, was observed to decrease only about 2° for wet paint samples.

Figs. 3.5.9 and 3.5.10 show the change of cutting force with time and thickness for methacrylate exposed to distilled water. In the first 20 minutes, the cutting force drops sharply. This probably reflects either a high permeability of water or high sensitivity of adhesion to the presence of water. Experiments on diffusion and equilibrium solubility properties of the coatings might help determine which of these is the most important parameter. The rates of decrease in cutting force are very similar for all coating thicknesses from 1.7 mils to 3.9 mils. Assuming a diffusivity for water of about 10^{-8} cm^2/s, the diffusion times for the thin and thick sides of the paint wedge are calculated to be about 30 min and 160 min, respectively. The fact that such differences are not apparent in the cutting force versus time plots may indicate that another phenomenon is involved in the loss of adhesion.

When methacrylate was dried in air at room temperature after being exposed to liquid water for 15 hours, the cutting force regained about 90% of its original value. The rate of recovery of cutting force is

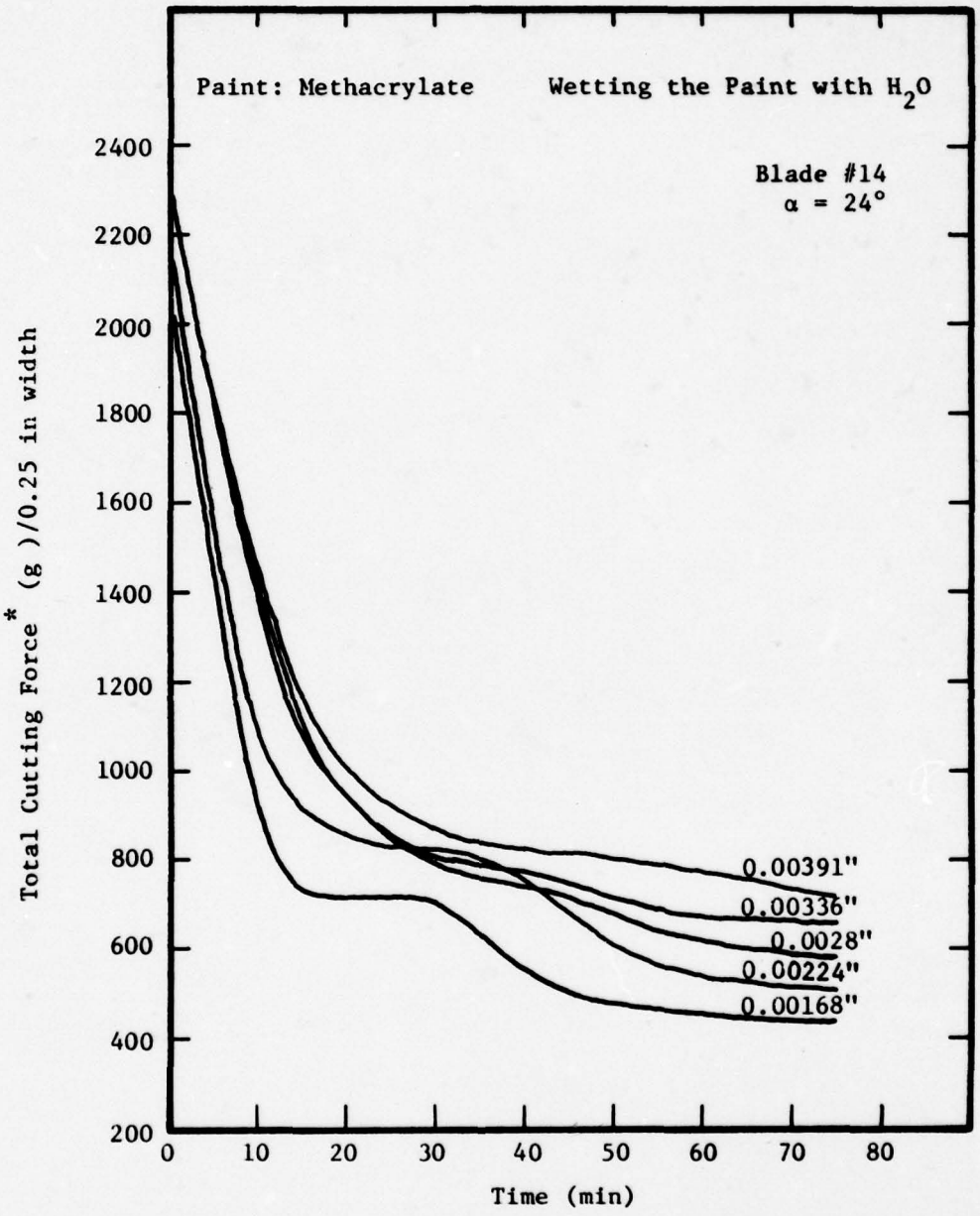

Fig. 3.5.9. Cutting force vs wetting time at different thicknesses.

* Includes friction force and blunt knife effect.

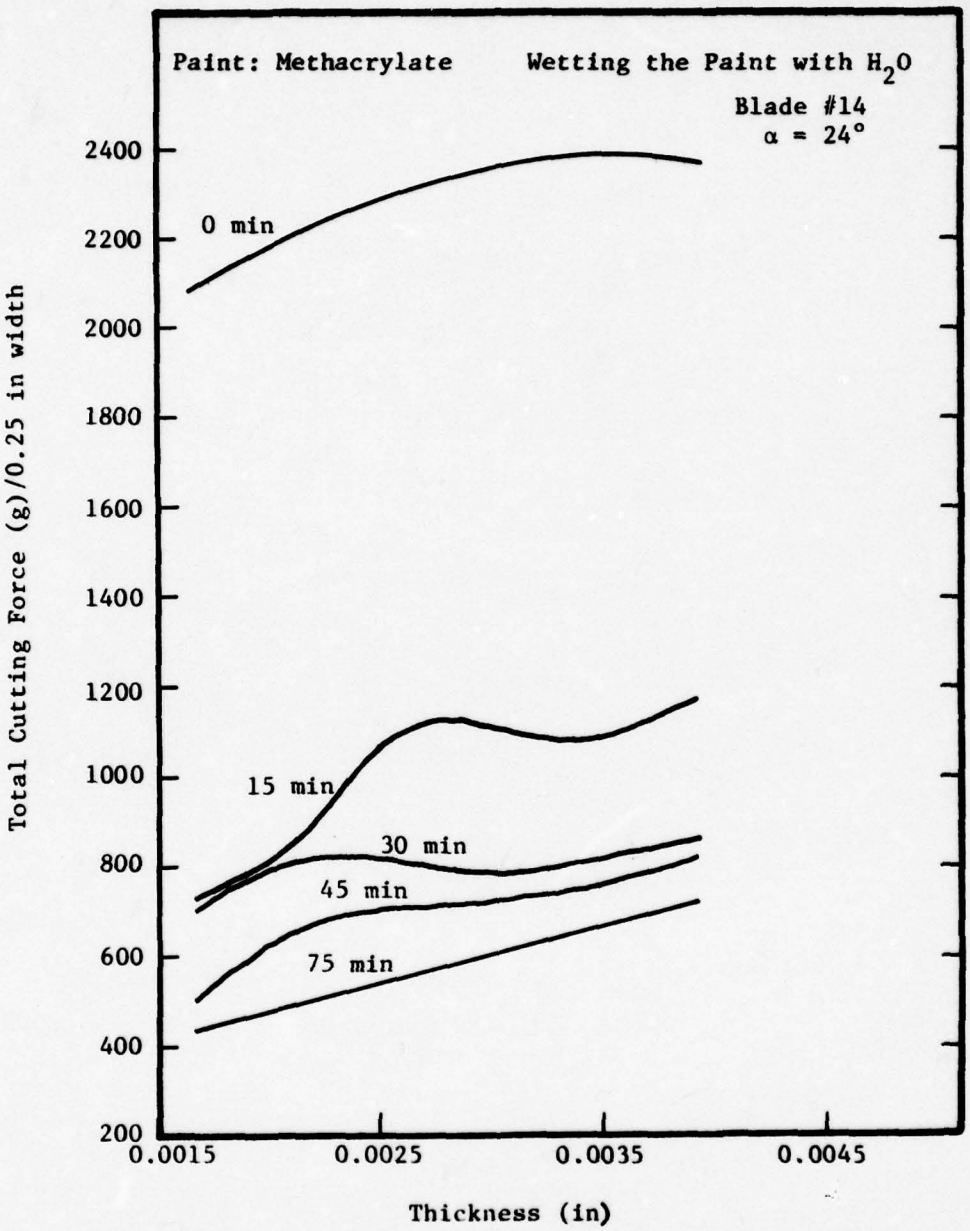

Fig. 3.5.10. Cutting force vs thickness at different wetting times.

shown in Figs. 3.5.11 and 3.5.12. During the initial 30 minutes, the adhesion remained approximately constant. This is expected because after soaking for a long period of time, the coating at the substrate-coating interface is saturated with water. The variation of interfacial water concentration thus depends on the coating thickness, and this may explain why the thick end (4.5 mils) has a slower recovery rate than the thin end (1.7 mils).

When VR3 was exposed to distilled water and then dried, in a short-time experiment, the effect was slightly different. Figs. 3.5.13 and 3.5.14 show the change in cutting force during the distilled-water wetting and drying processes. The decrease of cutting force is slower for VR3 than for methacrylate. This is possibly a result of lower water permeability in VR3. The adhesion was completely destroyed in 45 minutes for all thicknesses. During the drying period, it was surprising to find that the thick end recovered faster than the thin end. This may have been the result of lower average water content at the thick end due to incomplete wetting as a result of the short exposure time of 45 minutes. On the thin end (0.8 mil), oxygen diffused through the coating and oxidized the iron substrate. Hence the substrate beneath the thin coating had started to rust, and in these regions the adhesion never recovered its original value.

When E epoxy was used for wetting experiments, the rate of change of cutting force was observed to be approximately constant for all thicknesses as seen in Fig. 3.5.15 and 3.5.16. Moreover, similar observations apply to the recovery rate. This could be a result of the structure of the epoxy, a highly cross-linked polymer, which exhibits uniform effects upon wetting with water.

Based upon these findings, and lacking an adequate theory of adhesion, one would conclude that water permeability has a great effect on the rates of decrease and recovery of adhesion during wetting and drying. Saturation with water is probably not required to reduce adhesion markedly, and water alone does not have a permanent effect on adhesion unless the interface between the coating and the iron substrate has been contaminated

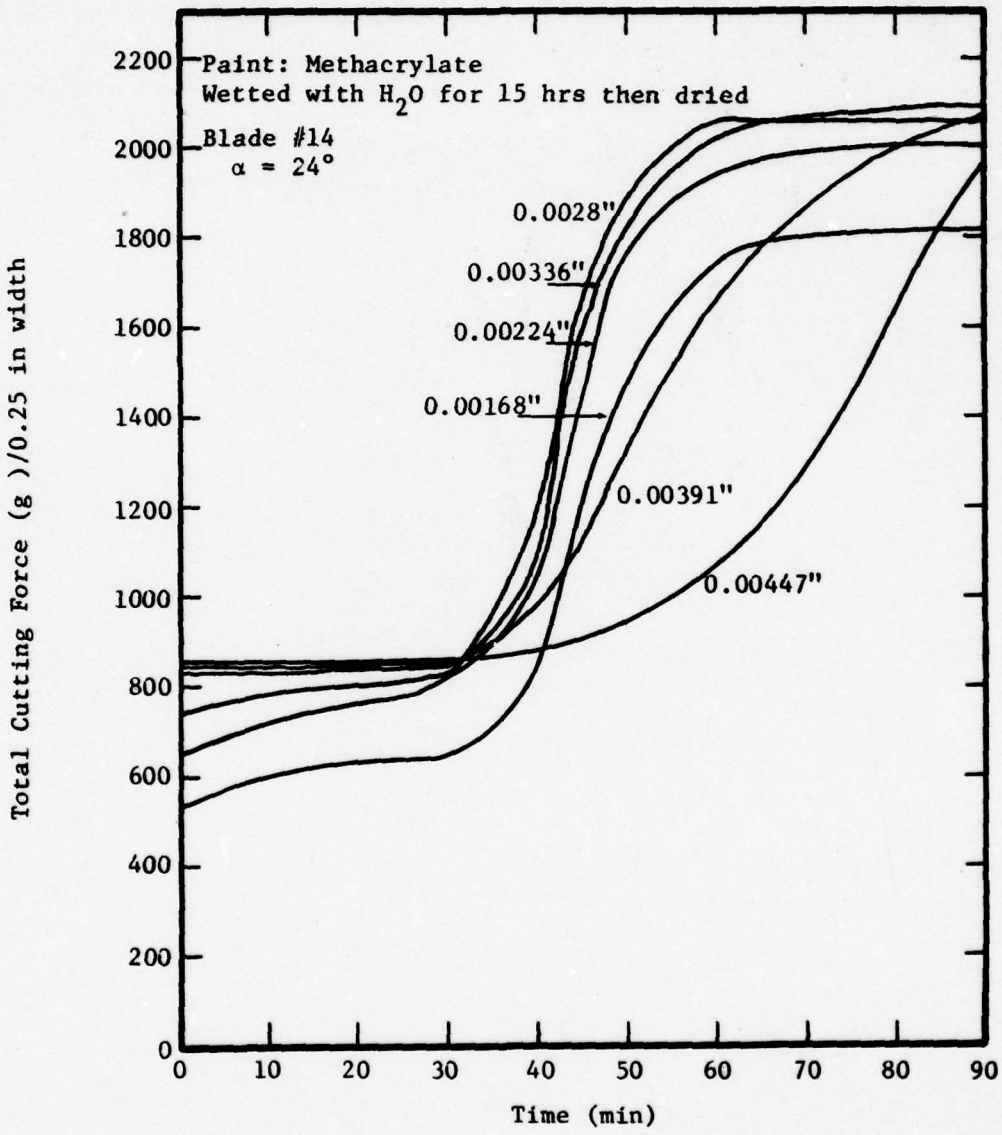

Fig. 3.5.11. Cutting force vs drying time at different thicknesses.

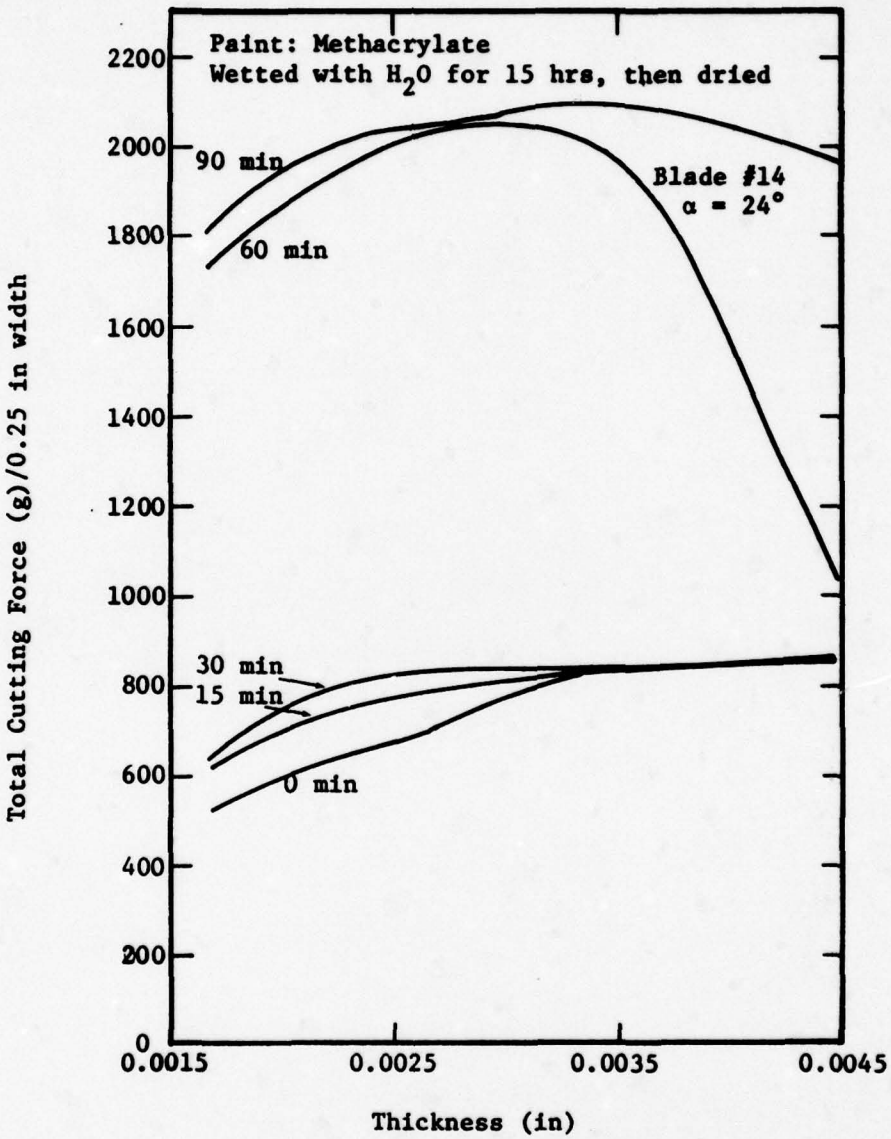

Fig. 3.5.12. Cutting force vs thickness at different drying times.

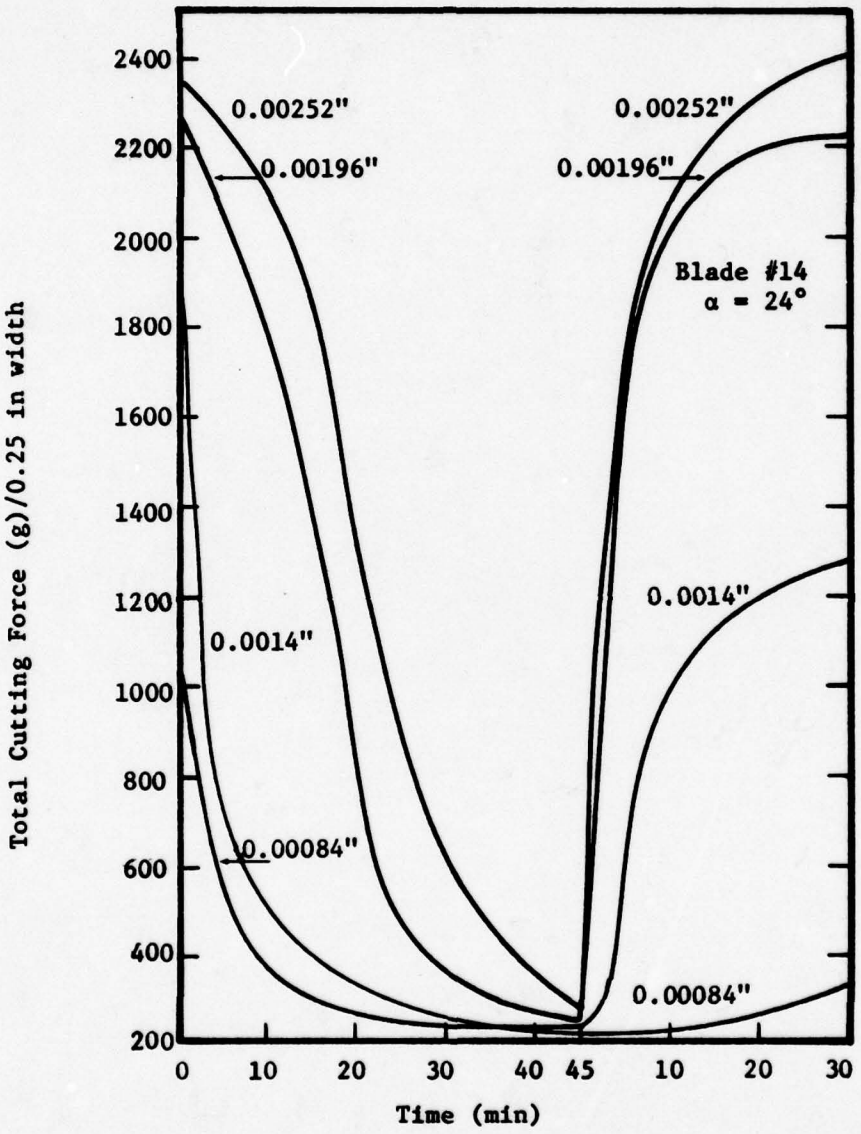

Fig. 3.5.13. Cutting force vs wetting and drying time of VR3 with H_2O at different thicknesses.

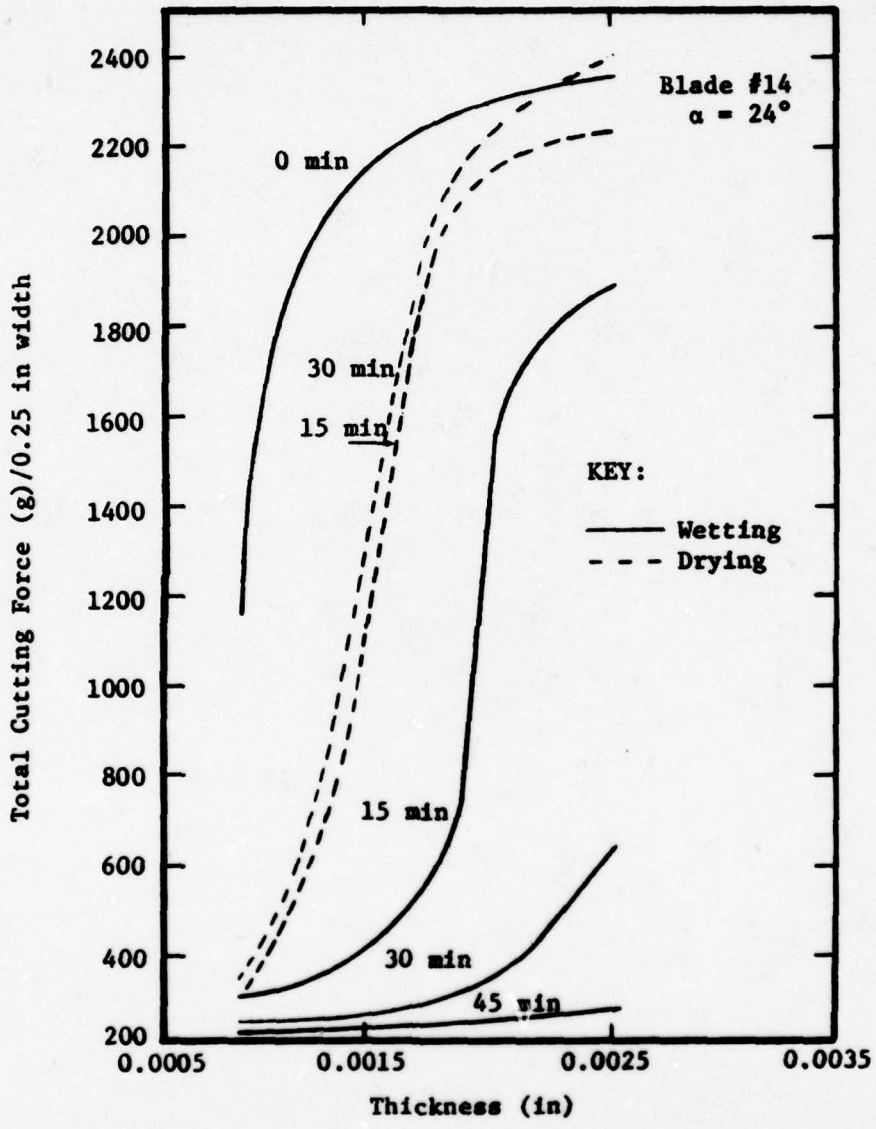

Fig. 3.5.14. Cutting force vs thickness at different wetting and drying times of VR3 with H_2O.

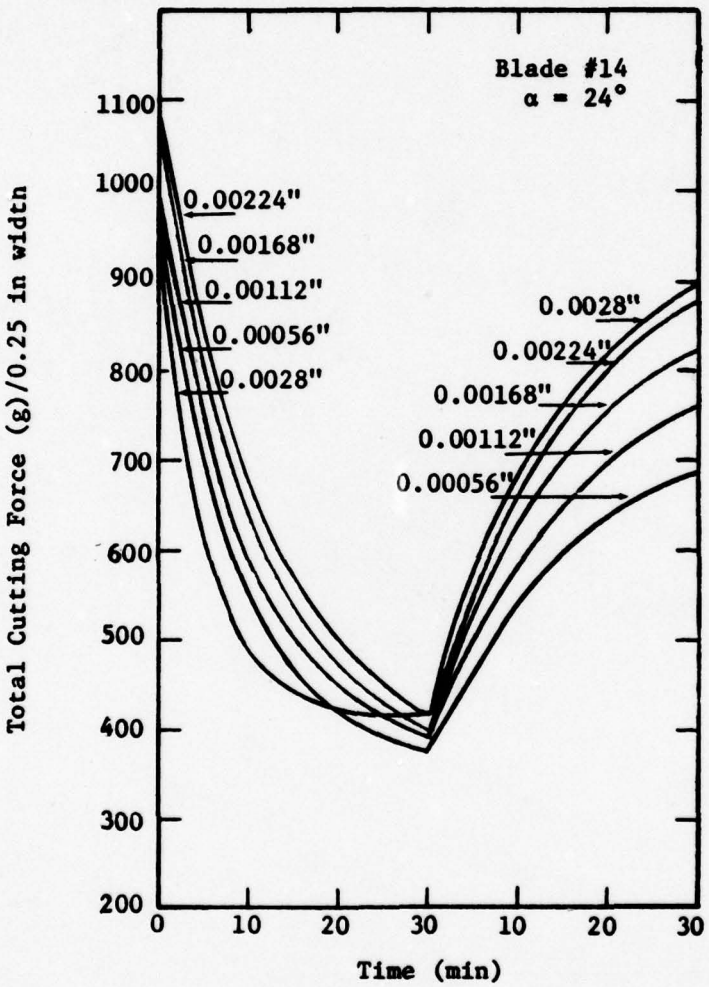

Fig. 3.5.15. Cutting force vs wetting and drying time of E epoxy with H_2O at different paint thicknesses.

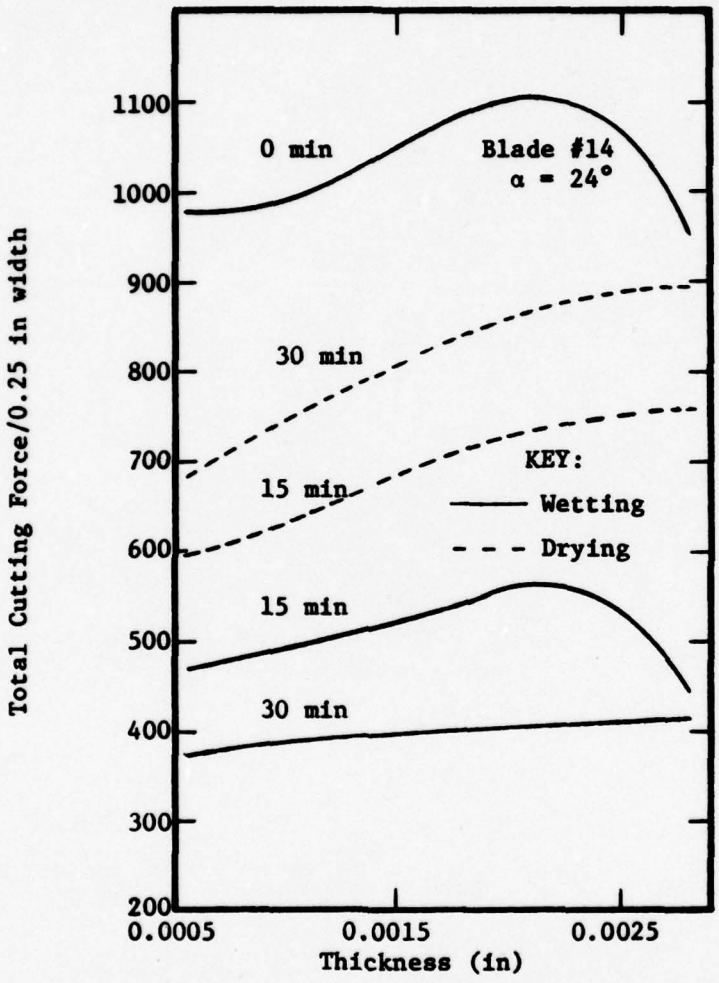

Fig. 3.5.16. Cutting force ve paint thickness at different wetting and drying time of E Epoxy with H_2O.

or altered in some way. A small degree of swelling in E epoxy may explain why this coating retains some adhesion after being wet with water. Taken as a unit, these experiments indicate that water, or some other solvent, is present when the adhesion fails, and the short failure time and extent of recovery suggest that corrosion is not involved in the initial loss of adhesion. On the other hand, the mere presence of water does not appear to be sufficient to explain the observations; a complex failure mechanism is indicated.

Salt Water

When coatings were wet with low-concentration (0.2 M) sodium chloride solution, the results were almost identical to those obtained using distilled water. When 1 M sodium chloride solution was used to wet VR3, the results showed slight differences. As seen in Fig. 3.5.17, the adhesion disappeared after soaking the coating for 5½ hours and upon drying only some regions of the coating recovered the original cutting force. It seemed that salt had permanently destroyed some interfacial bonding. Since the diffusivity of salt through the coating is estimated to be very small, the explanation appears to be that there are weak spots in the coating which allow salt to reach the metal interface. Contamination at the interface might be expected to reduce the bond strength. More weak spots appeared at the thin end than at the thick end of the paint layer.

Methanol

Methanol, which is a solvent for some paints, was used to wet the coatings being studied. Methacrylate was found soluble in methanol while VR3 and E epoxy were only softened. The effects on the adhesion of these coatings are shown in Figs. 3.5.18 and 3.5.19. It appears that in the presence of methanol, E epoxy looses adhesion completely, while VR3 still retains some adhesive strength. It is believed that VR3 did not soften as much as E epoxy. Upon drying, the VR3 coating appeared to shrink. As

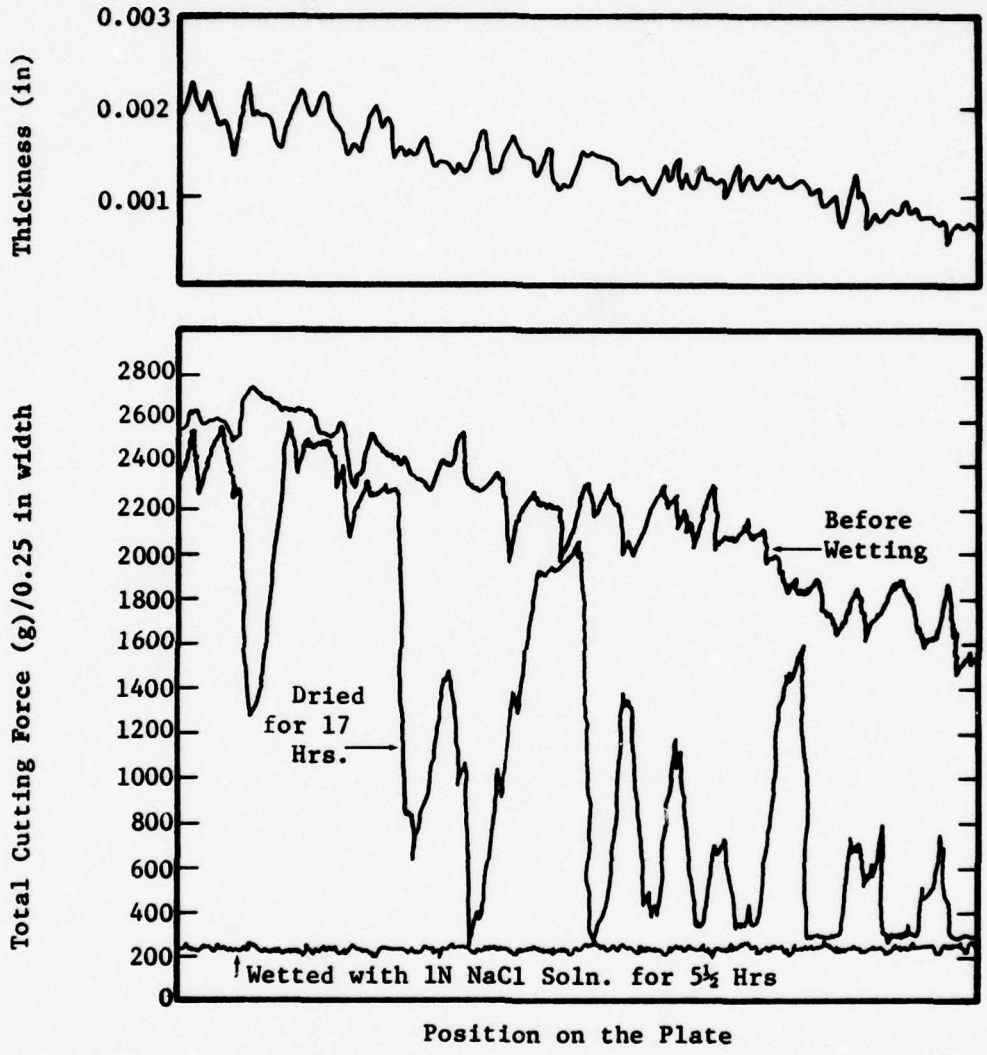

Fig. 3.5.17. Effect on wetting the VR3 paint with 1M NaCl soln.

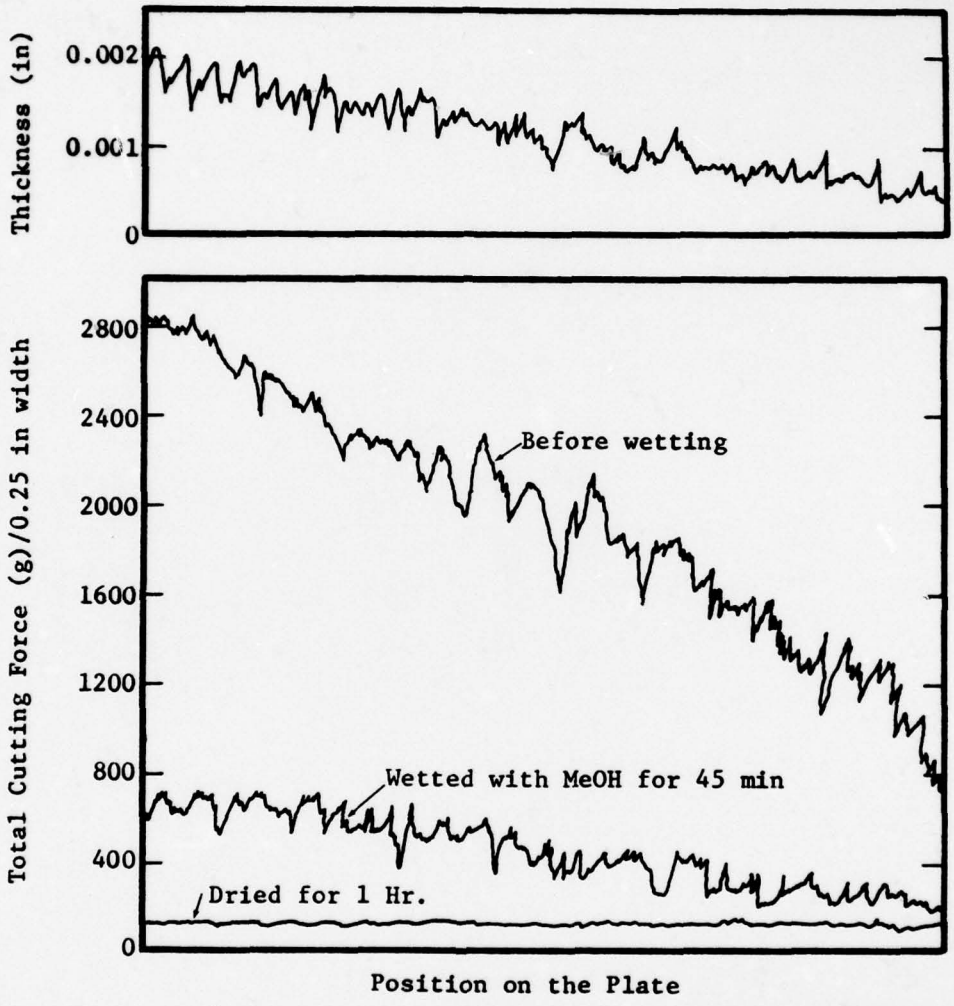

Fig. 3.5.18. Effect on wetting the VR3 paint with MeOH.

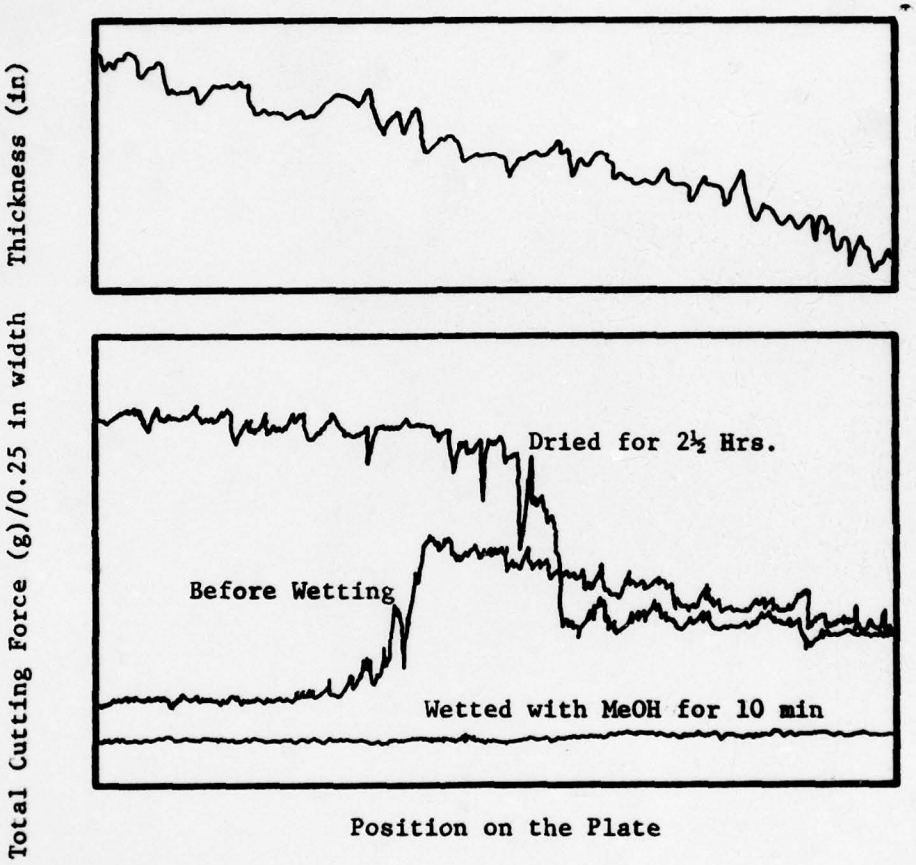

Fig. 3.5.19. Effect on wetting the E epoxy paint with MeOH

a result, the coating separated from the substrate; the adhesion became zero. When E epoxy dried, the cutting force at the thick end increased by a factor of four. This might reflect that methanol acts as a solvent and changes the bonding mechanism at the paint-metal interface. These experiments further demonstrate that polar molecules, in the absence of corrosion, can migrate through the polymer network and disrupt the polymer-metal adhesive bonds.

Electric Current (Anodic and Cathodic)

VR3, K epoxy, and methacrylate were used to study the effect of electric current on adhesion. Electric charge densities corresponding to from 1 to 1,000 monolayers of corrosion were passed through the coatings. Both sides of the substrate plate were filled with electrolyte (0.2 M NaCl) at the same time, but current was passed only over half the plate surface, the other half being used as a reference (see Fig. 3.5.3). The results obtained while passing anodic or cathodic currents showed that the temporary changes in adhesion are similar to those obtained without currents. It is thus difficult to separate the effect of electric current from the effect of electrolyte alone. Furthermore, there was no permanent effect noted from either electric current or electrolyte after the coating had been dried. More, longer-term, experiments are planned.

Although the hesiometer experiments are fairly involved and the true wet adhesion has not been measured, the facts support the conclusion that a complex mechanism is responsible for the loss of adhesion. One interesting fact is that initially the decreased adhesion associated with wetting is reversible. This fact as well as the results of the methanol, anodic and cathodic current, and water experiments indicate that corrosion is not important in the initial loss of adhesion. The time constants for water diffusion support the fact that the presence of water is not sufficient to explain the rate of adhesion loss. Therefore, a second, perhaps rate controlling, process is indicated as part of the overall mechanism. The increase in cutting force of E epoxy after drying out the methanol lends further support to the idea of a complex mechanism.

Nomenclature

C = the angle defined by Eq. 7.

F = the force.

F_c = the force required to cut a coating of thickness t from the substrate. This force is excluding the effect of a blunt knife.

$F_{c,cr}$ = the critical cutting force when the coating removal mechanism changes from cutting to peeling or cracking.

k = the slope of the shear strength vs compressive stress line.

L_1, L_2 = the length of the coating in the direction of knife travel before and after removal respectively.

r_L = coating chip length ratio.

S_n = the mean compressive or normal stress on the shear plane.

S_o = the shear strength of the coating under zero compressive stress.

S_s' = the shear strength.

t = the thickness of the coating.

T = the characteristic surface free energy.

w = the width of the coating that is being removed.

W = the weight of the knife.

α = the rake angle of the knife.

τ = the friction angle.

μ = the coefficient of friction between the coating and the face of the knife.

β = the angle the resultant (R) makes with the plane of the substrate (Fig. 3.5.4).

ϕ = the angle of the shear plane.

References (Section 3.5)

1. W. K. Asbeck, Paint Varn. Prod., 60, (3), 23 (1970).

2. W. K. Asbeck, Adhesion and Cohesion, Philip Weiss, Ed., Elsevier Publishing Co., New York, 120 (1962).

3. W. K. Asbeck, "Measuring the Adhesion of Coating," J. Paint Tech., 43 (556), 84-91 (1971).

4. M. E. Merchant, J. Appl. Phys., 16, 267 (1945).

5. M. E. Merchant, J. Appl. Phys., 16, 318 (1945).

6. R. Connally and C. Rubenstein, Int. J. Mach. Tool Des. Res., 8, 159-187 (1968).

7. C. Rubenstein and R. M. Storie, Int. J. Mach. Tool Des. Res., 9, 117-130 (1969).

8. W. K. Asbeck, IX FATIPEC Congress, 78-87 (1968).

APPENDIX A

COPOLYMERS AND THEIR GLASS TRANSITION TEMPERATURE

Random copolymers often exhibit their Tg at a temperature intermediate the pure homopolymer Tg's. A number of relations between Tg and copolymer composition have been suggested. Nielsen (1) suggested two simple relations which are given as follows:

$$Tg = V_1\ Tg_1 + V_2 Tg_2 \tag{1}$$

$$\frac{1}{Tg} = \frac{W_1}{Tg_1} + \frac{W_2}{Tg_2} \tag{2}$$

Where Tg_1 and Tg_2 are the glass transition temperatures of homopolymers, 1 and 2 given in °K, V_1 and V_2 are volume fractions, and W_1 and W_2 weight fractions of the corresponding homopolymers 1 and 2.

Wood (2) has proposed a two parameter empirical expression

$$K_1W_1(Tg-Tg_1) + K_2W_2(Tg-Tg_2) = 0 \tag{3}$$

where K_1 and K_2 are constants characteristics of the homopolymers.

This equation can be rearranged to

$$Tg = \frac{[Tg_1 + k(Tg_2 - Tg_1)W_2]}{[1 - (1-k)W_2]} \tag{4}$$

where $k = K_2/K_1$. This equation is known as Gordon-Taylor (3) equation and has found wide application to random copolymers. It should be kept in mind that the above equations are only applicable to random copolymers systems.

REFERENCES (Appendix A)

1. L. E. Nielsen, Mechanical Properties of Polymers, Reinhold, 1962.

2. L. A. Wood, J. Polymer Sci., 28, 319 (1958).

3. M. Gordon and J. S. Taylor, J. Appl. Chem., 2, 493 (1952).

APPENDIX B

Infrared Spectra

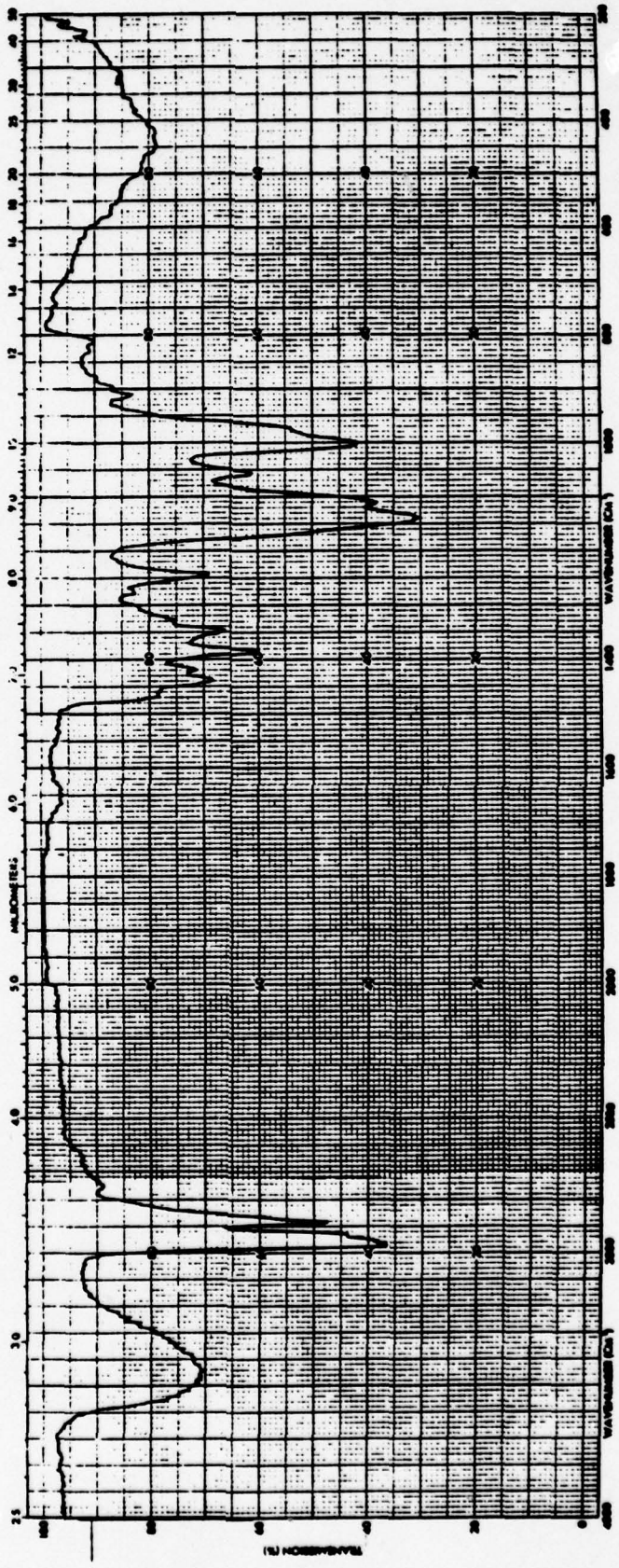

Fig. B-1. Paint System II (VR2) obtained from a solvent-cast film.

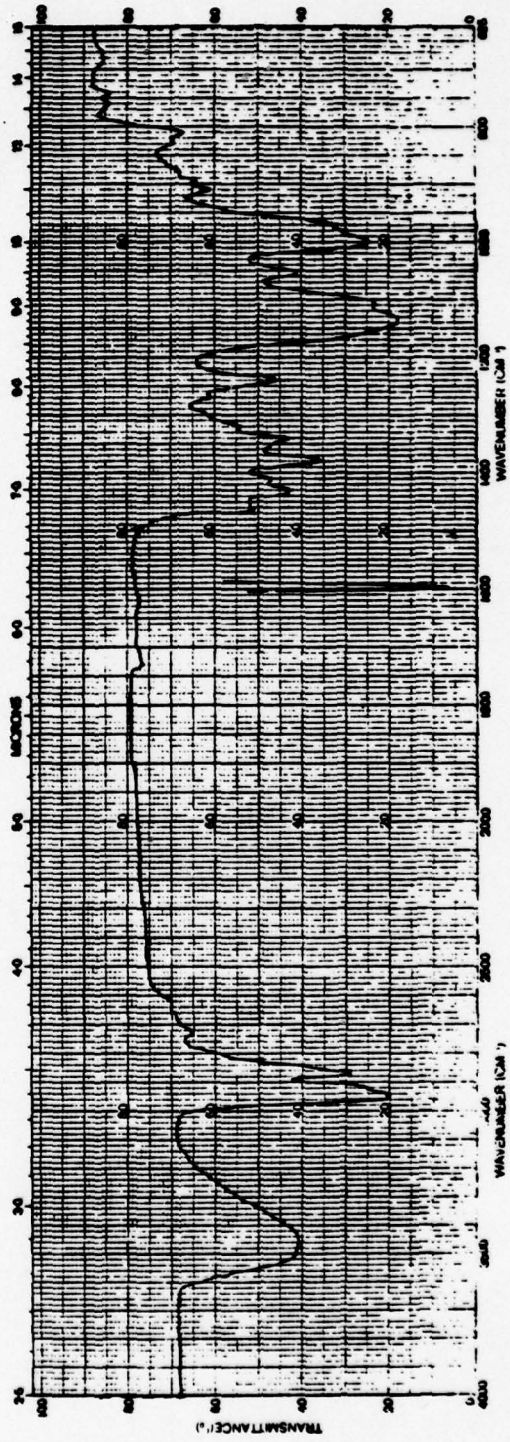

Fig. B-2. Paint System II (VR2) obtained from a KBr disc sample.

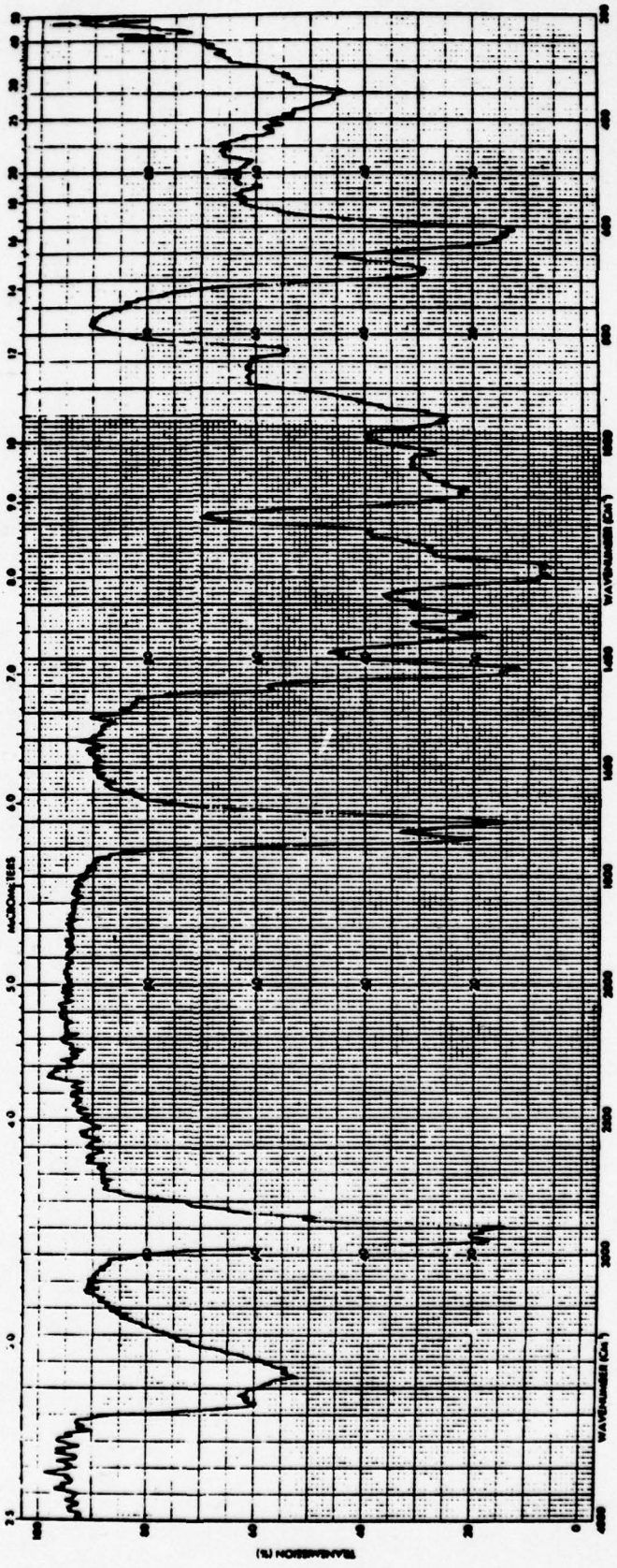

Fig. B-3. Copolymer of paint System III, obtained from a solvent-cast film.

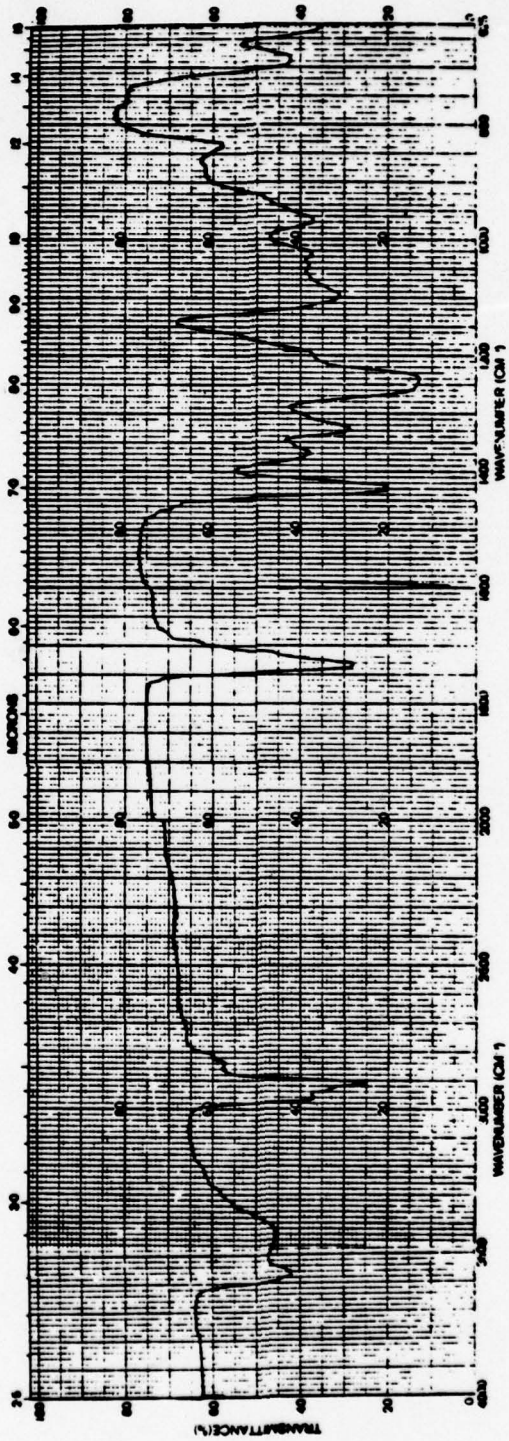

Fig. B-4. Copolymer of paint System III, obtained from a KBr disc.

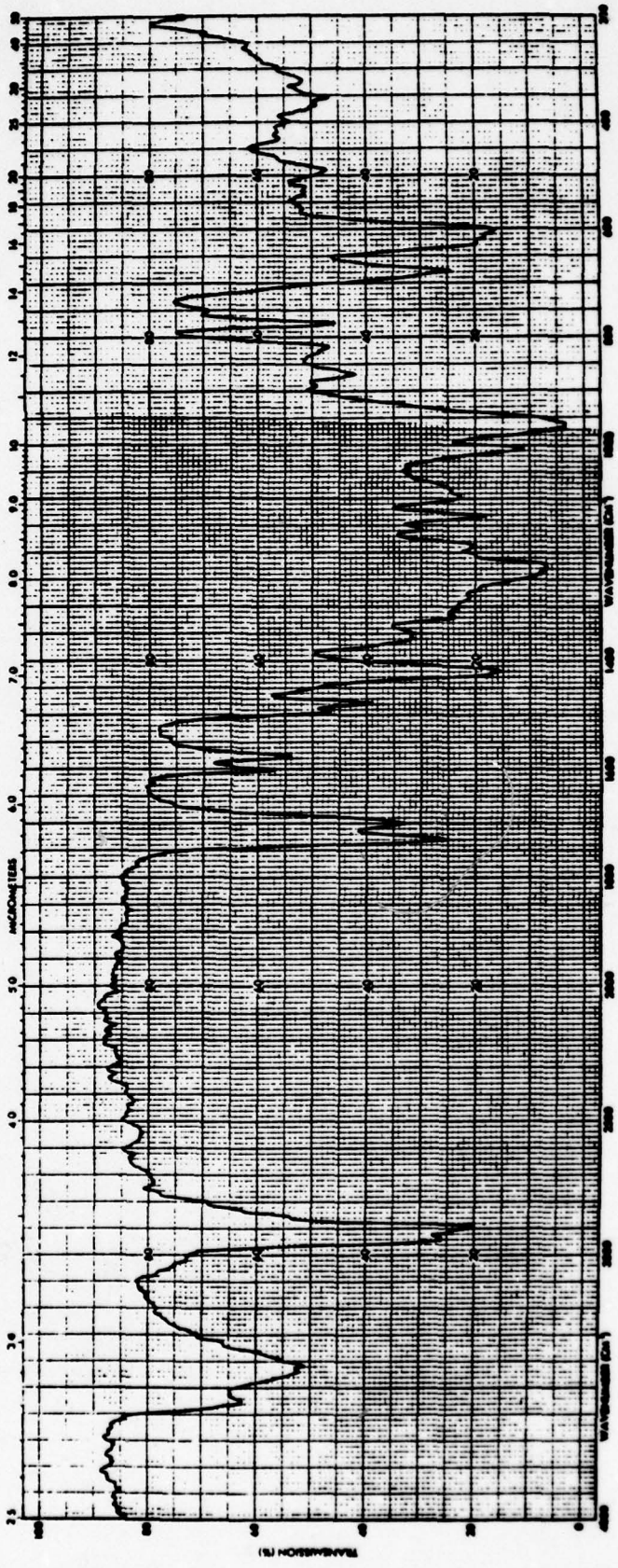

Fig. B-5. Paint System III (VR3) obtained from a solvent-cast film.

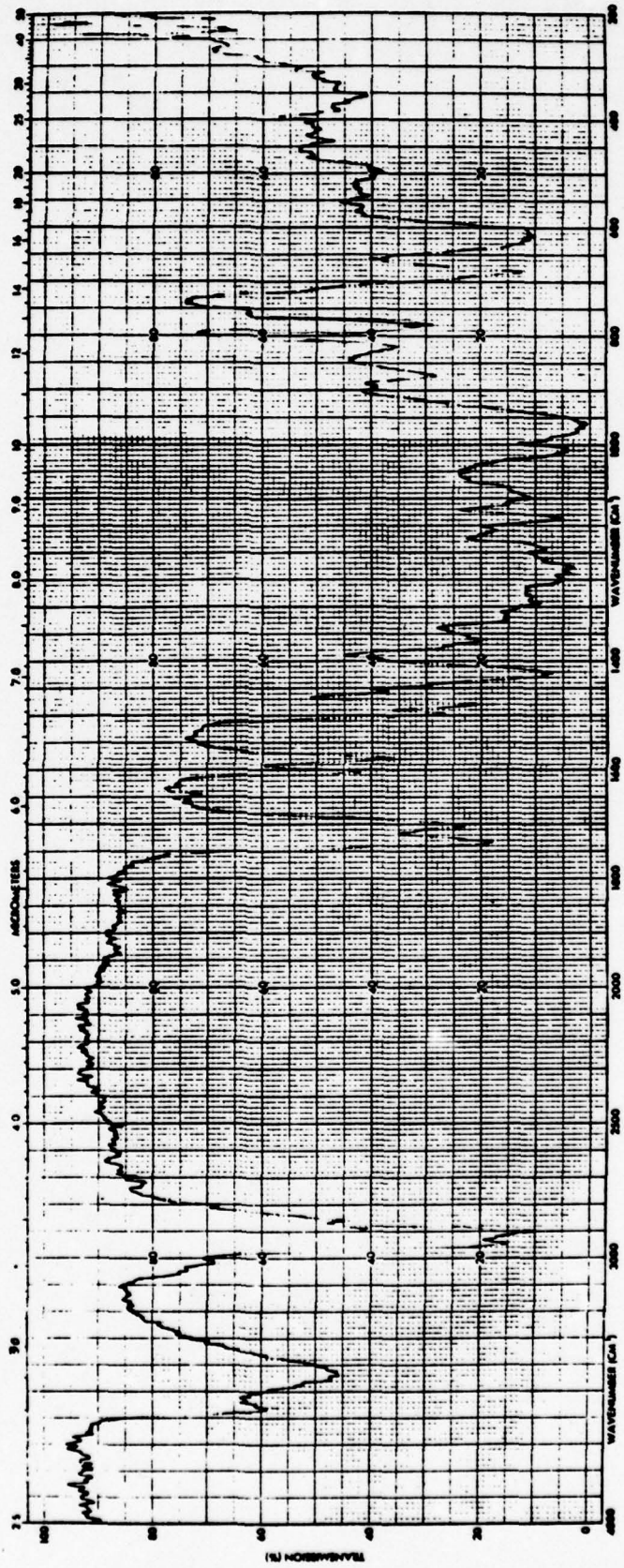

Fig. B-6. Copolymer of Paint System III with 17.2% by weight TCP. Spectrum was obtained from a solvent-cast film.

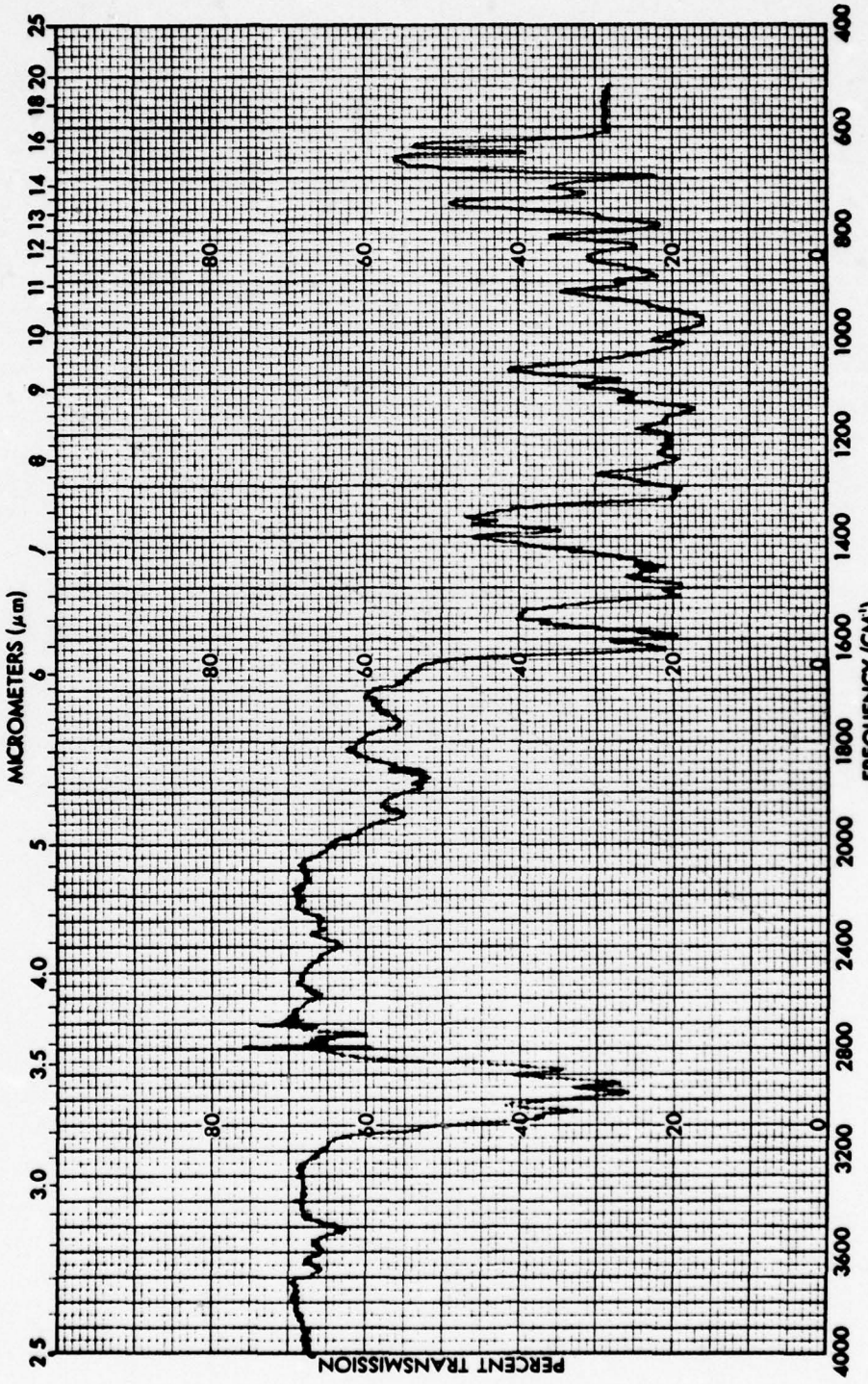

Fig. B-7. TCP plasticizer.

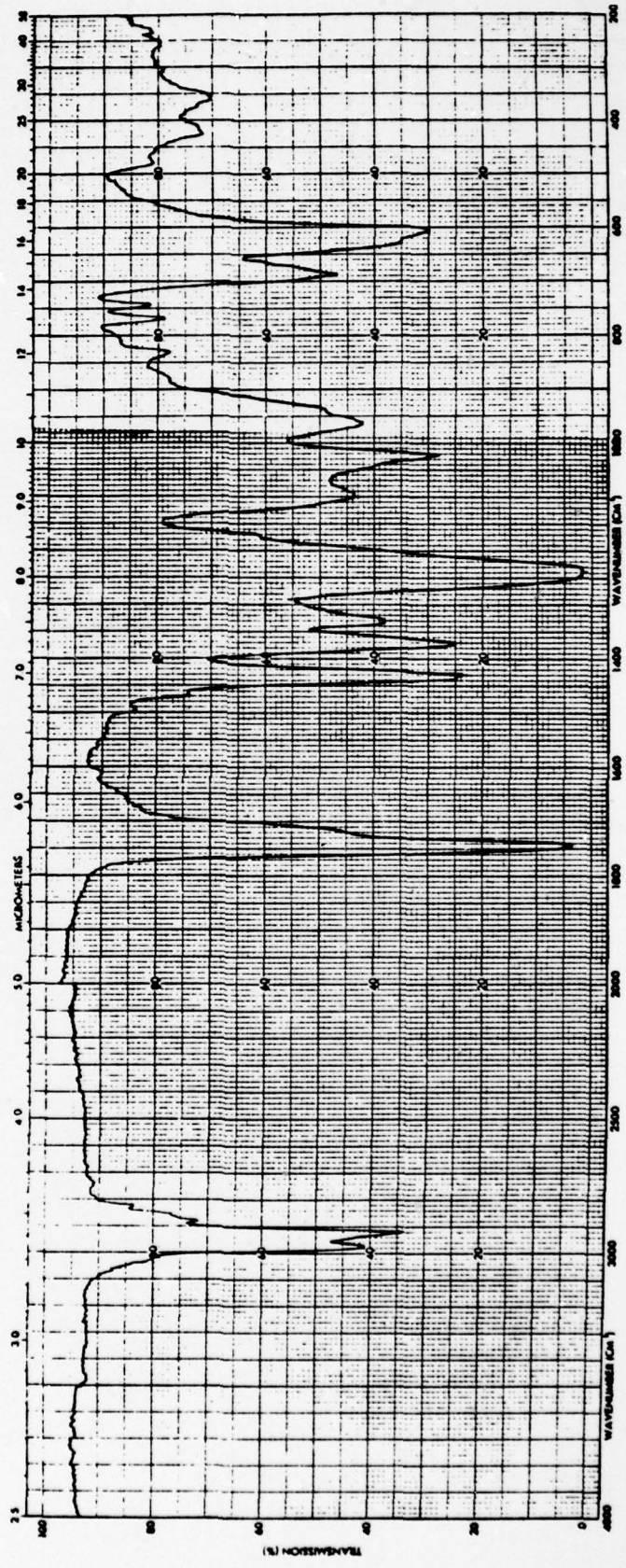

Fig. B-8. Copolymer of paint System IV only, obtained from a solvent-cast film.

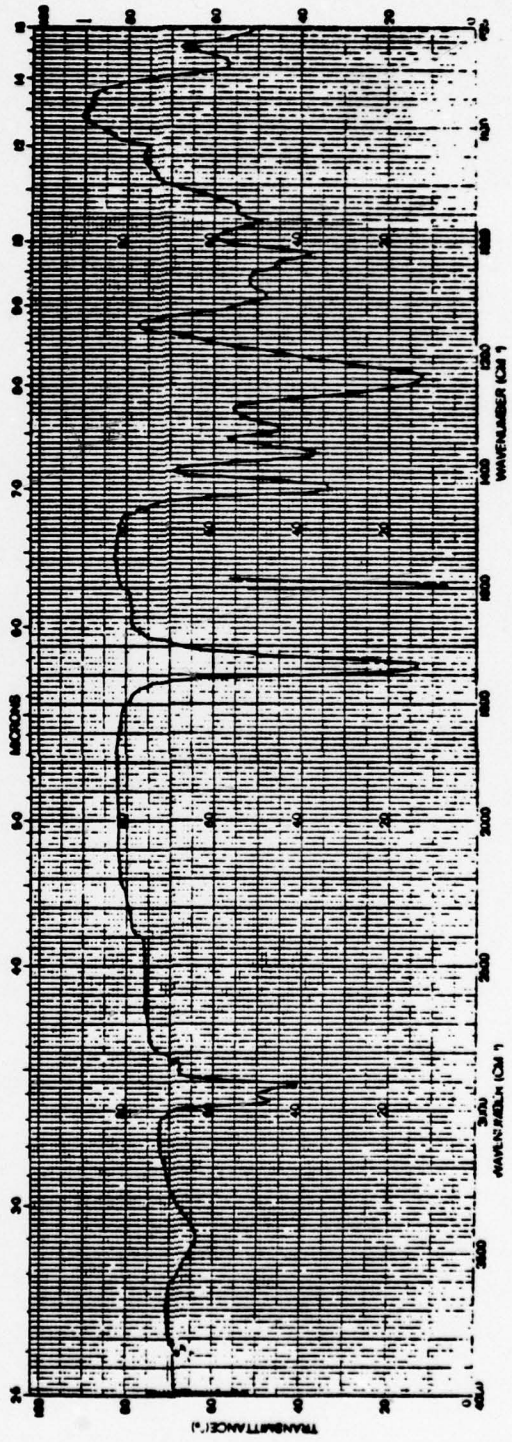

Fig. B-9. Copolymer of paint System IV only, obtained from a KBr disc sample.

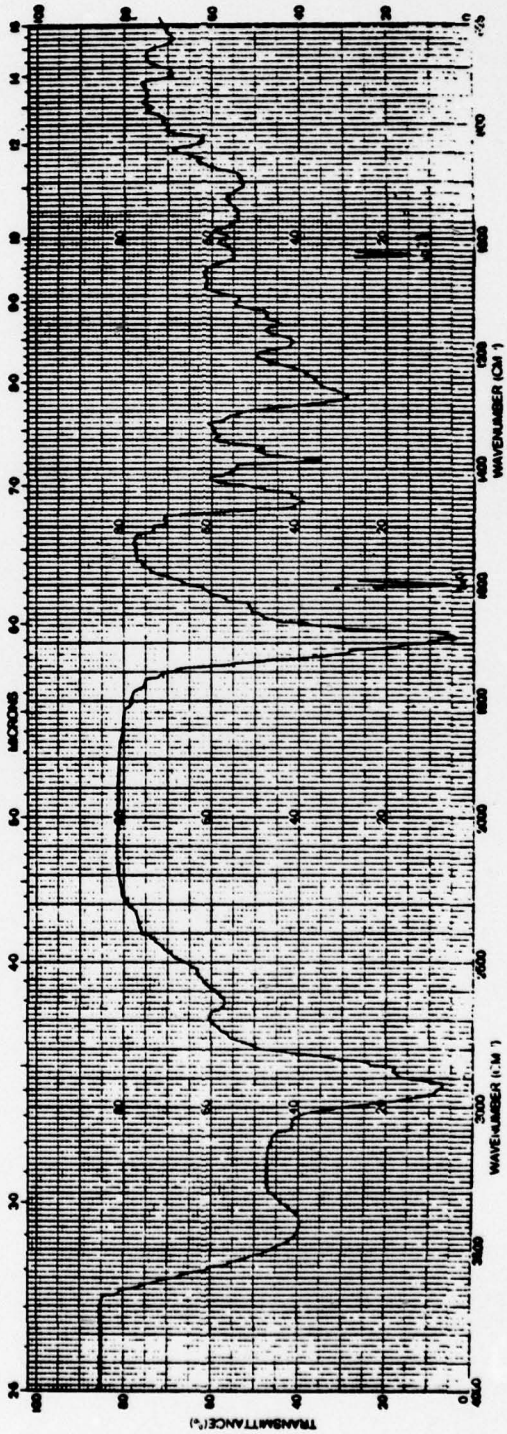

Fig. B-10. Rosin hardener from a KBr disc sample.

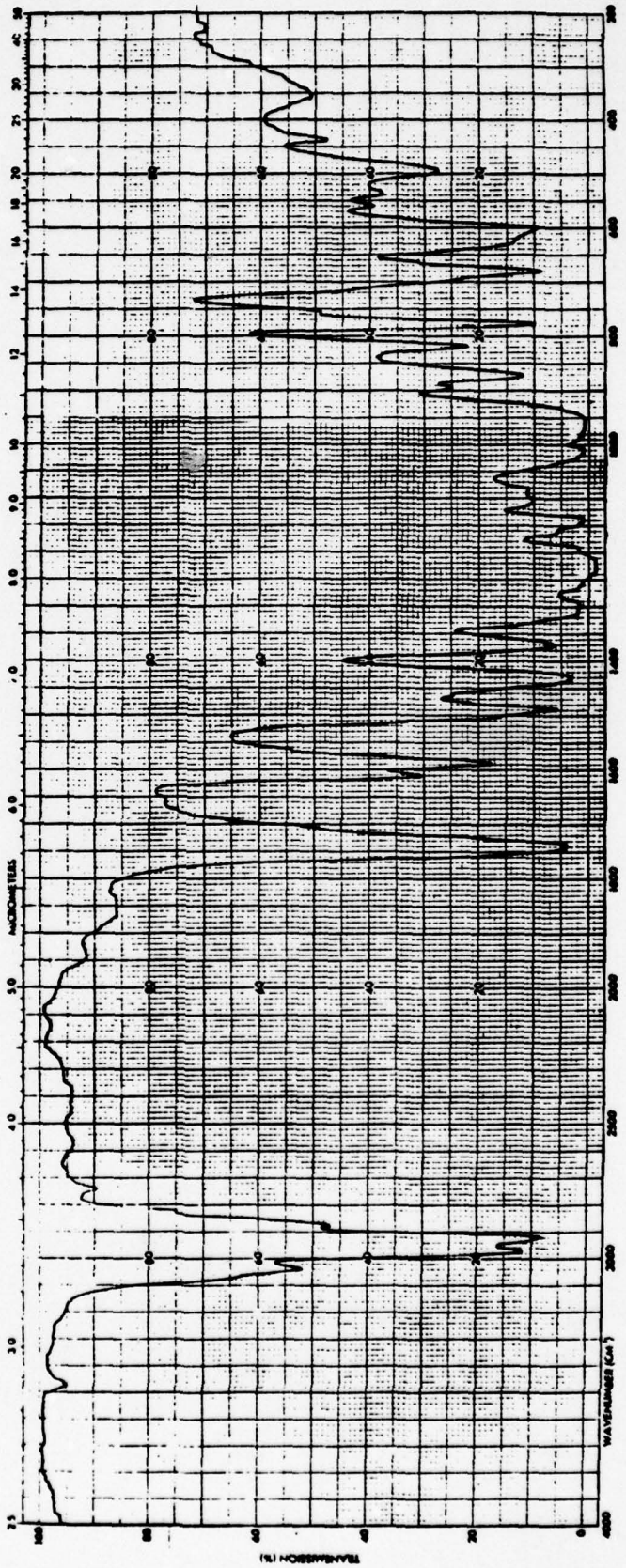

Fig. B-11. Copolymer of paint System IV with 27.6% by weight TCP from a solvent-cast film.

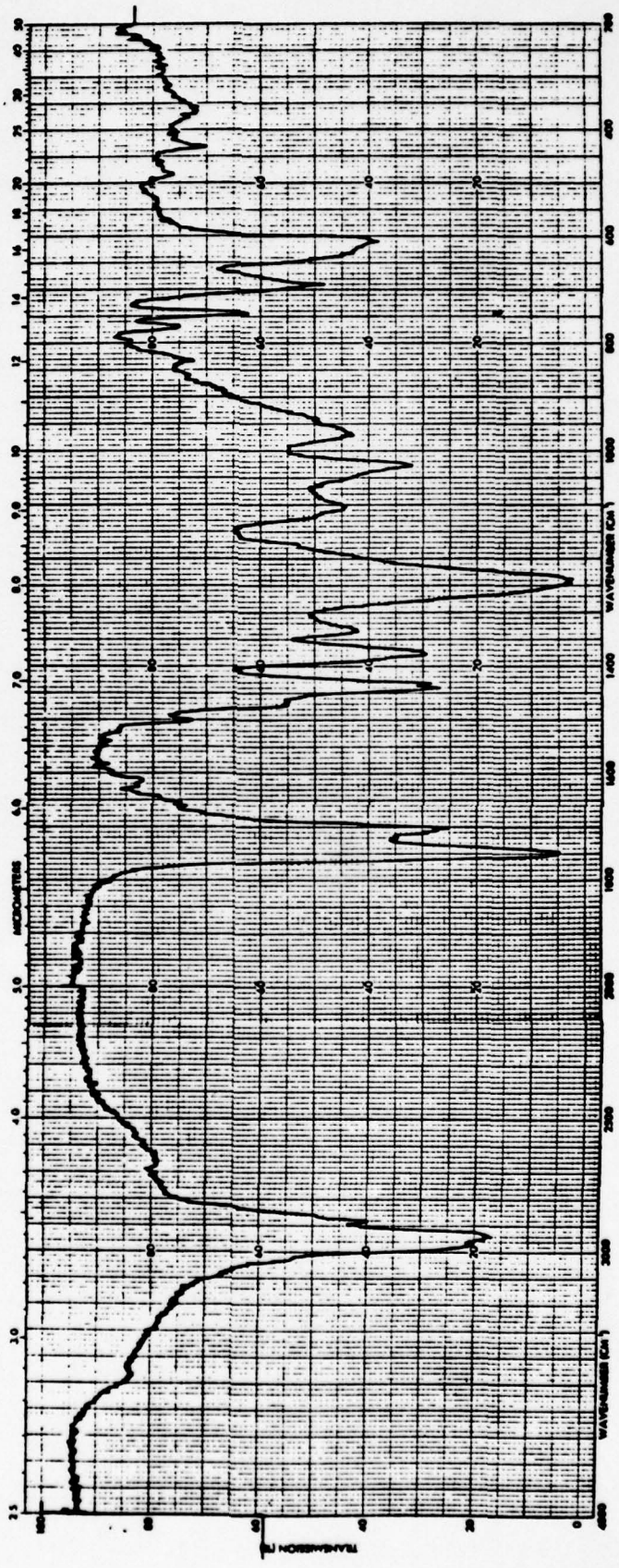

Fig. B-12. Copolymer of paint System IV with 20% by weight rosin hardener, obtained from a solvent-cast film.

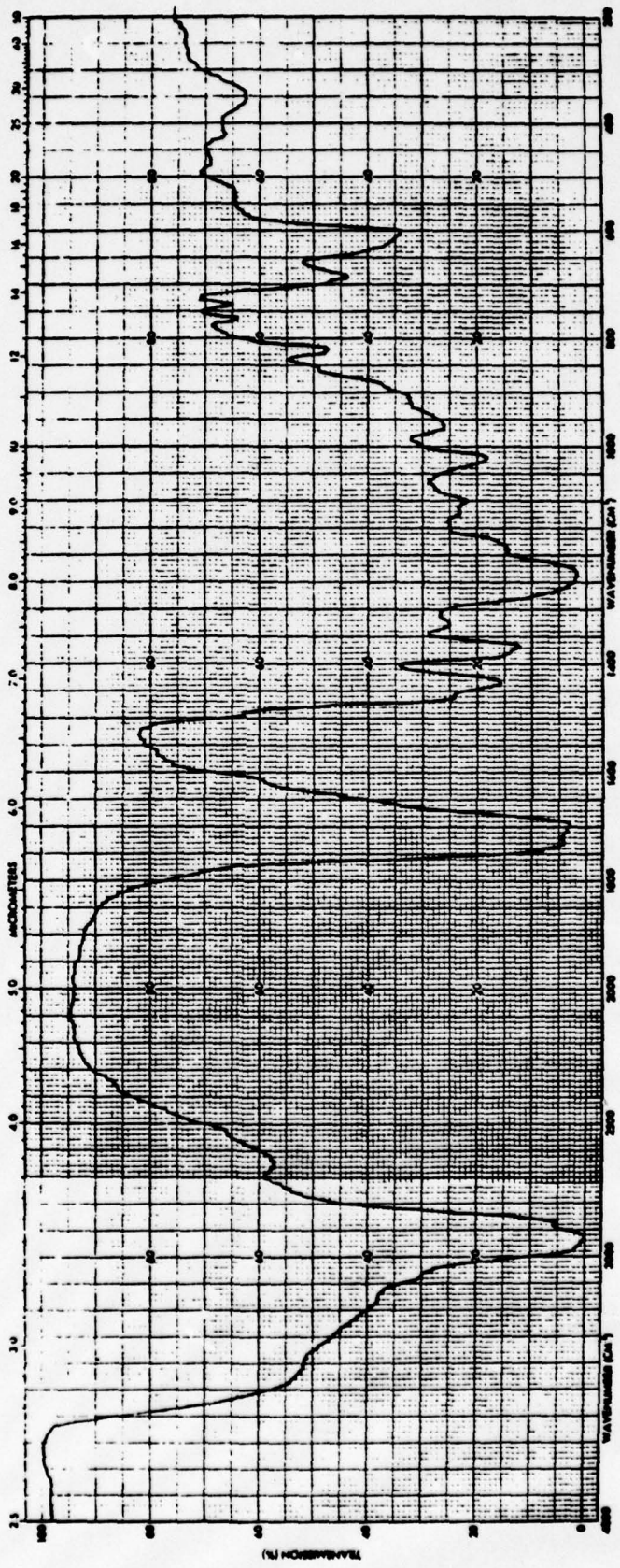

Fig. B-13. Copolymer of paint System IV with 50% rosin hardener from a solvent-cast film.

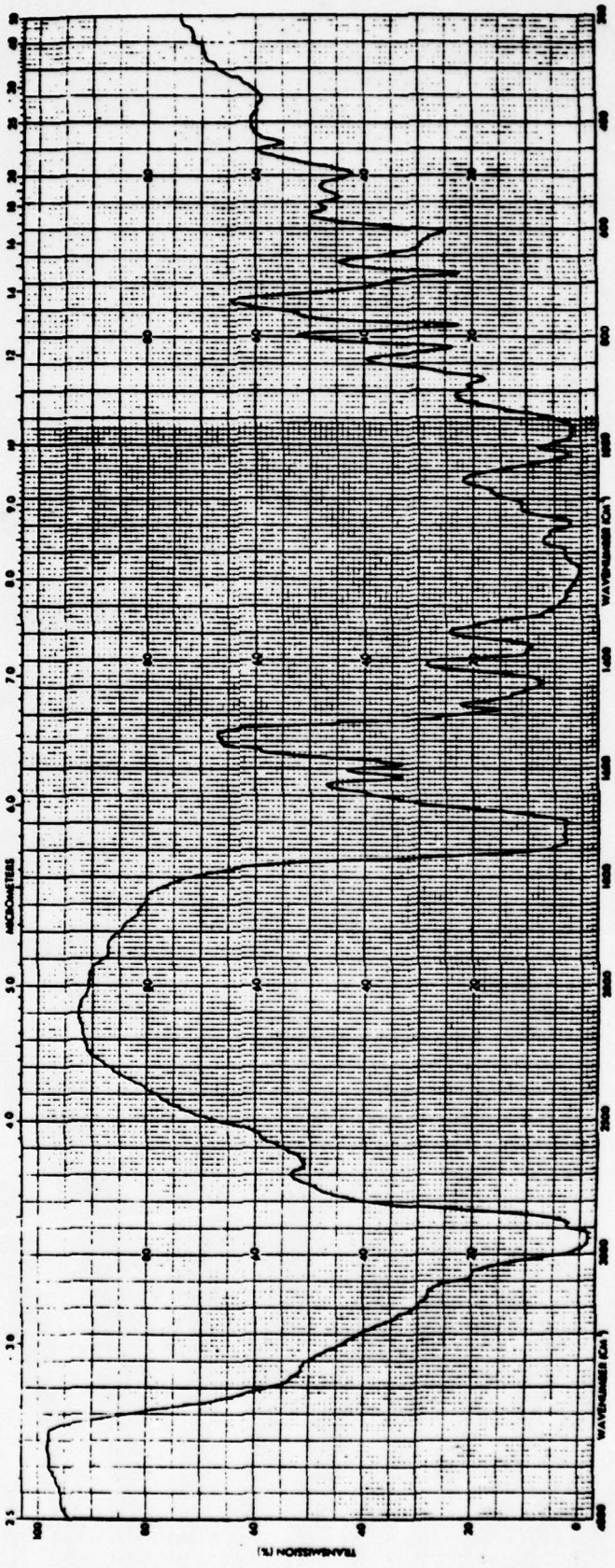

Fig. B-14. Paint System IV from a solvent-cast film.

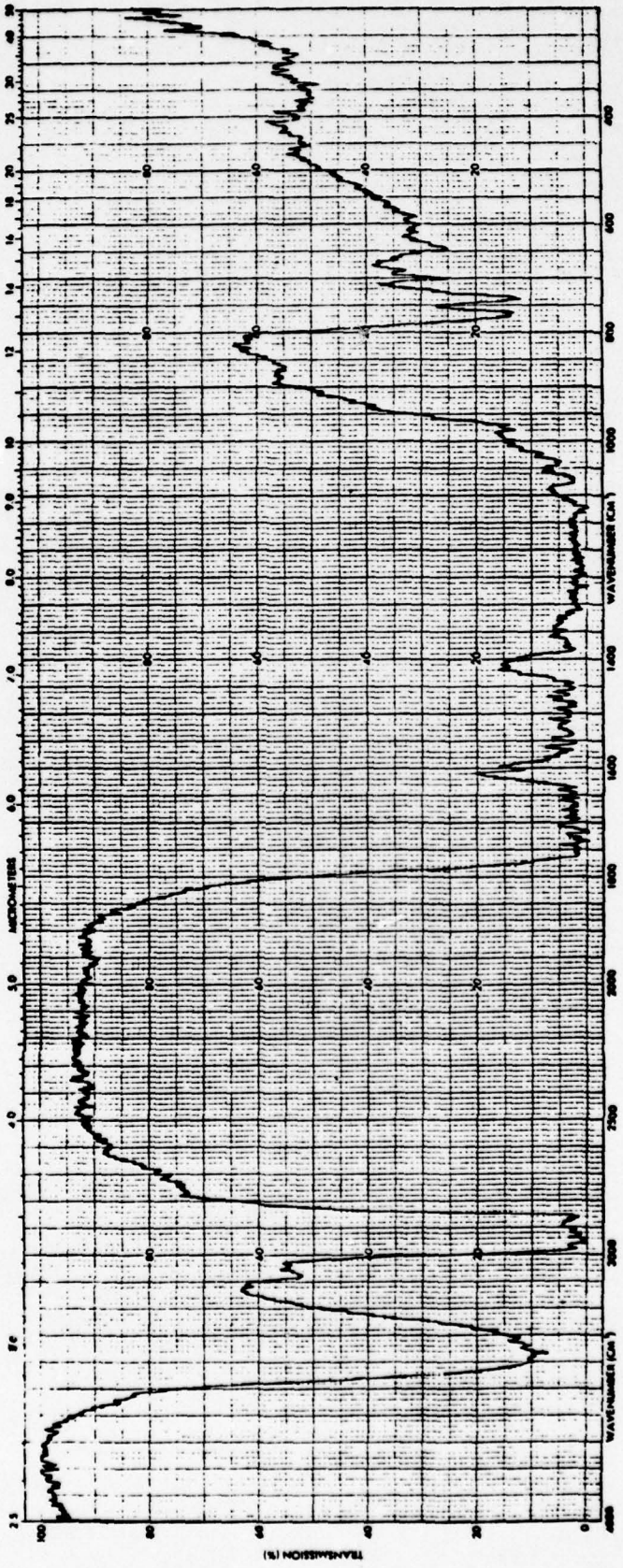

Fig. B-15. Paint System VIII from a solvent-cast film.

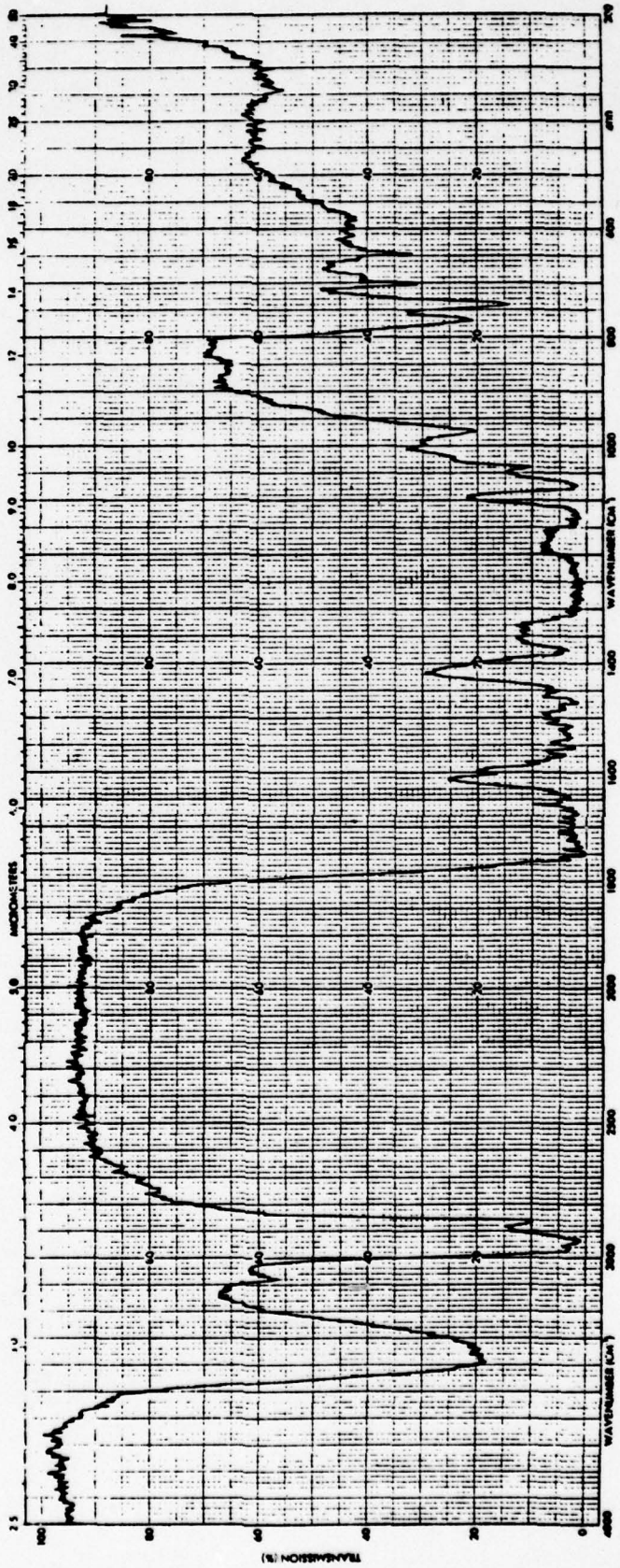

Fig. B-16. Paint System VII from a solvent-cast film.

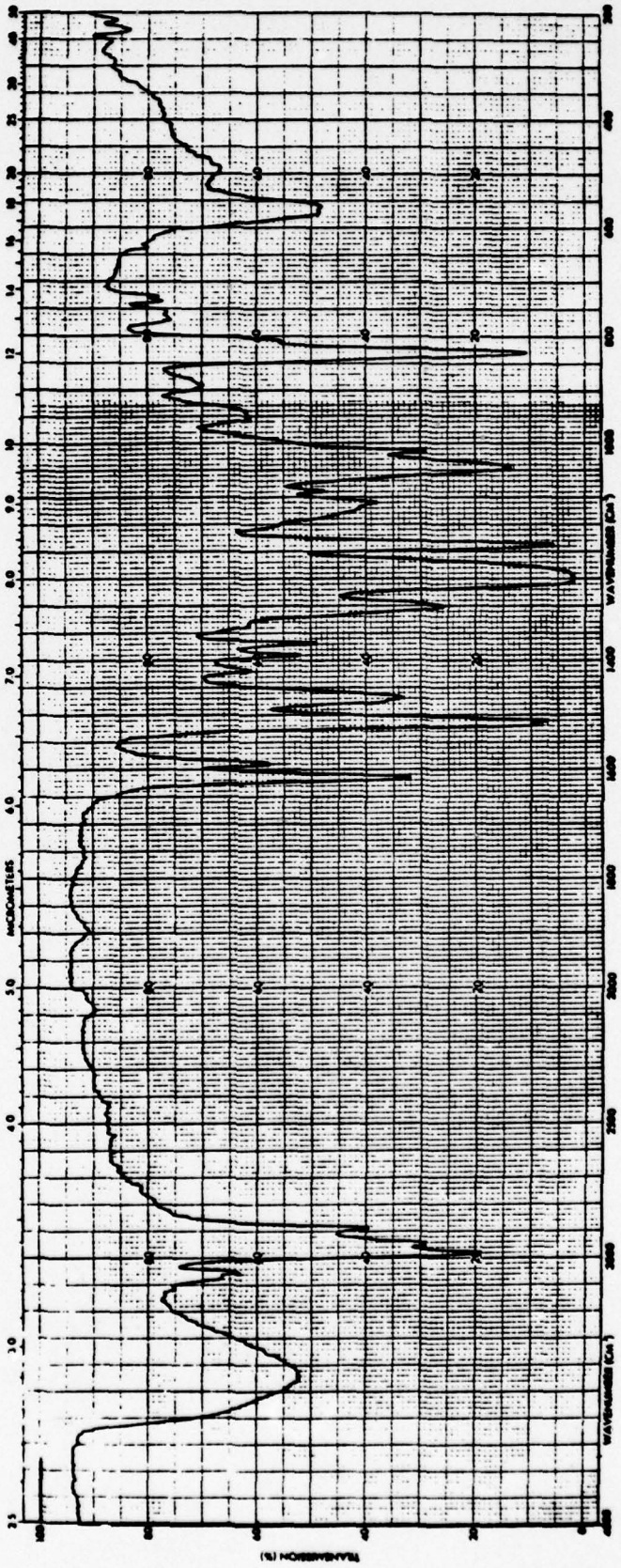

Fig. B-17. Paint System V from a solvent-cast film.

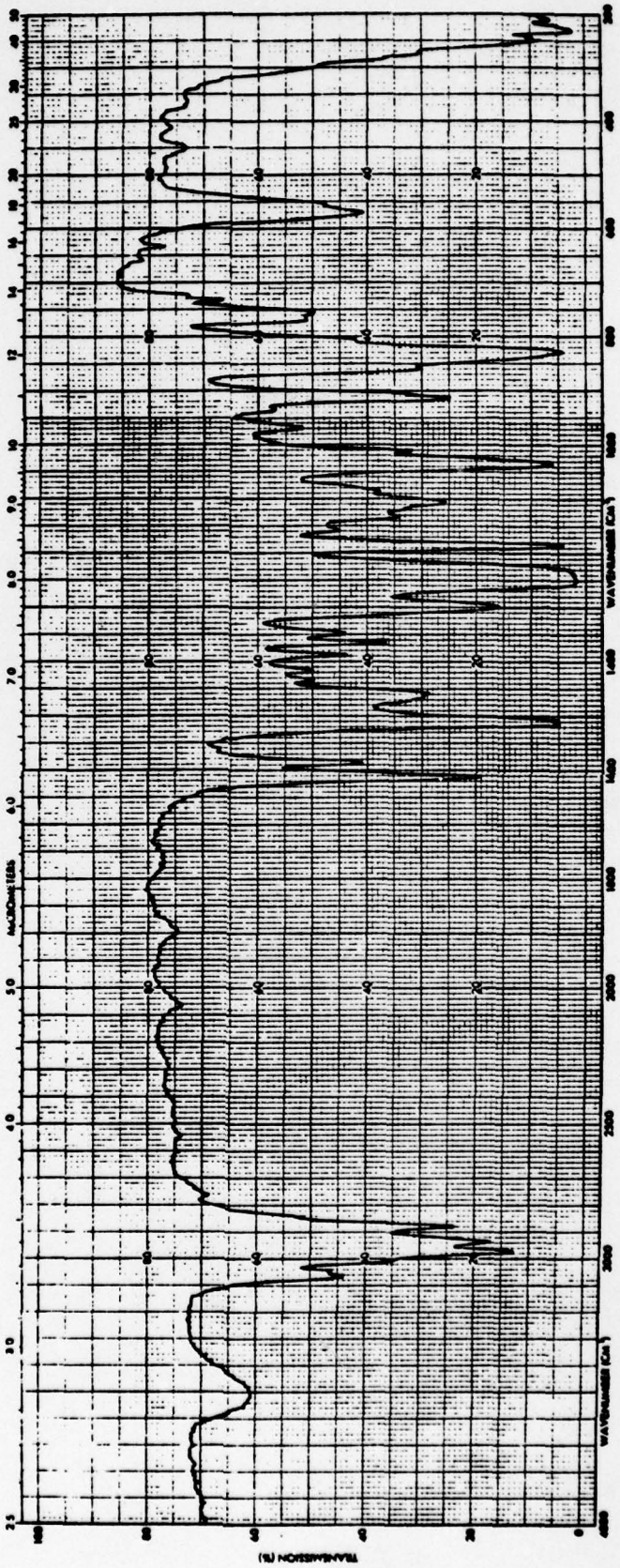

Fig. B-18. Shell Epon-815 epoxy resin for paint Systems I and VI.

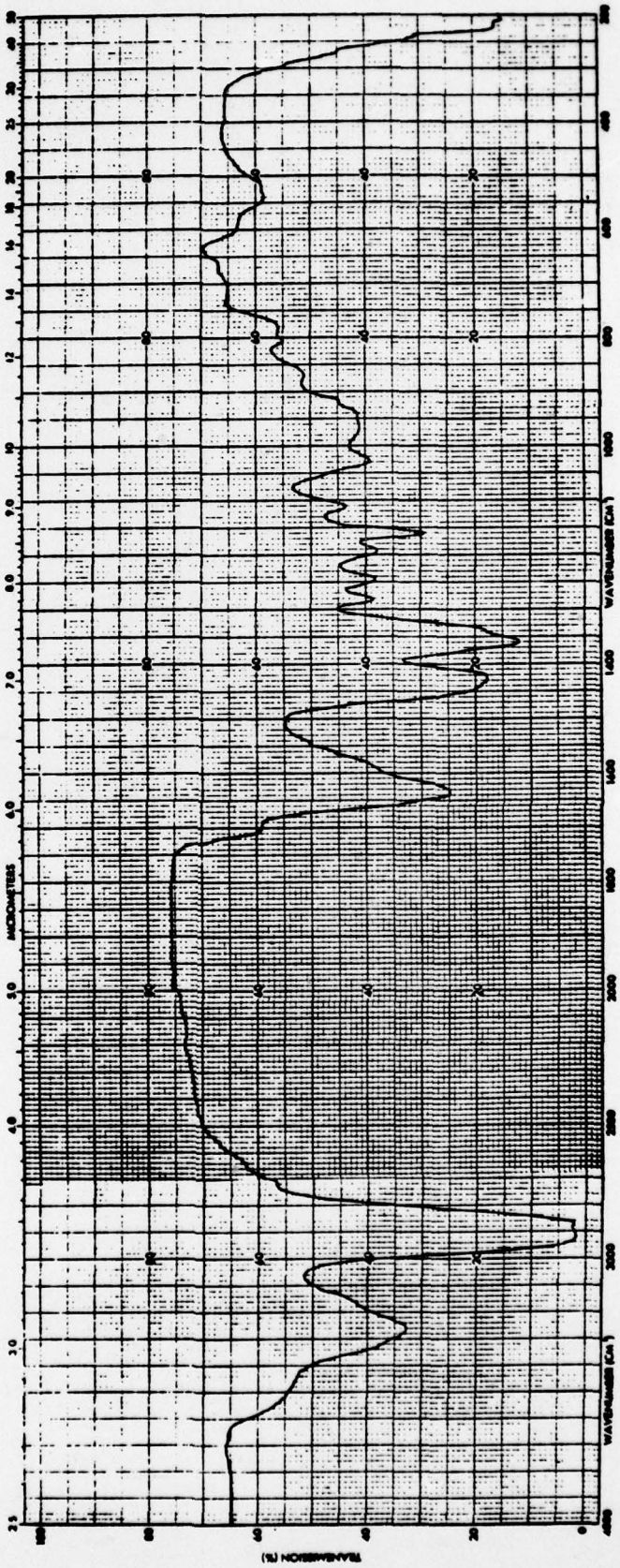

Fig. B-19. Amine curing agent for paint System VI.

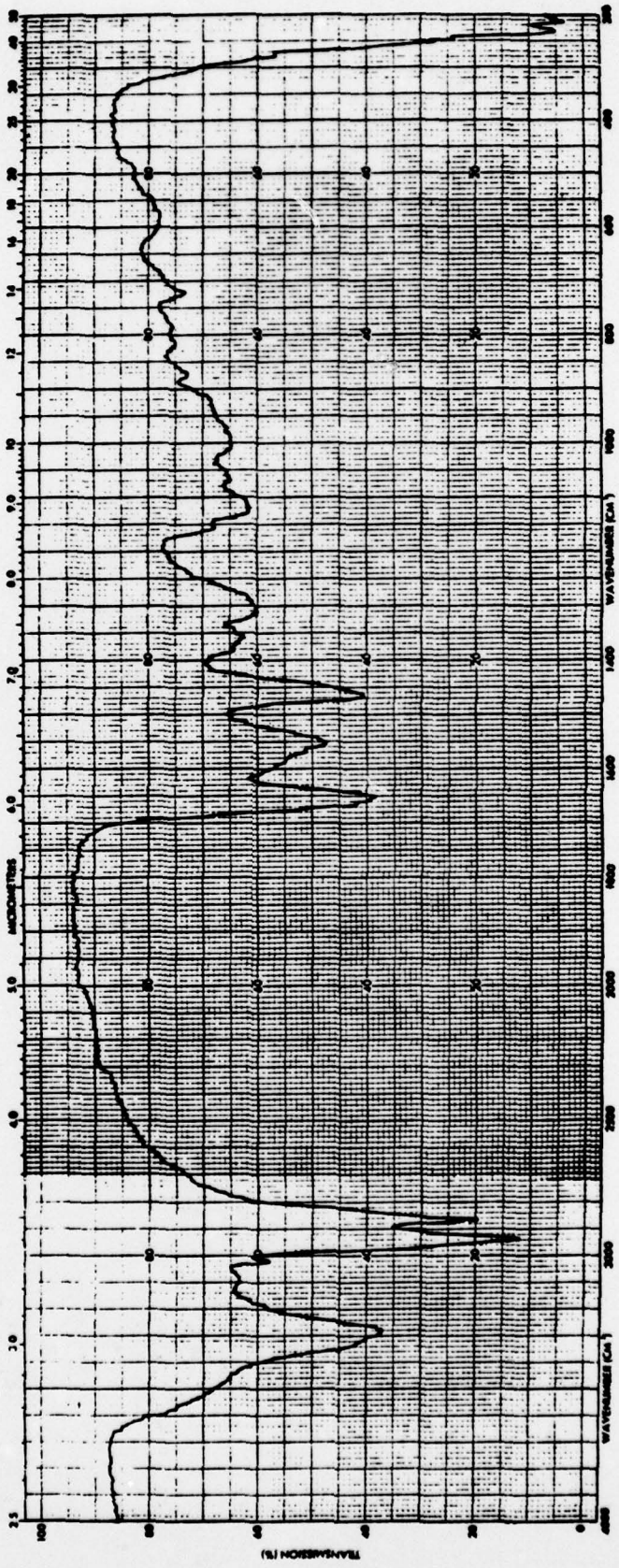

Fig. B-20. Gensamid amine curing agent for paint System I.

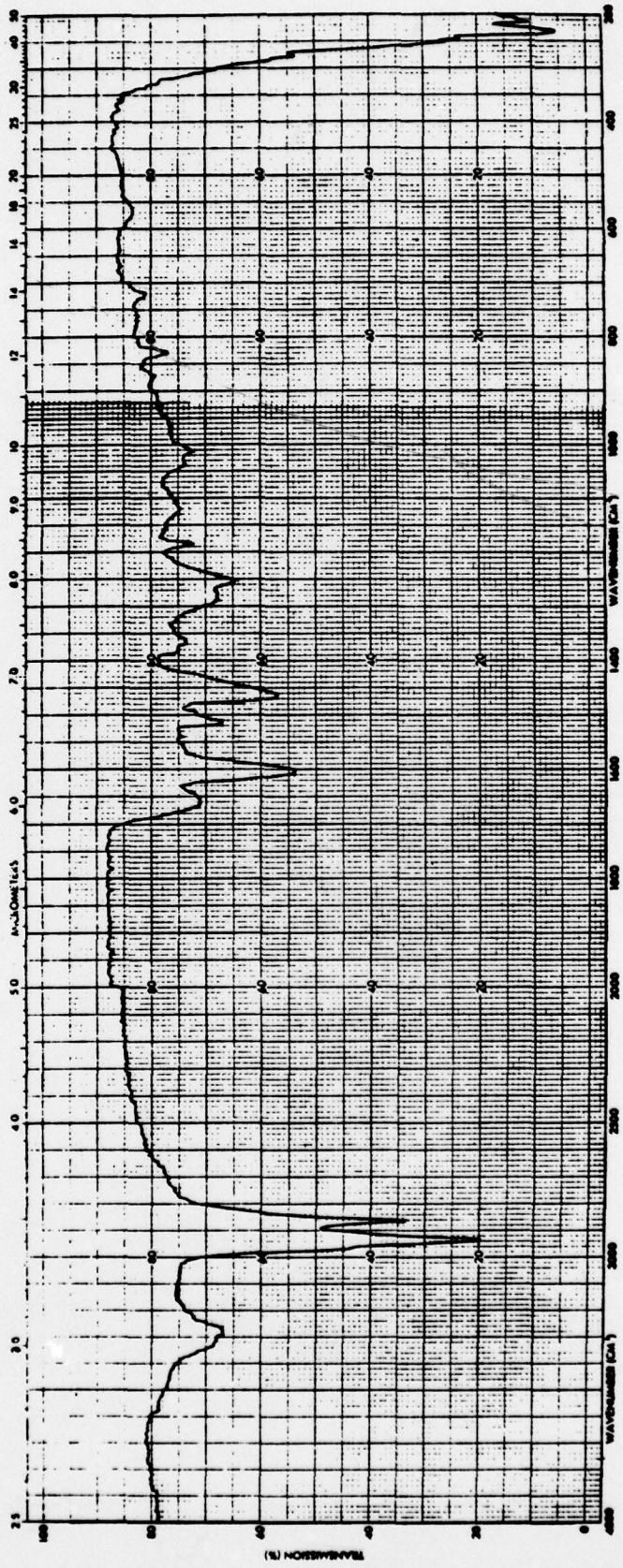

Fig. B-21. Versamid amine curing agent for paint System I.

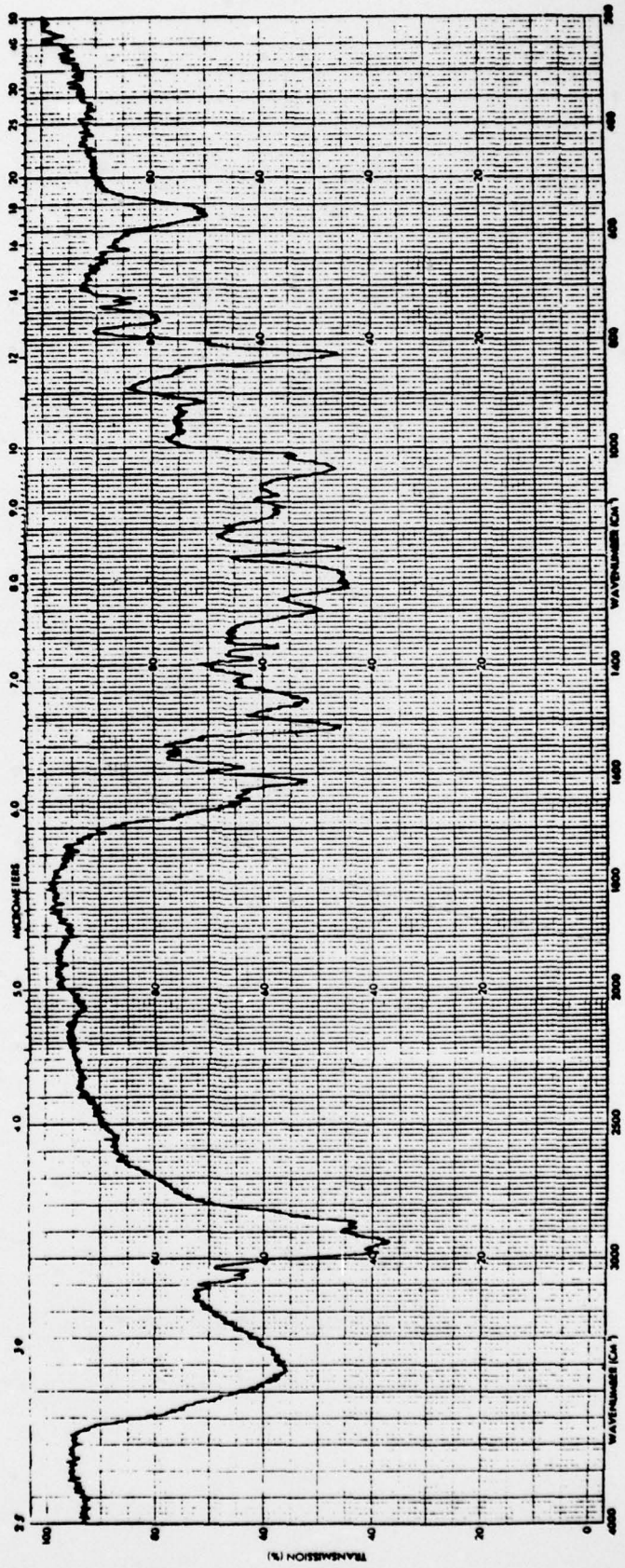

Fig. B-22. Paint System I.

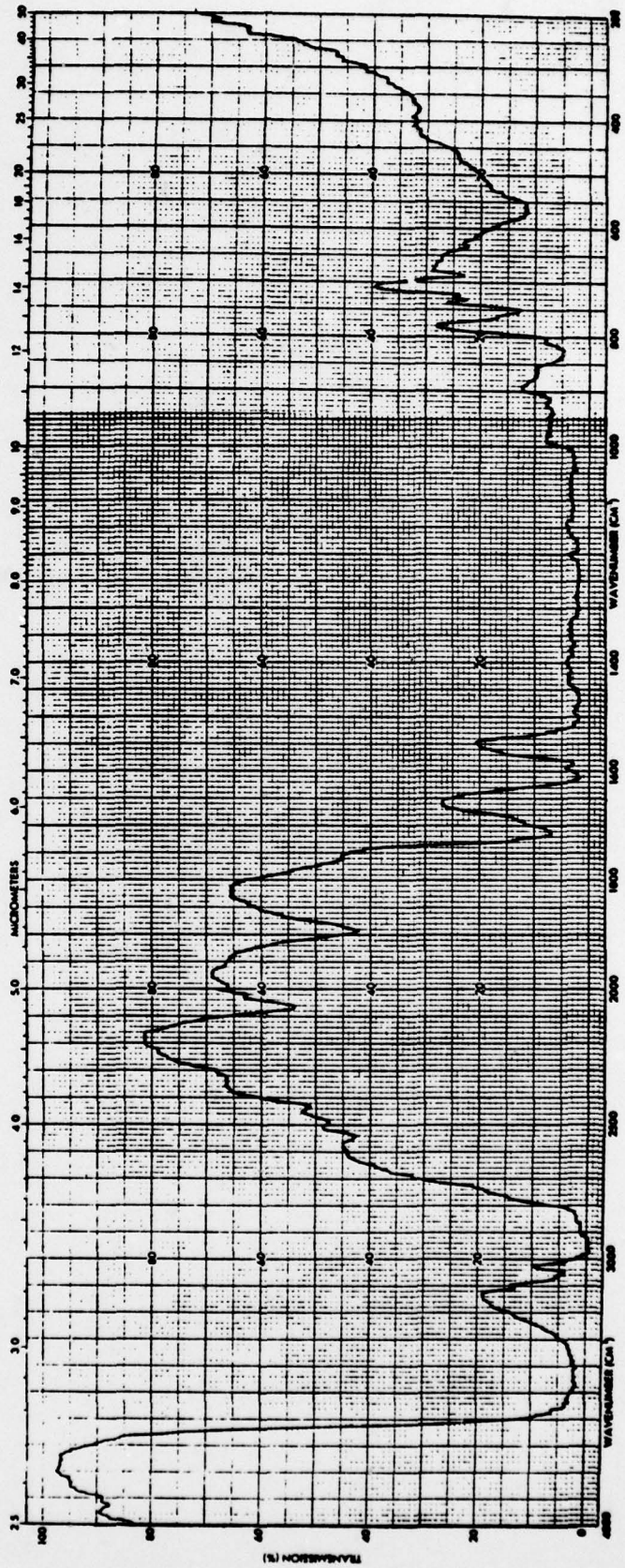

Fig. B-23. Paint System VI.

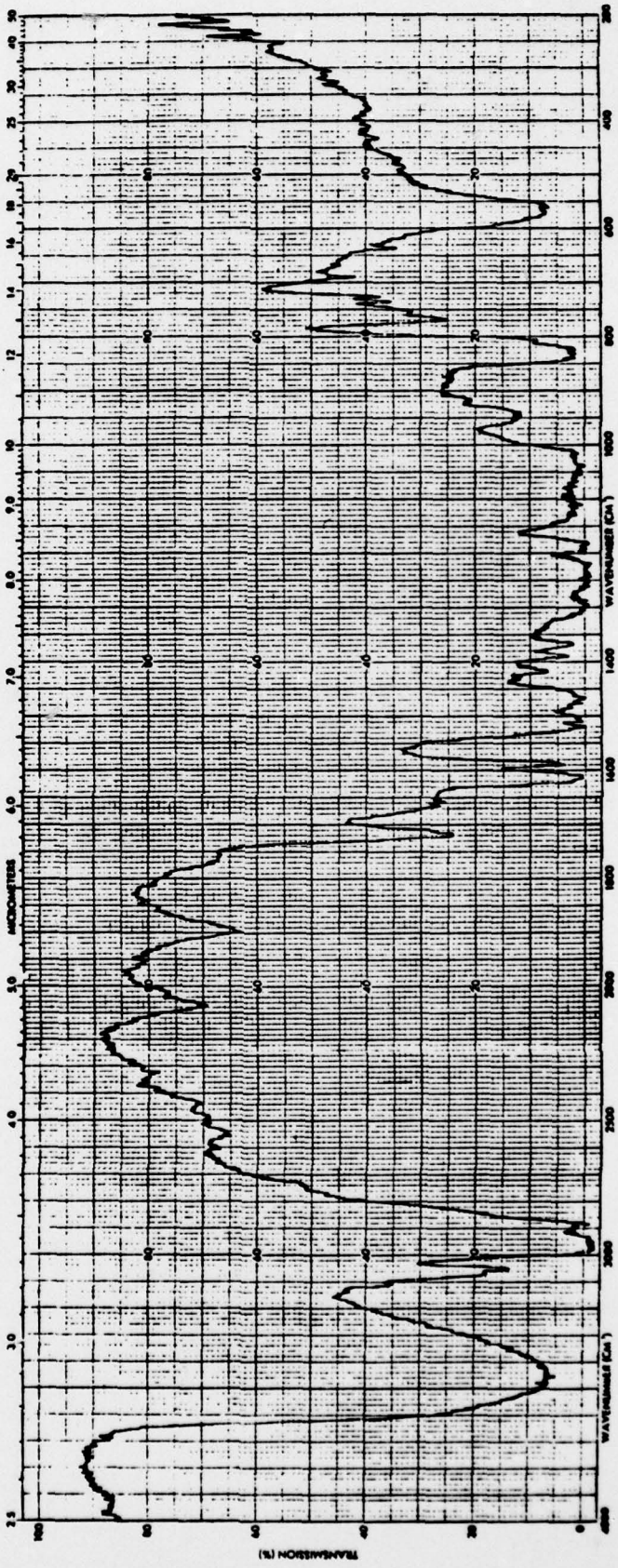

Fig. B-24. Paint System IX.

APPENDIX C

Ultraviolet Spectra

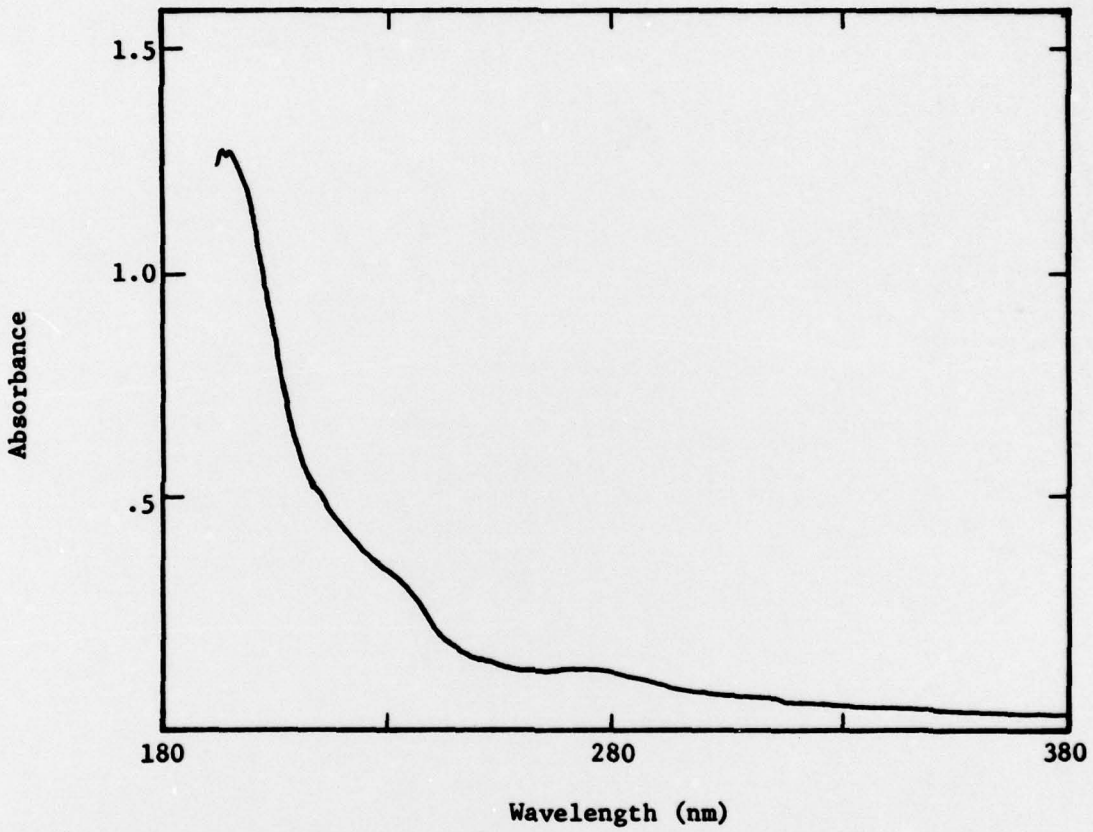

Fig. C-1. Paint System II (VR2).

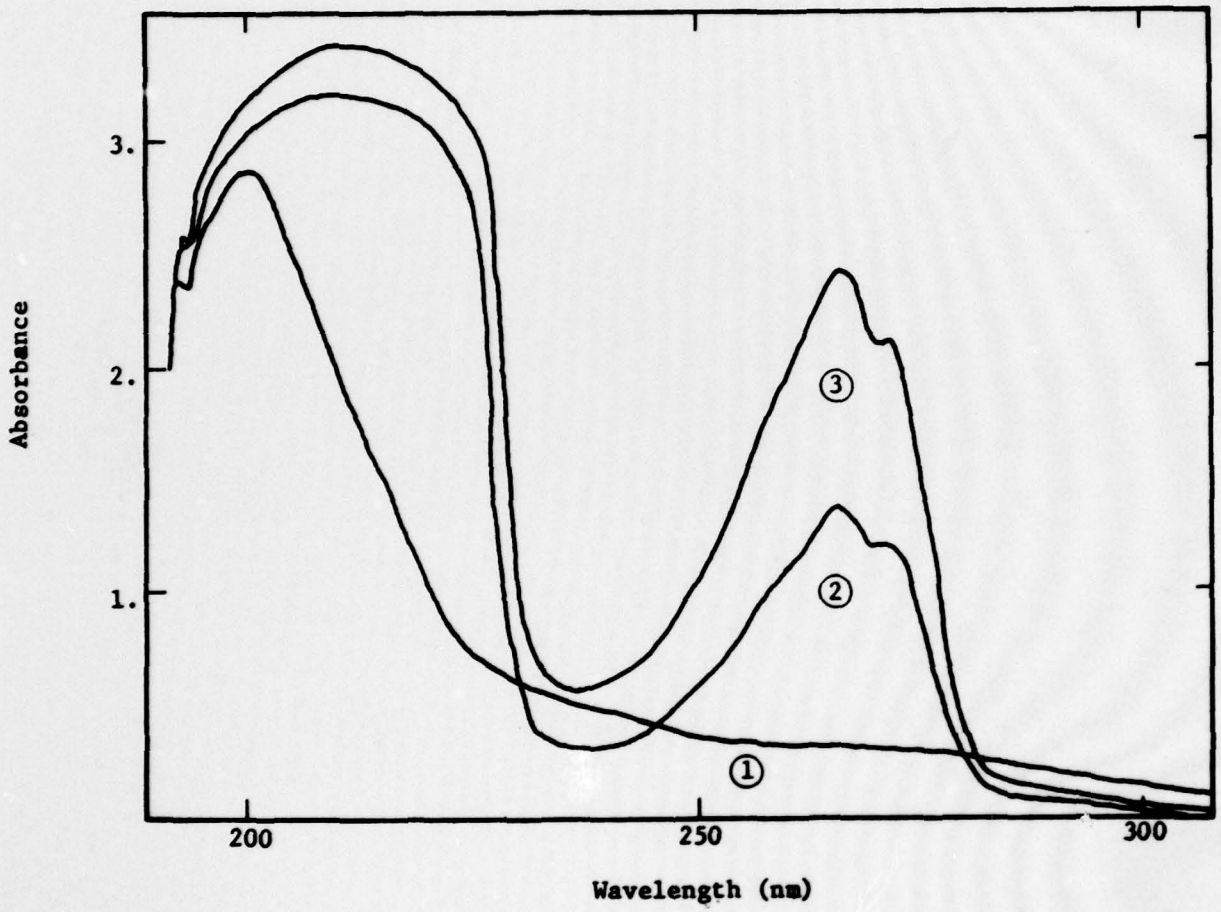

Fig. C-2. Paint System III (VR3) and special films containing copolymer and TCP. ① 0% TCP, ② 9.5% TCP (VR3), and ③ 17.2% TCP by weight.

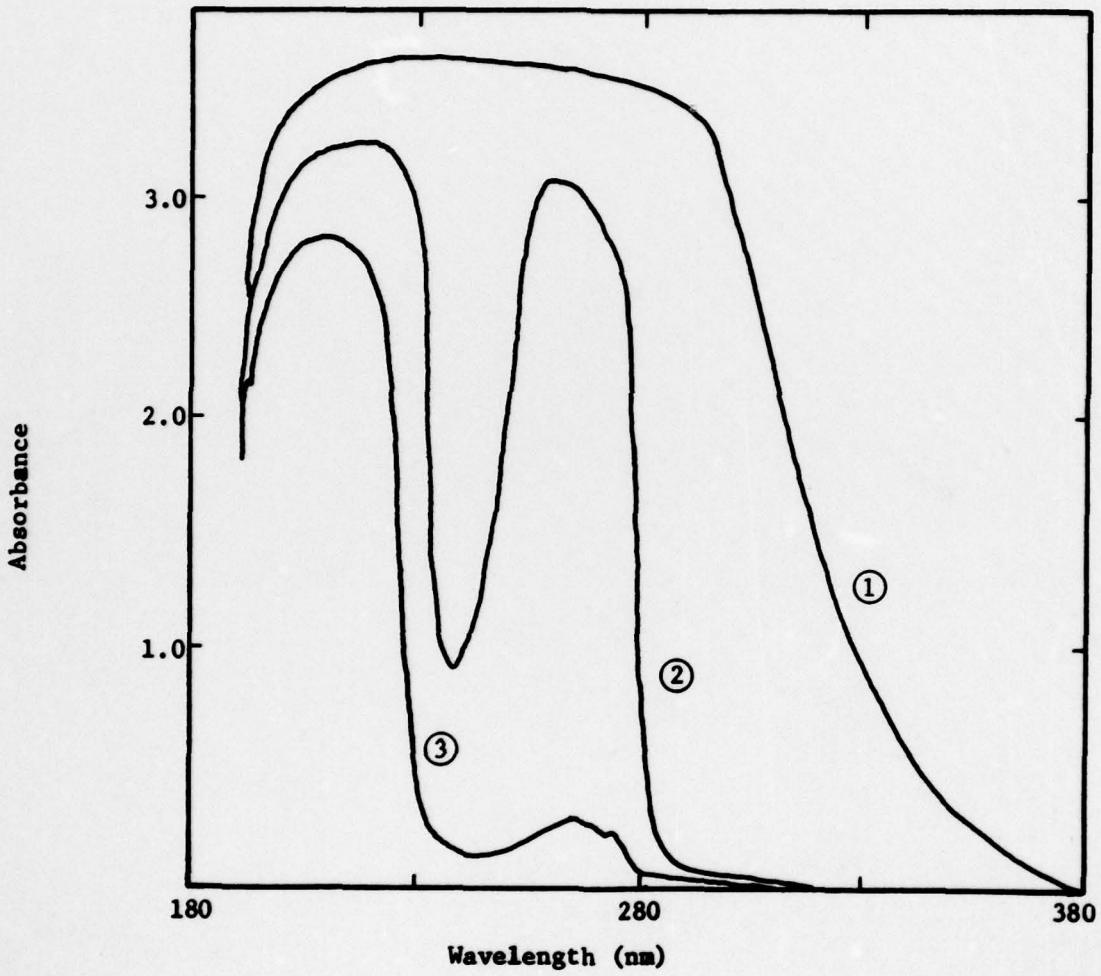

Fig. C-4. ① Paint System IV, ② copolymer with 27.6% by weight TCP, and ③ copolymer only.

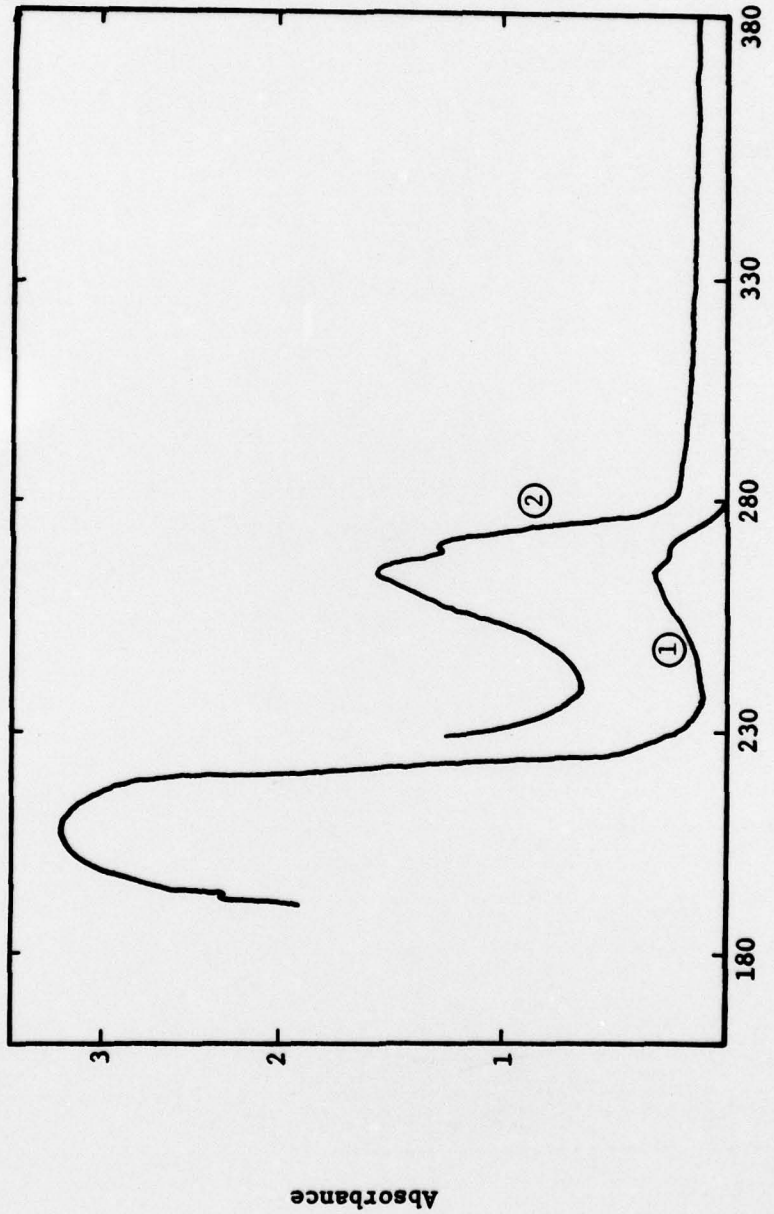

Fig. C-3. TCP in ethanol, ① Scale 1:1 and ② Scale 1:4.

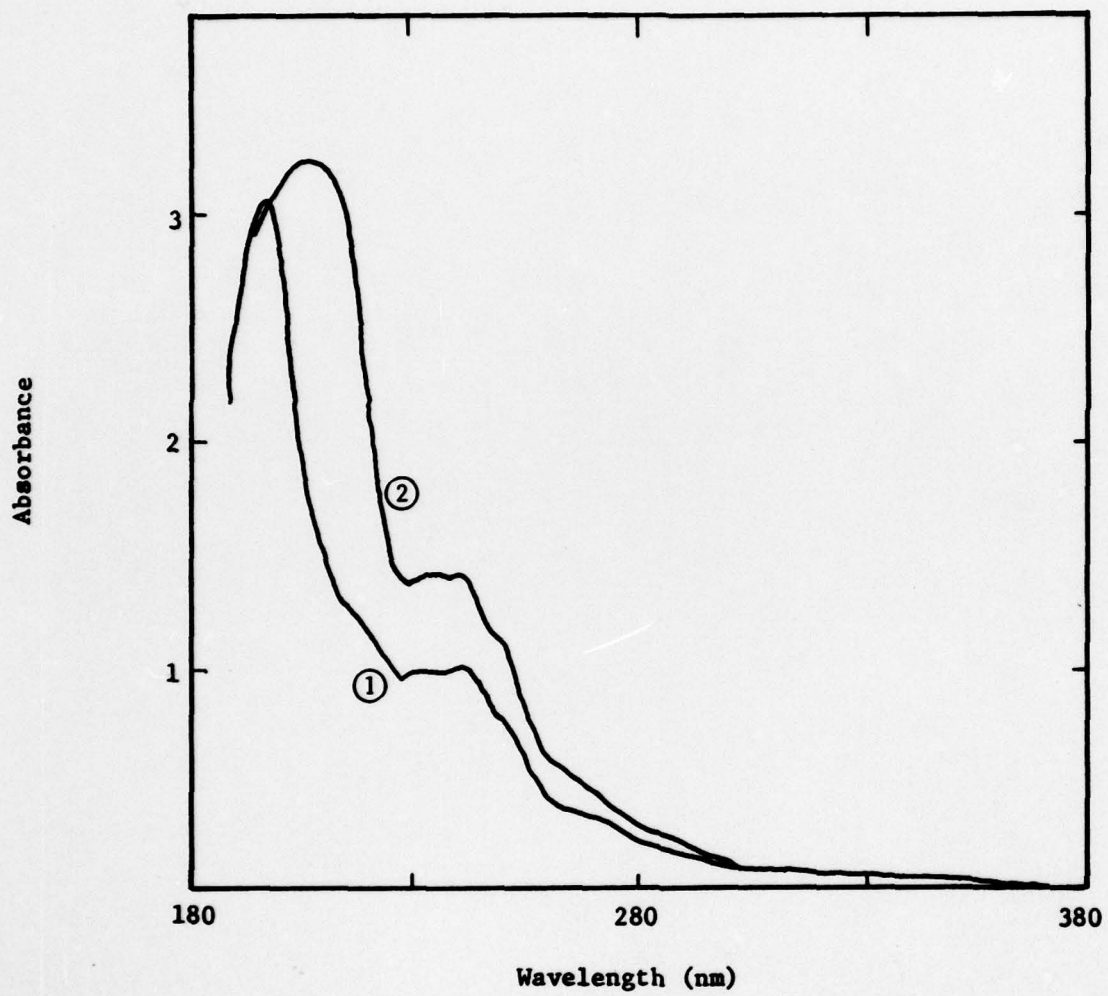

Fig. C-5. ① Copolymer of paint System IV and 20% rosin hardener and ② the rosin only in ethanol.

APPENDIX D

FILLERS

Many of the pigments and additives, for example, the rosin component in VR4, may be treated as a filler. Fillers are used in a polymeric material to increase its modulus or strength, change its coefficient of expansion, increase its toughness, and improve its abrasion resistance.

The addition of rigid inert fillers nearly always increases the modulus of a polymer since the modulus of most polymers is approximately 1×10^{10} dynes/cm^2, while the modulus for most common inorganic fillers is at least 1×10^{11} dynes/cm^2 at room temperature.

The modulus of a filled rigid polymer can often be approximated by (1)

$$G = G_1V_1 + AG_2V_2 \tag{1}$$

where G is the shear modulus of the filled material, G_1 and G_2 are the moduli of the pure polymer and filler respectively, while V_1 and V_2 are the corresponding volume fractions, and A is called the adhesion factor and can vary between zero and one. A is an empirical constant which gives a measure of the adhesion between the polymer and filler, and at the same time corrects for the theoretical inadequacies of the equation. The effect of fillers on the material's properties are important, especially in the case of paints, since pigments can be adequately treated as fillers.

Kerner (2) has derived the following relationship for the shear modulus G_o of the two-phase system (matrix and filler) in terms of the properties of the two phases. Assuming that the dispersed phase is spherical shaped particles and that there is perfect adhesion between the two phases, the equation is

$$G_o = G_1\left[\frac{V_2G_2/[(7-5\gamma_1)G_1 + (8-10\gamma_1)G_2] + V_1/15(1-\gamma_1)}{V_2G_1/[(7-5\gamma_1)G_1 + (8-10\gamma_1)G_2] + V_1/15(1-\gamma_1)}\right] \tag{2}$$

G_1 and G_2 are the shear moduli of the continuous phase and dispersed phase respectively. V_1 and V_2 are the corresponding volume fractions, while γ_1 is the Poisson's ratio of the material's continuous phase.

This result can be simplified to give Eq. D-1 under special conditions. The treatment of the effect of fillers has been extended by many investigators to account for the effect of particle shape, etc., (3).

REFERENCES (Appendix D)

1. L. E. Nielsen, Mechanical Properties of Polymers, Reinhold, 1962.

2. E. H. Kerner, Proc. Phys. Soc. of Lond. 69B, 808 (1956).

3. T. S. Cherv, J. Polymer Sci. Phys. Ed., 16, 959-965 (1978).